

OPTIMIZATION OF PEANUT DRYING, UTILIZING A MICROWAVE MOISTURE
METER IN THE IMPLEMENTATION OF A FEEDBACK CONTROLLED SYSTEM

by

MICAH ANTHONY LEWIS

(Under the Direction of Ernest W. Tollner and Samir Trabelsi)

ABSTRACT

The peanut drying process requires close monitoring of atmospheric conditions and human interaction for periodic evaluation of moisture content. If these tasks are not performed appropriately, the peanuts are at risk of being underdried or overdried. For this reason, the feasibility of implementing a feedback controlled system to optimize and further automate the peanut drying process on a wagon scale model was investigated. The feedback controller controls the temperature of the air used for drying as well as the duration of drying as it processes inputs including inlet air temperature, ambient air temperature, relative humidity and kernel (shelled peanuts) moisture content. A microwave dielectric method was used for nondestructive and rapid determination of kernel moisture content in unshelled peanuts from measurements of their complex permittivities in free space independent of bulk density. Use of such a controller would reapportion labor at peanut buying points, minimize energy consumption, and aid in preserving the quality of the peanuts.

INDEX WORDS: Feedback controller, Embedded system, Data acquisition, C/C++, Microwave sensing, Moisture content, Dielectric properties, Peanuts, Peanut drying, Unshelled peanuts, Shelled peanuts

OPTIMIZATION OF PEANUT DRYING, UTILIZING A MICROWAVE MOISTURE
METER IN THE IMPLEMENTATION OF A FEEDBACK CONTROLLED SYSTEM

by

MICAH ANTHONY LEWIS

B.S., Albany State University, 2004

M.S., University of Georgia, 2006

A Dissertation Submitted to the Graduate Faculty of The University of Georgia in Partial
Fulfillment of the Requirements for the Degree

DOCTOR OF PHILOSOPHY

ATHENS, GEORGIA

2011

© 2011

Micah Anthony Lewis

All Rights Reserved

OPTIMIZATION OF PEANUT DRYING, UTILIZING A MICROWAVE MOISTURE
METER IN THE IMPLEMENTATION OF A FEEDBACK CONTROLLED SYSTEM

by

MICAH ANTHONY LEWIS

Co-Major Professors: Ernest W. Tollner
Samir Trabelsi
Committee: Mark Haidekker
Stuart O. Nelson
Stanley Fletcher

Electronic Version Approved:

Maureen Grasso
Dean of the Graduate School
The University of Georgia
December 2011

DEDICATION

This dissertation is dedicated to my lovely wife, LaToya H. Lewis, our vibrant daughter, Avery

Janelle Lewis, and the Lewis family.

Elijah P. & Louise Lewis (Dad & Mom)

Jeffery, Dorothy & Corinthian

Elijah L., Gregoria, Mary Joy & Bonita

Frederick, Tashia, Xavier, & Lauren

To all of you, your support throughout the years has been worth more than pure gold.

This completed work is submitted in the memory of Mr. Lendon Lewis.

(July 16, 1965 to January 14, 2011)

Forever missed, never forgotten.

*You dreamed of the day Daddy and Mama would have two doctors, here it is. I know you're
looking down, shouting.*

ACKNOWLEDGEMENTS

First and foremost, I would like to acknowledge my Lord and Savior, Jesus Christ, for His strength and guidance throughout my graduate studies. His grace and favor were evident in the completion of this work. Without Him, none of this would have been possible.

I would like to thank my committee members for their tireless efforts and support throughout my research and project completion. I like to say that I assembled the “*dream team*” of engineering and physics. I am extremely grateful to USDA AMS FSMIP for funding in support of this work. Expressions of thanks go to the Georgia Federal State Inspection Service and the Peanut Inspection Service for assistance with deployment of microwave moisture sensors, provision of peanut grading equipment, and provision of peanut pod samples for research and evaluation. During this research, samples were provided by multiple peanut shellers throughout the country, and for that, I am grateful. I would like to acknowledge the multiple peanut buying points across the country that assisted in this research by allowing the insertion of the microwave moisture meter into the peanut grading process. Lastly, I would like to extend sincere thanks to USDA ARS Quality and Safety Assessment Research Unit for a place to perform research and grow as a scientist and engineer. To all that contributed to this research in any form or fashion, I express my deepest gratitude.

TABLE OF CONTENTS

	Page
ACKNOWLEDGEMENTS	v
LIST OF TABLES	ix
LIST OF FIGURES	xi
CHAPTER	
1 INTRODUCTION	1
1.1 Peanut History	1
1.2 Planting and Harvesting	2
1.3 Drying and Grading	3
1.4 Importance of Drying Efficiency	5
2 REVIEW OF LITERATURE	8
2.1 Present Techniques	8
2.2 Related Work	15
2.3 Literature Review Wrap Up	20
3 SOLUTION APPROACH	21
3.1 Research Objectives	22
3.2 System Design	23
4 PEANUT DRYING: SCALED DOWN	26
4.1 Current Drying System	26
4.2 Quarter-scale Drying System	28

5	FEEDBACK CONTROL SYSTEMS.....	35
	5.1 Feedback Control System Background.....	35
	5.2 Feedback Control System: Closed-Loop Regulation.....	37
6	MICROWAVE MOISTURE SENSING	45
	6.1 Nondestructive Testing	45
	6.2 Indirect Methods from Reference Methods	46
	6.3 Microwaves.....	48
	6.4 Microwave Measurement Methods.....	49
	6.5 Microwave Moisture Sensor Measurement Principle.....	52
	6.6 Peanut Moisture Content Determination (Unshelled, Shelled, & In-shell)	57
7	SOFTWARE IMPLEMENTATION	66
	7.1 Summary of Program Execution.....	66
	7.2 Modular Programming.....	67
8	DATA ACQUISITION.....	70
	8.1 Sensor Network.....	70
9	ANALYSIS OF STABILITY AND TYPE INDEPENDENCE OF THREE DENSITY INDEPENDENT CALIBRATION FUNCTIONS FOR MICROWAVE MOISTURE SENSING IN SHELLED AND UNSHELLED PEANUTS	75
	Abstract.....	76
	9.1 Introduction.....	77
	9.2 Materials and Methods.....	79
	9.3 Free-space Complex Permittivity Measurements	80
	9.4 Results and Discussion	88

9.5 Conclusion	103
References.....	103
10 INTEGRATING AN EMBEDDED SYSTEM WITHIN A MICROWAVE	
MOISTURE METER.....	106
Abstract.....	107
10.1 Introduction.....	108
10.2 Materials and Methods.....	111
10.3 Results and Discussion	123
10.4 Conclusion	127
References.....	128
11 AN AUTOMATED APPROACH TO PEANUT DRYING WITH REAL-TIME	
MONITORING OF IN-SHELL MOISTURE CONTENT WITH A MICROWAVE	
SENSOR.....	130
Abstract.....	131
11.1 Introduction.....	132
11.2 Materials and Methods.....	135
11.3 Results and Discussion	153
11.4 Conclusion	159
References.....	160
12 CONCLUSION AND FUTURE WORK	164
REFERENCES	168

LIST OF TABLES

	Page
Table 5.1: Data for open-loop coefficients and constants at low fan speed	40
Table 5.2: Data for open-loop coefficients and constants at high fan speed	41
Table 9.1: Ranges of physical characteristics and measurement data of kernel and pod samples used for calibration	83
Table 9.2: Regression statistics corresponding to equations (9.8) and (19.0) for moisture content prediction for kernels of specified peanut types at 6 GHz and 23 °C.....	90
Table 9.3: Regression statistics corresponding to equations (9.8) and (9.10) for moisture content prediction of pods of specified peanut types at 6 GHz and 23 °C	91
Table 9.4: Regression statistics corresponding to equations (9.8), (9.10) and (9.11) for type-independent moisture content determination for peanut kernels and pods at 6 GHz and 23 °C	96
Table 9.5: Ranges of physical characteristics and measurement data for kernel and pod samples used for validation.....	99
Table 10.1: Resolution for various standard bit configurations over a 0 to 2.5 V range	114
Table 10.2: Voltage values measured throughout the level shifter.....	115
Table 10.3: Results from measurements taken on unshelled Georgia Runner type peanuts comparing the embedded system to the laptop-controlled system	124
Table 10.4: One-way analysis of variance results for system comparison	127
Table 11.1: Possible dimensions for small-scale peanut drying trailer	139

Table 11.2: 2-bit control for heating elements.....	142
Table 11.3: Breakdown of water added to peanuts.....	151
Table 11.4: Data for comparison between moisture content determination with oven method and microwave moisture meter.....	159
Table 11.5: <i>SEP</i> and ANOVA results for moisture content determination	159

LIST OF FIGURES

	Page
Figure 1.1: Peanut digger inverting peanuts for drying in windrows	3
Figure 1.2: Probe patterns for pneumatic probe in extraction of representative sample	4
Figure 1.3: Peanut kernel and shell contaminated with aflatoxin.....	7
Figure 2.1: PECMAN decision support system for peanut drying	13
Figure 2.2: Opticure2000© dryer controller software main screen	14
Figure 2.3: Setup window for Opticure2000 dryer controller system	15
Figure 3.1: Complete system diagram and data flow	24
Figure 4.1: Wagon-type peanut drying trailers loaded with peanuts	27
Figure 4.2: Official moisture meters for peanut grading; GAC shown left, PT-2 shown right	28
Figure 4.3: Peanut drying trailer connected to BlueLine dryer	29
Figure 4.4: Schematic diagram of quarter-scale peanut drying trailer.....	30
Figure 4.5: Quarter-scale peanut drying trailer.....	30
Figure 4.6: Block diagram for electrical circuits in ChallengAir 560 dryer	32
Figure 4.7: Original controls in ChallengAir 560 dryer	33
Figure 4.8: ChallengAir 560 with modified controls.....	33
Figure 4.9: Dryer shown connected to solid-state relays for automated control	34
Figure 5.1: Block diagram of closed-loop feedback system.....	36
Figure 5.2: Block diagram for open-loop air inlet process	38
Figure 5.3: Dryer response at low fan speed.....	39

Figure 5.4: Dryer response at high fan speed	40
Figure 5.5: Open-loop control and temperature distribution throughout bed of peanuts	42
Figure 5.6: Block diagram for closed-loop control of inlet air temperature shown with P- controller	43
Figure 5.7: Temperature of inlet air shown in comparison with temperature distribution throughout bed of peanuts.....	44
Figure 6.1: Electromagnetic spectrum	49
Figure 6.2: Free-space transmission method measurement principle.....	53
Figure 6.3: Free-space measurement system with vector network analyzer	55
Figure 6.4: Laptop-controlled free-space measurement system using microwave components ...	56
Figure 6.5: Enclosed version of microwave moisture meter	57
Figure 6.6: Peanuts shown in different forms	58
Figure 6.7: Complex-plane representation for kernels and pods	56
Figure 6.8: Variation of ψ with moisture content for kernels and pods.....	57
Figure 6.9: Variation of ψ with moisture content and temperature for kernels and pods.....	64
Figure 6.10: Predicted kernel moisture content versus reference moisture determined by oven drying	65
Figure 6.11: Temperature distribution of peanut pod samples	65
Figure 7.1: Flowchart for main program execution	68
Figure 8.1: Modified LM35 temperature sensors	72
Figure 8.2: Linear regression for determination of relative humidity	73
Figure 8.3: Antennas for microwave meter mounted within drying trailer	74
Figure 9.1: Free-space measurement system with pod sample shown	81

Figure 9.2: Complex-plane representation of dielectric properties of kernels (upper) and pods (lower) of indicated peanut types at 6 GHz and 23 °C	84
Figure 9.3: Structural differences shown for various peanut types	87
Figure 9.4: Variation of ψ_1 with kernel moisture content for Valencia type kernels measured at 6 GHz and 23 °C	88
Figure 9.5: Variation of ψ_1 with moisture content for kernels of indicated type measured at 6 GHz and 23 °C (shown with individual calibrations).....	90
Figure 9.6: Variation of ψ_1 with moisture content for pods of indicated type measured at 6 GHz and 23 °C (shown with individual calibrations)	91
Figure 9.7: Variation of ψ_1, ψ_2, ψ_3 with moisture content for kernels of combined indicated types at 6 GHz and 23 °C	94
Figure 9.8: Variation of ψ_1, ψ_2, ψ_3 with moisture content for pods of combined indicated types at 6 GHz and 23 °C.....	95
Figure 9.9: Predicted kernel moisture content for ψ_1, ψ_2, ψ_3 (top to bottom) versus reference moisture determined by oven drying	97
Figure 9.10: Predicted pod peanut moisture content for ψ_1, ψ_2, ψ_3 (top to bottom) versus reference moisture determined by oven drying	98
Figure 9.11: Variation of r^2 and <i>SEC</i> for ψ_1, ψ_2, ψ_3 as frequency increases (peanut kernels).....	100
Figure 9.12: Variation of r^2 and <i>SEC</i> for ψ_1, ψ_2, ψ_3 as frequency increases (pod peanuts).....	101
Figure 9.13: Variation of <i>SEP</i> for ψ_1, ψ_2, ψ_3 as frequency increases (peanut kernels).....	102
Figure 9.14: Variation of <i>SEP</i> for ψ_1, ψ_2, ψ_3 as frequency increases (pod peanuts).....	102
Figure 10.1: Previous version of microwave moisture meter (controlled by external laptop)	110
Figure 10.2: USB connection on rear of moisture meter	111

Figure 10.3: SensorCore (Tern, Inc.) microcontroller shown with 16-button keypad and graphical LCD	113
Figure 10.4: Schematic diagram of level shifter circuit simulated in Multisim	116
Figure 10.5: Implementation of level shifter circuit	117
Figure 10.6: Voltage divider implemented for level shifter circuit	118
Figure 10.7: Circuitry solution for negative supply voltage	119
Figure 10.8: Complete circuit for signal conditioning	120
Figure 10.9: Microwave moisture meter shown with LCD and keypad (embedded system).....	120
Figure 10.10: Flowchart for main program execution	122
Figure 10.11: Variation of dielectric properties with moisture content shown on laptop-controlled system and VNA	125
Figure 10.12: Variation of dielectric properties with moisture content shown on embedded system and VNA	126
Figure 11.1: Complete system diagram and data flow	135
Figure 11.2: Circuitry for sensor network.....	138
Figure 11.3: Quarter-scale peanut drying trailer.....	140
Figure 11.4: Unmodified ChallengAir 560 dryer	142
Figure 11.5: Modified ChallengAir 560 dryer.....	143
Figure 11.6: Dryer response at different heat settings	144
Figure 11.7: Flowchart for main program execution	146
Figure 11.8: Drying trailer with dryer connected	148
Figure 11.9: Schematic diagram for thermocouple distribution	149
Figure 11.10: Drying trailer shown with thermocouples placed throughout	150

Figure 11.11: Antennas mounted within drying trailer.....	153
Figure 11.12: Relative humidity versus time during drying process	154
Figure 11.13: Temperature of ambient air and peanuts versus time during drying process	155
Figure 11.14: Inlet air temperature and temperature distribution of peanut bed versus time shown for first 10 minutes.....	156
Figure 11.15: Inlet air temperature and temperature distribution of peanut bed versus time shown for last 10 minutes.....	157
Figure 11.16: Moisture content determination (pods and kernels) compared between microwave meter and oven method.....	158

CHAPTER 1

INTRODUCTION

1.1 Peanut History

The origin of peanuts can be traced back to South America, possibly Brazil or Peru, approximately 3500 years ago. Graves of the ancient Inca civilization, found along the western coast of South America, often contained jars filled with peanuts, and recovered pottery artifacts include jars shaped like peanuts and decorated with peanuts (American Peanut Council, 2007). By the time of the arrival of the Spanish conquistadors in America, the growth of peanuts had spread as far north as Mexico. The Spanish explorers took peanuts back to Spain; and through further trade and exploration, peanuts were spread to Africa and Asia.

It was not until the 1700's that peanuts were introduced to North America as a result of the slave trade from Africa as food for swine (University of Georgia, 2003). Around 1800, the commercial growth of peanuts began in South Carolina for food, oil, and a substitute for cocoa (American Peanut Council, 2007). In 1860, peanut consumption in the United States increased substantially because of the Civil War. Peanuts served as a vital source of food for soldiers. However, aside from the consumption of peanuts by soldiers, the demand remained low because harvesting was done by hand. It wasn't until 1900 that proper equipment was invented for planting, harvesting, and grading peanuts. After this time, peanut production increased dramatically (Putnam et al., 2000).

Today, peanut production is very high in the United States. The growth of peanuts is no longer limited to the southeastern states. It has spread throughout the southern part of the

country, providing different types for different uses. For market, the four basic types of peanuts are Runner, Virginia, Spanish and Valencia. Types of peanuts can be distinguished by their growth location, branching habit, and branch length (Virginia-Carolina Peanut Promotions, 2007). Within each type are different varieties that address various growing needs. For each type, the same routines are followed in planting, harvesting, and processing.

1.2 Planting and Harvesting

Peanuts are planted traditionally after the last frost, which is usually April or May. This time is preferred because the soil temperature is usually between 65 to 70 °F. The seeds are planted at a depth of one to two inches and spaced apart by three to four inches. Favorable growing conditions include a climate with 160 to 200 frost-free days, warm weather, adequate moisture, and rich fertile soil (Virginia-Carolina Peanut Promotions, 2007). When the majority of peanuts have reached maturity, harvesting begins. Harvesting occurs in two phases, digging and combining. During the digging phase, diggers are driven along rows of peanuts; and while passing, they cut the taproots of the peanut plants, lift the plants from the soil, and lay the plants down inverted in windrows so that the peanuts are exposed for natural drying (Figure 1.1). Since the moisture content of the peanuts at this time can range from 25% to 50% w.b., they are allowed to remain in the windrows for two to three days to allow the moisture to drop.

The second phase of harvesting is combining. After the peanuts have had a reasonable chance to dry in the field, they are collected using combines, also known as threshers. The combine lifts the entire plant and separates the peanuts from the vine. The peanuts are then blown into a hopper located on top of the combine. The vines are laid back in the field to aid in soil fertility and increase organic matter. Upon completion of harvesting, peanuts are loaded into drying wagons and transported to buying points for grading.



Figure 1.1: Peanut digger inverting peanuts for drying in windrows

1.3 Drying and Grading

When harvested peanuts arrive at buying points, a small sample is extracted from the wagon. After being cleaned and shelled, the sample is analyzed for kernel moisture content. The moisture content at this time could still be reasonably high, $> 20\%$. After the determination of initial kernel moisture content, the wagon is taken to the drying shed for the peanuts to be dried to a target kernel moisture content of $\leq 10.49\%$ w. b. It is imperative that peanuts be dried below 10.5% kernel moisture content for grading and storage.

To facilitate the drying process, peanuts are loaded into drying wagons. These wagons are 6.4 m long, 2.4 m wide, and 1.27 m deep above a perforated floor, which is at the top of a 23 cm high air plenum (Butts and Williams, 2004). Then dryers (propane or natural gas) are connected to the wagons through canvas ducts, and heated air is blown into the airspace below the bed of peanuts. The airspace pressurizes, forming an air plenum, and heated air is forced up through the peanuts to decrease the moisture content of the bed (Butts, 1995). Peanuts are dried

in this fashion until the target moisture is reached. When the peanuts are finished drying they are moved from the drying shed to a tower where the wagon is probed at various locations to extract pneumatically a representative sample for grading. Initially, a 3 kg sample is extracted. It is then halved to create a primary sample and a backup sample in case of spillage or other mishaps. Figure 1.2 shows probe patterns for the pneumatic probe used to sample the peanuts.

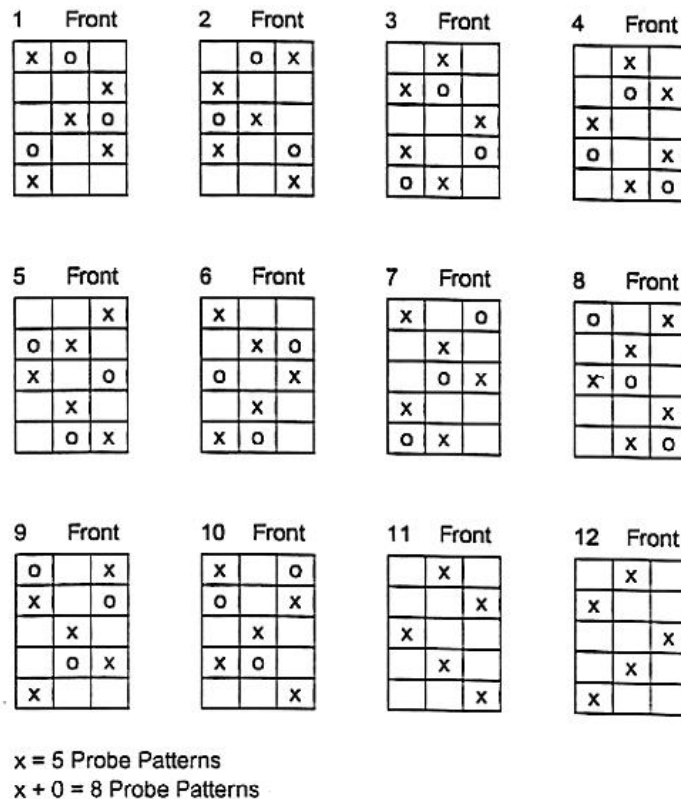


Fig. 3. Example of several five- and eight-probe patterns used by the USDA to sample farmers stock peanuts for grade and support price.

Figure 1.2: Probe patterns for pneumatic probe in extraction of representative sample

Peanuts are inspected and graded to determine the overall quality and on-farm value for commercial sale. The grading process is facilitated by the Agricultural Marketing Service (AMS) and the Federal-State Inspection Service (FSIS) at buying points near the peanut fields (American Peanut Council, 2007). During this process, the representative sample of unshelled

and unclean peanuts taken from each wagon is analyzed to determine the following five parameters:

1. amount of foreign material – percentage of the weight of foreign material (dirt, rocks, sticks, miscellaneous debris) compared to that of the entire uncleaned sample
2. size of peanut pods (unshelled peanuts)
3. meat content – percentage of the weight of kernels (shelled peanuts) as compared to the weight of entire unshelled sample
4. amount of damaged kernels – kernels visually inspected for rancid, moldy and decay characteristics
5. kernel moisture content – initial samples have to be cleaned and then shelled to expose the peanut kernels (acceptable moisture content ≤ 10.49 %)

These five parameters are used to establish the grade of a specific lot of peanuts. This determines how much the farmer is paid per ton for the peanut lot. While being graded, if the kernel moisture content is determined to be ≥ 10.50 %, the corresponding sample is marked with a label “NO SALE”, and the corresponding lot of peanuts has to be taken back to the drying shed and further dried.

1.4 Importance of Drying Efficiency

There are decision support systems and other control systems that are presently used to estimate the drying time based on initial atmospheric conditions and the initial kernel moisture content of the bed of peanuts (Butts et al., 2003; Butts et al., 2004; Microtherm Inc, 2000). However, these systems demand heavy user interaction such as sampling for kernel moisture content and updating current atmospheric conditions, and they are susceptible to permitting overdrying or underdrying if not updated appropriately. To sample kernel moisture content, a sample of a few hundred grams of peanuts is taken from the trailer. At this point, the sample still contains foreign material; therefore, the sample has to be cleaned using machinery that separates

the peanut pods from foreign material found in the sample. After the sample is cleaned, it is shelled to remove the peanut kernels from the hulls. Then the kernels are analyzed for kernel moisture content. This process is repeated every time kernel moisture content of the drying bed of peanuts is analyzed.

Overdrying affects the buying station and the farmer. When peanuts are overdried, energy has been wasted lowering the peanuts to undesirable kernel moisture content. When peanuts are low in moisture, more splits and loosely shelled kernels are generated during handling and cleaning; resulting in a decline in quality for the peanuts and ultimately a lower grade. The amount the farmer is awarded per ton is decreased because of a lower grade.

Underdrying is expensive in costs, labor and time for a buying point. When underdried peanuts are graded, they generate a “NO SALE” due to moisture; meaning a kernel moisture content of 10.5% or greater. Since they are rejected, they have to be further dried and regraded. This slows the progress of the buying station.

Other control criteria, such as drying temperature, have to be monitored closely. Drying temperatures exceeding 95 °F can cause undesirable flavor and poor milling properties in peanuts (Beasley and Dickens, 1963). However, drying temperatures that are too low can cause slow drying rates. A slow drying rate can cause mold to form on the peanut pods and eventually penetrate to the kernels. The most common mold observed in peanuts is *aspergillus flavus*. It is a common mold known to attack corn and peanuts that are high in moisture for long periods of time. Figure 1.3 shows peanut pods affected by *aspergillus flavus*. Its spores are allergenic, and many strains produce significant quantities of aflatoxin, a carcinogenic and acutely toxic compound (Klich, 2007).

Control systems available for peanut drying, at most, are able to measure atmospheric conditions in real-time. However, they lack a means to measure the main parameter of interest, kernel moisture content. Knowledge of kernel moisture content in real-time could aid in the development of an automated system to fully control the drying process, eliminating the occurrences of overdrying and underdrying. A system able to monitor atmospheric conditions and kernel moisture content would be essential in optimizing drying control.



Figure 1.3: Peanut kernel and shell contaminated with aflatoxin

Problems in drying efficiency were observed beginning in 2008 when the first of several visits to buying stations throughout Georgia were made. Testimonials of buying point managers, farmers and inspectors also gave indications that the drying process could use innovative improvements. Therefore, this research addresses the implementation of a feedback control system to efficiently govern and facilitate the drying process. This dissertation is written in manuscript style and initially provides the reader with an overview of the system and a description of each component of the system in detail. Then, the latter chapters show published works that support the goals of this research.

CHAPTER 2

REVIEW OF LITERATURE

2.1 Present Techniques

Over the years, computer simulation models have been developed to estimate the time required to dry farmer stock peanuts. These models require initial inputs along with periodic maintenance and updates to keep the estimated drying time current. Initial estimated drying time is subject to change as atmospheric conditions fluctuate. The models have proven effective; however, the efficiency of each model depends greatly on the effective management of operations. For example, kernel moisture content, the most important and governing parameter, has to be sampled manually. The following models described are used today throughout the peanut industry.

PEADRY (Colson and Young, 1990) is a computer program written in BASIC, based on a thin-layer drying model for in-shell Virginia-type peanuts in which the pod is treated as two separate components (kernels and hulls) and the moisture movement is considered proportional to a combination of moisture content gradients (liquid diffusion) and vapor pressure gradients (vapor diffusion). The initial version of PEADRY (PEADRY3) was based on the following drying relationship:

$$\frac{dM}{dt} = -k(M - M_e) \quad (2.1)$$

where M is the moisture content, dry basis, in decimal form, M_e is the equilibrium moisture content, dry basis, decimal form, k is a drying constant, in h^{-1} , and t is time, in h. Equation 2.1 has been used to describe the thin-layer drying of many products. It is based on the assumption

that resistance to moisture movement and gradients within the material are negligible. Therefore, with peanut drying, the following assumptions are made: there is a single drying gradient for the pod as a whole, resistance to moisture transfer occurs only at the surface, and moisture transfer is proportional to the difference in pod moisture content and its equilibrium moisture content for the condition of the surrounding air. Kernel and hull moisture contents are calculated from the pod moisture content, assuming that they are in equilibrium with each other (Colson and Young, 1990).

The latest version of PEADRY (PEADRY8) is improved from the initial version in that not only does it describe the drying of the whole peanut pod accurately; it also accurately describes the drying of the hulls and kernels separately. The differential in Equation 2.1 is replaced with a finite difference, and the moisture contents are solved for at the end of a time step, yielding Equations 2.2 and 2.3:

$$M_{k2} = -K_L \times TI \times (M_{k1} - M_{ke}) - K_V \times TI \times (rh_k - rh_h) + M_{k1} \quad (2.2)$$

and

$$M_{h2} = -H_L \times TI \times (M_{h1} - M_{he}) - H_V \times TI \times (rh_h - rh) + M_{h1} \\ - (M_{k2} - M_{k1}) \times \frac{D_k}{D_h} \quad (2.3)$$

where M_{k1} is kernel moisture content at the beginning time step, M_{k2} kernel moisture content at the end of time step, TI is time increment, h , M_{h1} is hull moisture content at beginning of time step, M_{h2} is hull moisture content at end of time step, rh is relative humidity of surrounding air, rh_k and rh_h are equilibrium relative humidity of kernels and hulls, respectively, K_L and K_V are kernel liquid and vapor drying parameters, respectively, in h^{-1} , H_L and H_V are hull liquid and vapor drying parameters, respectively, in h^{-1} , M_{ke} and M_{he} are equilibrium moisture content of kernels and hulls, respectively, and D_k and D_h are the dry matter density of peanut kernels and

hulls, respectively, in kg/m^3 . The inputs required are ambient air temperature, plenum air temp, air flow rate, initial peanut moisture and peanut volume (Butts et al., 2004). The wet bulb and dry bulb temperatures of the air after heating must also be supplied. PEADRY has been observed to accurately simulate peanut drying; however, extensive programming and response time hinder mass incorporation in decision support systems.

PNUTDRY is a peanut drying simulation program also written in BASIC. It is based on the Hukill method for bulk drying of grains (Troeger, 1989). William Hukill served as a research engineer for the USDA for 43 years and is commended for his innovative contributions to the understanding and application of drying principles to agricultural crops (Foster, 1986). The Hukill method consists of the deep-bed drying analysis in which air is forced up through drying grain or other material.

PNUTDRY requires the following inputs: ambient air temperature, plenum air temperature, air flow rate, initial peanut moisture, peanut volume and daily minimum and maximum temperatures (Butts et al., 2004). In this model, the pod is treated as a single entity. The following regression is used to determine the reciprocal of the time required to reduce the pod moisture to 7%:

$$RTIME = A_0 + A_1 \cdot T_{PRS} + A_2 \cdot DTPR + A_3 \cdot DTPR^2 \quad (2.4)$$

where coefficients A_0 , A_1 , A_2 and A_3 depend on minimum daily temperature of ambient air (T_{DMN}) and range in daily temperature (T_{DRN}) in degrees Celsius, T_{PRS} is the user specified temperature rise, and $DTPR$ is the difference in maximum temperature rise needed to achieve maximum allowable plenum temperature of the drying air and T_{PRS} . The next regression was developed to estimate the natural logarithm of the ratio of drying time at nonstandard conditions to that at standard conditions:

$$LNRTIM = B_0 + B_1 \cdot RSMC^2 + B_2 \cdot RSMC + B_3 \cdot SMSF \quad (2.5)$$

where coefficients B_0 , B_1 , B_2 and B_3 depend on T_{DMN} and T_{PRS} , RSMC is standard moisture content ratio and SMSF is standard moisture and standard airflow ratio (Butts et al., 2003; Butts et al., 2004).

With the calculations of RTIME and LNRTIME, the time to dry the peanuts to the desired peanut pod moisture content can be determined. The time required to dry peanuts from the desired peanut pod moisture content to 7% is calculated as:

$$T_{ref} = \frac{1}{RTIME} \quad (2.6)$$

Next, the ratio of actual time to dry peanut pods from a given peanut pod moisture content to 7% w.b. to T_{ref} is calculated as:

$$T_{rel} = e^{LNRTIM} \quad (2.7)$$

The time required to dry peanuts from the initial pod moisture content to 7% is calculated as:

$$T_i = T_{ref} \times T_{rel} \quad (2.8)$$

Finally, the time required to dry peanuts from the initial to the desired peanut pod moisture content is calculated as:

$$T_D = T_i \times T_f \quad (2.9)$$

As with PEADRY, PNUTDRY has been observed to accurately simulate peanut drying. Simplifications in programming have rendered it useful in the design of peanut dryers of desired capacity with optimum drying conditions.

PECMAN (Peanut Curing Manager) is a decision support system that assists drying facility managers with inventory control throughout the drying process (Butts and Hall III, 1994). It provides scheduling of sampling and estimation of current moisture content and time remaining on the dryer. It is provided by USDA ARS National Peanut Research Laboratory and is used widely throughout peanut growing regions. The model was created for average atmospheric conditions one would expect during the harvest season. The user enters initial moisture, and the system gives an estimated drying time to reach the ideal moisture content. It has been revised since initial development using equations retrieved from simulations with PNUSTRY. The time remaining on the dryer is calculated by subtracting the elapsed time since the last moisture content sampling from the estimated drying time:

$$T_{remain} = T_D \left(1.95349 \times \frac{MC_k - FMC_k}{IMC_k - FMC_k} - 0.02114 \right) \quad (2.10)$$

where T_D is current day temperature of the ambient air, °C, MC_k is moisture content of peanut kernels in percent wet basis, IMC_k is initial moisture content of peanut kernels, and FMC_k is desired final moisture content of peanut kernels (Butts et al., 2003; Butts et al., 2004).

The change in moisture content is calculated by using the following regression:

$$\Delta mc = -0.0022t^2 + 0.2382t + 0.2497IMC_k - 3.4658 \quad (2.11)$$

where t is the elapsed time on the dryer. Using the change in moisture content, Δmc , the current moisture content is determined by subtracting Δmc from the initial moisture content. Figure 2.1 shows a screen display of the PECMAN decision support system (Butts et al., 2003; Butts et al., 2004).

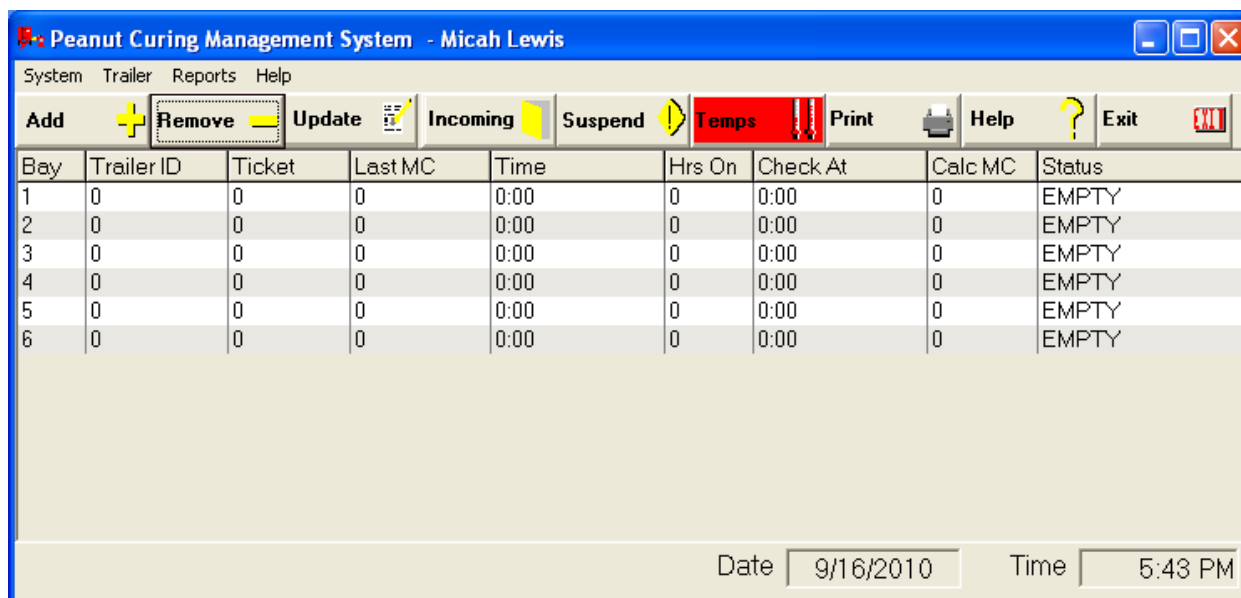


Figure 2.1: PECMAN decision support system for peanut drying

The OptiCure2000© is an agricultural dryer control system, produced by Microtherm¹, Inc., which monitors, controls, manages and logs drying temperature for peanuts (Microtherm Inc, 2000). Microtherm uses electrical engineering and software design to develop specialized products meeting customer specifications. OptiCure2000© blends software and hardware to provide the drying operator with a fully-functional interface and provide automated on/off and temperature control of the dryer(s). It may control up to 192 dryers simultaneously.

Like the previously described support systems and simulation models, OptiCure2000© calculates the estimated total drying time from inputs given by the user. These inputs consist of initial kernel moisture content, target kernel moisture content and atmospheric conditions. Once drying begins, ambient air temperature and relative humidity are monitored in real-time via sensors, and adjustments are made to the set point of the dryer as well as the calculated drying time. This dryer control system has been observed to reduce fuel consumption and yield higher

¹ Mention of company or trade names is for descriptive purposes only and does not imply endorsement by The University of Georgia

quality peanuts. Since the set point of the dryer is automatically adjusted according the ambient atmospheric conditions, a noticeable reduction in fuel consumption is observed. Also, since peanuts are dried consistently with appropriate temperature and monitored efficiently, quality of the peanuts is preserved, increasing the amount the farmer is awarded per ton. Figures 2.2 and 2.3 show screen displays of the control interface for OptiCure2000©.

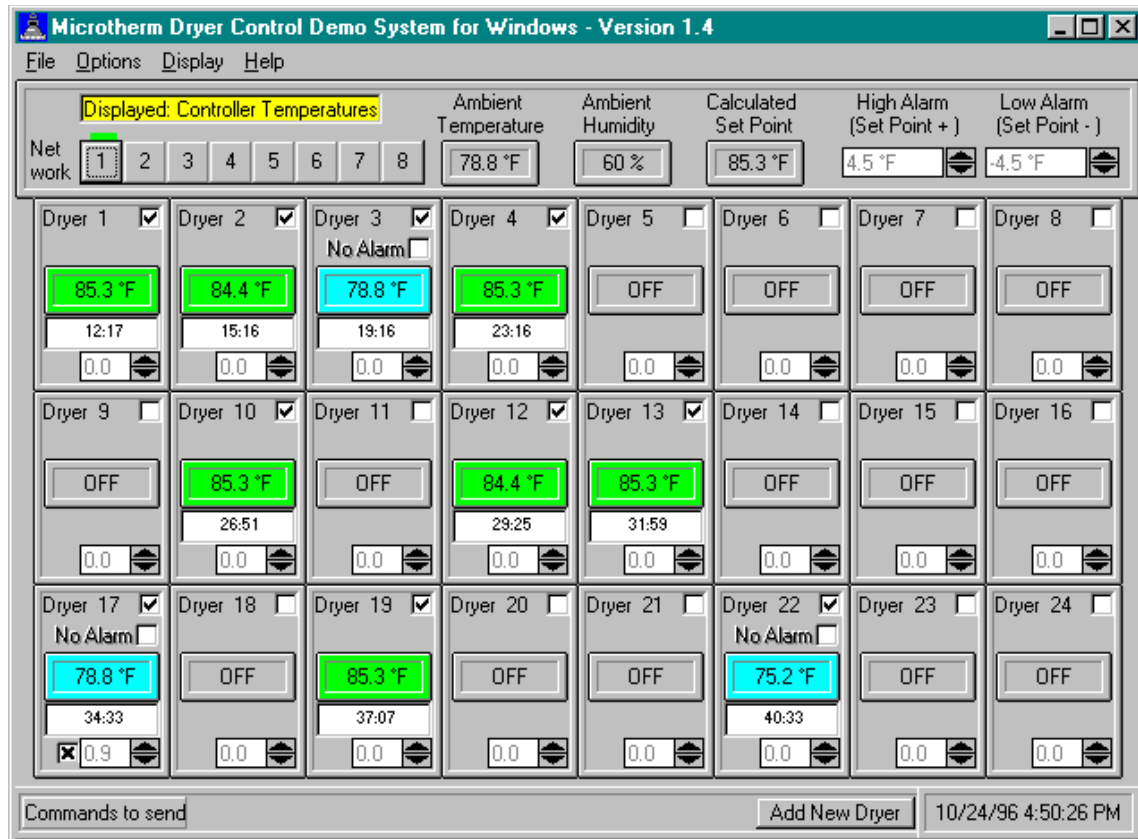


Figure 2.2: Opticure2000© dryer controller software main screen

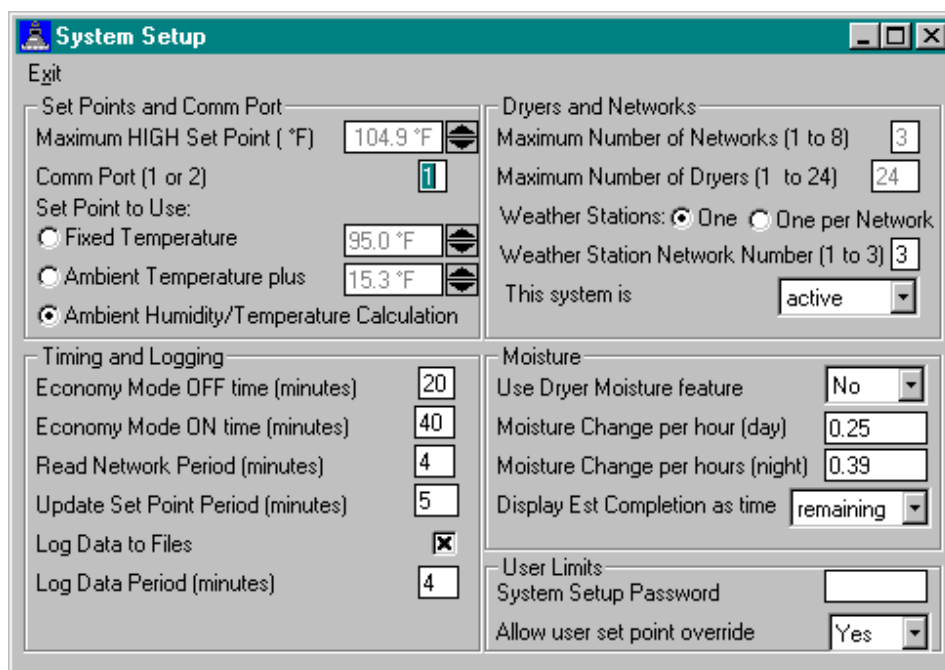


Figure 2.3: Setup window for Opticure2000 dryer controller system

2.2 Related Work

Although most of the peanut grading process has remained unchanged for the last 50 years, there is ongoing research to address problems and enhance certain aspects of the process. This section discusses other published works that address the limitations and inefficiencies in today's peanut drying process.

Much of the published work on innovations in peanut drying discusses the monitoring of weight loss to indirectly observe the change in moisture content of the drying bed of peanuts (Allgood et al., 1995; Allgood et al., 1993; Blankenship and Davidson, 1980; Blankenship and Davidson, 1984). In the prevention of overdrying, Blankenship and Davidson (1980) developed a laboratory-scale method for automatic termination of drying operation using a preset final weight based on the desired kernel moisture content. With this method, a subsample (0.5 to 0.9 kg) was extracted from the sample of peanuts needing to be dried. The subsample was then cleaned of all

foreign material and shelled. Moisture content and dry weight of kernels and hulls were determined by using the reference oven drying method (ASAE, 2002). Then, these properties were used in the calculation of a predicted cutoff weight (PCW) for the original sample. The drying apparatus for the system was on a 20 kg balance beam scale, and once the weight of the drying peanuts reached the PCW setting, a limit switch installed on the scale cut off power to the drying fan (Blankenship and Davidson, 1980).

Tests were performed with samples ranging in initial kernel moisture content from 12.6% to 40.0% wet basis. The average final kernel moisture content for all samples was 10.4% w.b., with a standard deviation of 1.5%. Final sample weights were 0.6% lower than the PCW setting on average. Therefore, it was concluded that the final peanut weight could be calculated with enough accuracy to govern the termination of laboratory dryer operation. The authors noted that the method, if implemented on a larger scale, would prevent overdrying, reduce labor considerably, and preserve sample integrity better than conventional drying methods.

In other published work, the method using a PCW setting was implemented on a larger scale (Blankenship and Davidson, 1984). Blankenship and Davidson tested a similar system for monitoring and automatic cutoff of full-scale peanut drying equipment. In this research, the predicted final weight of the peanuts was determined as in the laboratory-scale experiment. Three load cells were placed under the axles of each peanut drying trailer to monitor the weight during drying. As before, drying was terminated once PCW was reached. Results were similar to those observed in the laboratory-scale experiment, and the authors concluded that the method would be advantageous in reducing the risk of overdrying and maintaining peanut quality. Safety hazards and the time and labor needed to raise the trailers made this approach infeasible for commercial drying facilities (Blankenship and Davidson, 1984).

Further work on determining kernel moisture content by monitoring weight loss of the peanuts is discussed in work by Allgood et al. (1993 and 1995). As in standard procedure, upon arrival to the buying point, a sample was extracted from the peanut trailer to determine initial kernel moisture content. After sample extraction, the trailer was pulled across an electronic platform scale to obtain the rear axle load. Then, the trailer was backed onto a bending beam type weighing platform. Once in place, the drying system was initiated, using the initial kernel moisture content and initial rear axle load as inputs. Drying was terminated once the desired kernel moisture content was reached, as indicated by the weight loss.

Results show that 95 % of trailers tested had predicted moisture contents within 1 % of their actual kernel moisture content determined by grading. This reported accuracy allows the weighing system to be implemented within the dryer process for automated dryer control. The system's in-process determination of moisture content eliminates the need for manual sampling while drying, minimizing required human interaction. Drawbacks of such systems include a finite, undetermined life expectancy of the weighing platforms. Also, the price to install a weighing platform in every stall of a drying bay can be initially expensive (Allgood et al., 1993).

The previous three methods discussed governing the drying process by using weight loss to predict kernel moisture content. Although proven reliable in their predictions, these methods do not provide a sense of how uniform the moisture content is throughout the entire drying trailer. Also, weight loss not related to moisture content can give false predictions as to how dry a sample is, resulting in underdrying. This could occur with the blowing out of loose foreign material as air is forced up through the bed of peanuts.

A controller based on the wet-dry bulb temperature differential is discussed as a means for peanut drying control (Paine, 1969). The controller helps ensure proper drying rate.

Parameters such as temperature and flow rate of the air being blown into the peanuts have a direct effect on drying rate. Peanuts drying at a rate too fast are susceptible to off-flavor and poor milling quality (Beasley and Dickens, 1963; Butts et al., 2004; Paine, 1969). Correct operation of peanut dryers requires a knowledge of the combined effects of temperature, relative humidity, air-flow rates, and drying fronts (Paine, 1969). These phenomena play crucial roles in the establishment of ideal drying zones, conditions favorable for optimal peanut drying rate. The ideal drying zone consists of proper conditions regarding temperature and water vapor in the air used for drying. Wet-bulb and dry-bulb thermometers were used because of their use with the psychometric chart, and together they accurately define the condition of the air.

Tests showed that a 12.5 °F differential between the dry-bulb temperature and the wet-bulb temperature (dry-bulb > wet-bulb) resulted in ideal conditions for optimal drying rate. This differential setting was applied to a peanut dryer by means of a new control system. The new controller minimized manual adjustment normally required by an operator; and therefore, made optimal drying conditions achievable even with operators having minimal skill.

Steele (1982) implemented a microprocessor control system for peanut drying to minimize energy consumption and preserve peanut quality throughout the drying process. Control criteria were established to ensure that the fan and burner were in use only when conditions were most conducive. With the new controls, the fan was only operated for a certain percentage of each hour, and the time off increased one minute every two hours. The burner was powered off if conditions were such that ambient air promoted drying just as well as heated air.

The experiment was repeated for three peanut harvest seasons, and great reductions in energy consumption were observed each year. On average, liquefied petroleum gas consumption was reduced 49%, and electric energy consumption was reduced 39% (Steele, 1982). These

reductions in energy conservation translated into a net saving of \$5.61 per ton or a 25% reduction in total peanut drying costs. At the time of the experiment, \$1500 was spent implementing the system. However, reductions in energy consumption were such that expenditures for the system were regained during the first harvest season.

The final related work discussed deviates from the topic of peanut drying. However, the control system implementation and the scope of the project are highly relative to the research presented in this dissertation. Li et al. (2006) discuss the development of a microwave power control system with temperature feedback to automatically adjust the power supplied to a magnetron based on the temperature of the product . This system was implemented to preserve the quality of final products and reduce burning during the microwave drying process. An infrared (IR) temperature sensor was used to measure the temperature of the product being dried. Power supplied to a magnetron was adjusted according to the differential between the set point temperature and the current temperature of the drying product. The system consisted of a commercial microwave oven, Motorola HC11 microcontroller with keypad, IR temperature sensor, zero-crossing detector to trigger measurement on the falling edge of the AC power source, and a triac control to control the high-voltage transformer for the magnetron.

Results show temperature stability around the set point with a maximum error of ± 1.5 °C. In the reported test of the drying process, carrot cubes initially at 83.10% moisture content were dried at a set temperature of 70 °C. Carrot cubes lost over 85% of their moisture in 180 minutes, and less than 2% of the cubes had any burn damage (Li et al., 2006). Less deterioration in surface color of carrot cubes was observed for the feedback controlled system compared to other microwave drying systems.

2.3 Literature Review Wrap Up

All related work examples, except for the last one, show that research has been carried out to rectify problems identified in peanut drying for at least the last four to five decades. While many of the methods showed promise, underlying factors have hindered their adoption as commercially available innovations for the peanut drying process. At present, the peanut grading process is still a labor-intensive task, having little small change since initialization. One factor missing from the existing techniques used in drying, as well as related tasks, is nondestructive, in-shell kernel moisture content determination.

The kernel moisture content is the main parameter of interest in the drying process, and it is the only parameter, besides temperature, that the drying system is working to control. However, since it is difficult to obtain, control for it is often indirect and misguided. Therefore, providing a simple, in-process, accurate method for determination of kernel moisture content while drying would significantly reduce troubles faced presently with drying. For this reason, this dissertation discussed the implementation of a system to govern peanut drying in which the kernel moisture content is measured accurately in real-time. The following chapters discuss the components that make up the system and the functionality of the system as a whole.

CHAPTER 3

SOLUTION APPROACH

As the current peanut drying process was assessed and a solution was approached, the following limitations were apparent:

- kernel moisture content is sampled manually, and the frequency with which it is sampled can determine the efficiency with which the peanuts are dried
- atmospheric conditions affect the drying process (ambient temperature and relative humidity)
- peanuts dried with air temperature > 95 °F are susceptible to off-flavor development and degradation in milling quality
- peanuts dried with air having a relative humidity $> 85\%$ are actually being further moistened
- air blown into peanuts should be no greater than 15 °F above the ambient temperature.

With these limitations in mind, the research process was designed such that each limitation was addressed specifically. The first noted limitation, determination of kernel moisture content, was the most important focal point of the research. A means of monitoring the kernel moisture content in real-time would greatly reduce the high demand for human interaction and minimize occurrences of overdrying and underdrying. The other limitations had been addressed frequently in related work and, therefore, needed no major innovations; just efficient implementation to facilitate conditions specified.

3.1 Research Objectives

With the realization of the importance for a nondestructive, real-time method for kernel moisture content determination and a sensor network to facilitate the control of drying parameters, the following research objectives were devised:

- Show feasibility of using dielectric properties to determine moisture content in unshelled and shelled peanuts
- Show feasibility of relating dielectric properties of unshelled peanuts (peanut pods) to moisture content of shelled peanuts (peanut kernels)
- Investigate the effects of peanut type on dielectric properties, and the influence on moisture content determination
- Develop quarter-scale simulation of peanut drying system
- Use microwave moisture meter for in-shell determination of kernel moisture content in small-scale drying system
- Integrate sensor network and feedback control to facilitate drying process within specified conditions.

The first two objectives were not performed initially in this research. The use of dielectric properties to determine moisture content in peanuts as well as cereal grain and oilseed has been shown (Kraszewski and Kulinski, 1976; Nelson and Trabelsi, 2004; Nelson et al., 1998; Trabelsi et al., 1999b; Trabelsi and Nelson, 2004b; Trabelsi and Nelson, 2006a). However, because of their importance, they were included to provide a foundation for the use of the microwave moisture meter, which is discussed in detail in chapter six.

3.2 System Design

To provide a methodical approach to the research, a system design was devised to define the scope of the system and illustrate the functions of each component. The system consists of four major components: the sensor network, data acquisition unit, microcontroller unit, and display. Figure 3.1 shows how the four components interact within the system as data flow between them. As data are retrieved from the sensor network, they enter the data acquisition unit as analog data. They exit as digital data and enter the microcontroller unit where they are converted to float values representing the appropriate measured parameter. The data are then assessed and compared against stored conditions and criteria within the microcontroller unit. From those comparisons, decisions are made, and the appropriate control action is relayed to the dryer unit.

The sensor network consists of three temperature sensors, a relative humidity sensor, and a microwave moisture meter to determine kernel moisture content. The sensors are monitored continuously. The temperature sensors are used to measure the ambient air temperature, the temperature of the inlet to the drying trailer, and the peanut bed temperature at the location where the microwave meter is applied. The sensor network is discussed in more detail in chapters ten and eleven.

The data acquisition unit is responsible for acquiring the data from the sensors and converting the values from analog to digital. The data acquisition unit uses an analog-to-digital converter (ADC) for data conversion. The ADC converts an input analog voltage into a digital number that is proportional to the magnitude of the analog voltage. Data acquisition is discussed further within chapter ten in section two.

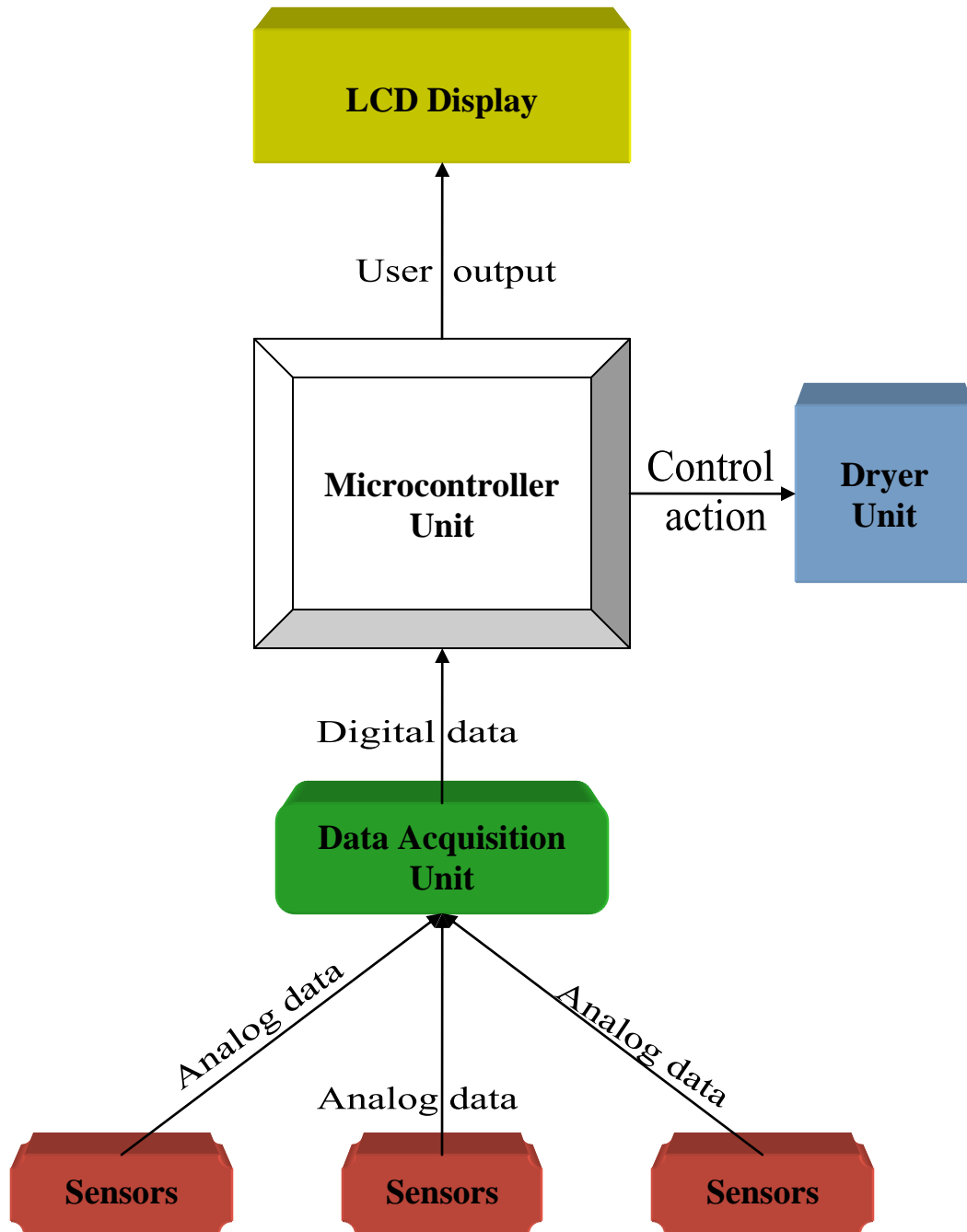


Figure 3.1: Complete system diagram and data flow

The microcontroller unit calculates the measured parameters from the data retrieved from the sensors. Then, it uses stored conditions based on the limitations discussed in section 3.1 to increase the temperature of the drying air, decrease the temperature of the drying air, or

terminate the drying process. It also sends the calculated kernel moisture content to the liquid-crystal display (LCD) for real-time monitoring by the user. The microcontroller unit is discussed in more detail in chapters seven and ten.

The four components work together to provide data acquisition, feedback control and real-time monitoring. The feedback control governs the temperature of the air blown into the peanuts. The microwave moisture meter provides determination of kernel moisture content such that it can be monitored continuously, in real-time.

CHAPTER 4

PEANUT DRYING: SCALED DOWN

4.1 Current Drying System

The drying process is required for peanuts to be lowered to a moisture content that meets storage and production regulations. When peanuts are brought to the buying point, they could have a kernel moisture content as high as 20% w.b (Beasley and Dickens, 1963; Butts et al., 2008). It is the responsibility of the buying point to properly dry the peanuts down to a kernel moisture content between 7% and 10% (Butts et al., 2004). Any lot of peanuts having kernel moisture content above 10.49% will be labeled as “NO SALE” during grading and will have to be dried further.

After peanuts are allowed to stay in windrows to dry naturally, they are harvested using combines. Peanut drying trailers are brought to the peanut fields from the various buying points. The peanuts are then loaded into the drying trailers and transported to the nearest buying point using a slow moving vehicle if trailer is of wagon-scale type. The trailers of semi-type are transported by truck. Such trailers can be transported longer distances than those of the wagon-type. Figure 4.1 shows wagon-type peanut drying trailers loaded with peanuts. These wagons are 6.4 m long, 2.4 m wide, and 1.5 m deep above the air plenum. The depth of the air plenum is 23 cm (Butts and Williams, 2004).

When a specific lot of peanuts arrives at a buying point, it is processed in and given an identification number so that the peanuts may be accounted for at all times during the grading process. Then a sample is extracted for determination of kernel moisture content. The operator

manually extracts the sample and then prepares the sample for measurement. Sample preparation includes cleaning of the sample with a foreign material extractor and shelling the sample with a rub board type sheller. After the sample is prepared, the peanut kernels are measured with an official moisture meter; either the GAC manufactured by DICKEY-john® or the Steinlite Model PT-2 moisture meter. Both meters require that the sample be shelled to measure kernel moisture content. They also require a separate calibration for each peanut type. Both meters are shown in Figure 4.2.



Figure 4.1: Wagon-type peanut drying trailers loaded with peanuts

After the initial kernel moisture content of the peanuts is determined, it along with atmospheric conditions such as relative humidity and temperature are used to estimate drying time (Butts et al., 2003; Butts et al., 2004; Butts and Hall, 1994). When a stall is available, the peanuts are taken to the drying bay where the peanut trailers are connected to forced-air, axial-flow dryers powered by propane or natural gas. The dryers are usually 76 cm in diameter and run

at 1750 rpm. Two common manufacturers are BlueLine Dryers and Peerless Manufacturing Company. A canvas duct with a wooden frame at the end is inserted into the plenum inlet at the rear of the trailer, Figure 4.3. Air is blown into the plenum, and as the plenum pressurizes, heated air is forced up through the peanuts (Butts and Williams, 2004). The specifications for the perforated floor are provided by the Industrial Perforators Association. The holes can be drilled to provide 23% and 40% open area. To make 40% open area, 3.17 mm holes are drilled on 4.76 mm staggered centers (Butts and Williams, 2004).



Figure 4.2: Official moisture meters for peanut grading; GAC shown left, PT-2 shown right

The dryers are equipped with thermostats, and the temperature of the air blown into the peanuts is regulated using the gas valve pressure. The air is regulated to maintain operation within specified control criteria discussed in chapter eleven, section two.

4.2 Quarter-scale Drying System

In the design of experimentation, a small-scale drying system was needed to start initial tests and perform what would be considered as a proof of principle investigation. A quarter-scale drying trailer was decided upon because of its manageable size and credible representation of the

large-scale peanut drying trailer. All aspect ratios present in the original peanut drying trailer were preserved in the implementation of the small-scale trailer. The quarter-scale trailer measured 1.5 m long, 0.563 m wide, and 0.297 m deep above the air plenum. The plenum was 0.054 m deep. The total volume of the trailer above the plenum was 0.251 m³. Table 11.1 provides dimensions for the other trailer sizes considered. A schematic diagram of the quarter-scale trailer is shown in Figure 4.4, and the actual trailer is shown in Figure 4.5.



Figure 4.3: Peanut drying trailer connected to BlueLine dryer

The trailer was constructed so that no metallic parts would be above the air plenum. A wooden frame was built around the upper perimeter of the drying trailer, and the sides were made of 0.75" thick polystyrene sheathing.

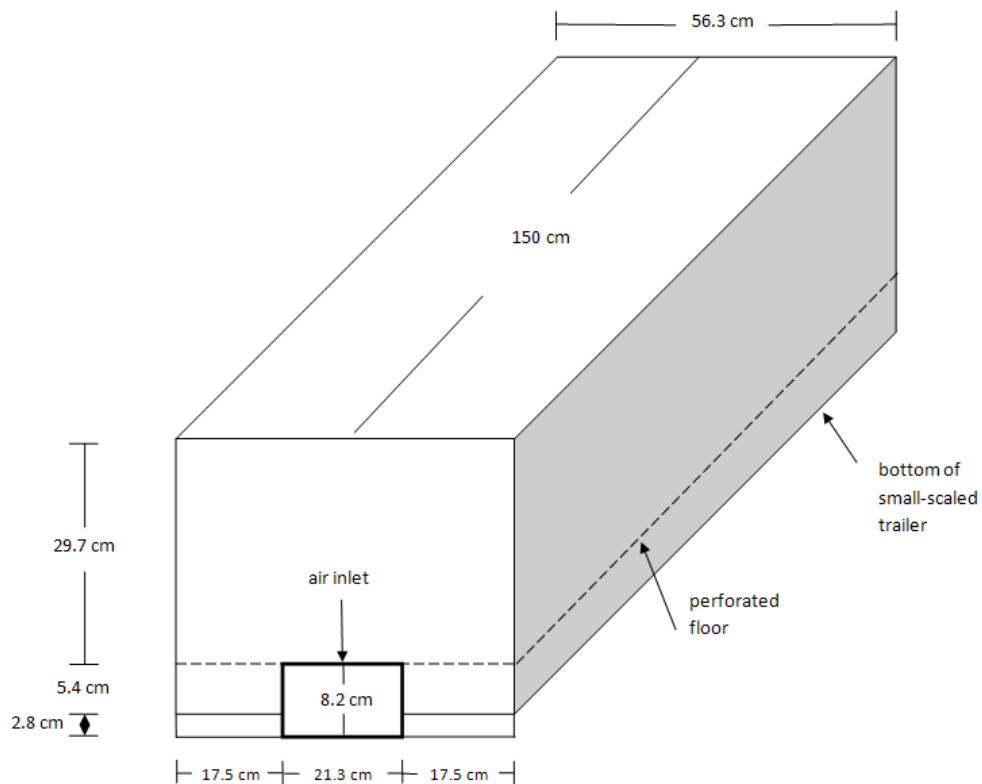


Figure 4.4: Schematic diagram of quarter-scale peanut drying trailer

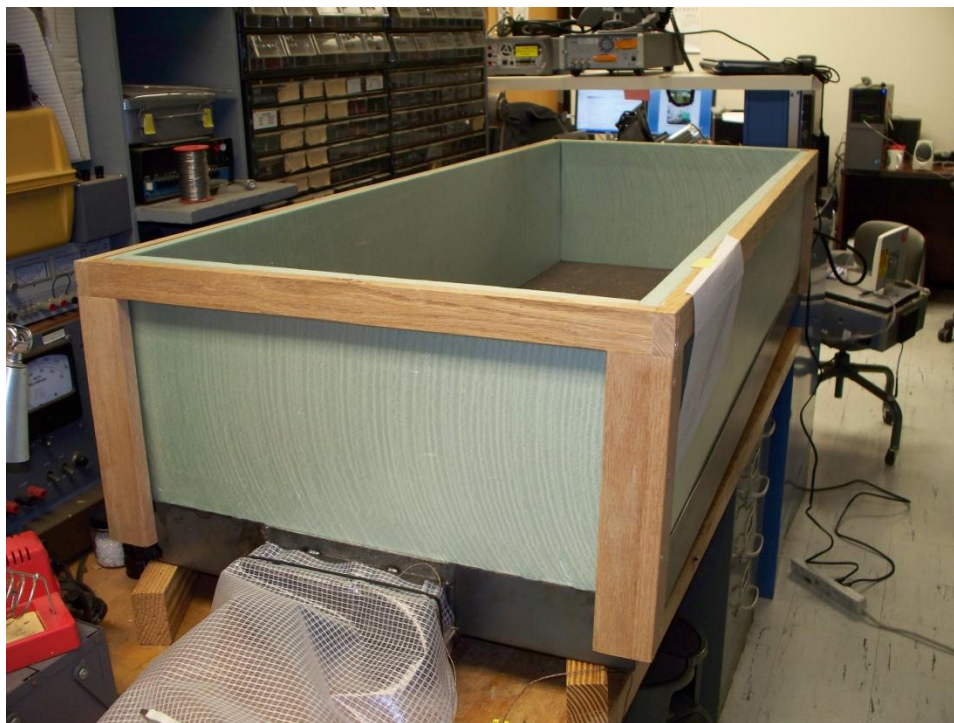


Figure 4.5: Quarter-scale peanut drying trailer

This material was selected for the sides because of the versatility it allows in installing the microwave moisture meter. The dielectric constant of the polystyrene sheathing is close to that of air; therefore, the sheathing does not affect the measurements. The dielectric constant of the sheathing is 1.03, and the dielectric constant of air is 1.0006. If necessary, measurements could be taken such that one antenna was on the outside of the trailer. Figures 6.3 and 6.4 show that the sample holder used for laboratory experiments was also made of polystyrene sheathing.

Selection of the appropriate dryer was just as important as choosing the appropriate dimensions for the drying trailer. At buying points, axial-flow dryers are used in the creation of forced-air drying. The air passes through the fan in a direction that is parallel to the fan axis (Hall, 1957; Loewer et al., 1994). Vane-axial-flow fans have guide vanes upstream or downstream from the fan impellor. These vanes reduce turbulence and improve fan performance. Such fans are advantageous for deep-bed drying.

However, when looking for a dryer to include in the small-scale system, most of the dryers were of the centrifugal-blower type. Centrifugal dryers have a blower wheel located at the center of a spiral housing with air moving blades along the outer edge (Hall, 1957; Loewer et al., 1994). As the blower wheel turns, centrifugal force causes the pressure to drop at the center of the blower wheel, and the pressure rises in the spiral housing outside the blower wheel. This causes air to flow axially into the center of the blower wheel and then out radially through the impeller blades (Loewer et al., 1994).

Therefore, a centrifugal dryer was chosen for this research, the ChallengeAir 560 advance cage dryer manufactured by Double K industries. It was one of few small-scale dryers that included heating elements for provision of heated air. Original controls on the dryer were two fan speeds, three heat settings, and a 60-minute timer. The block diagram for the electrical circuits of

the dryer was used to modify the dryer so that it could be controlled automatically through software and hardware modifications, Figure 4.6.

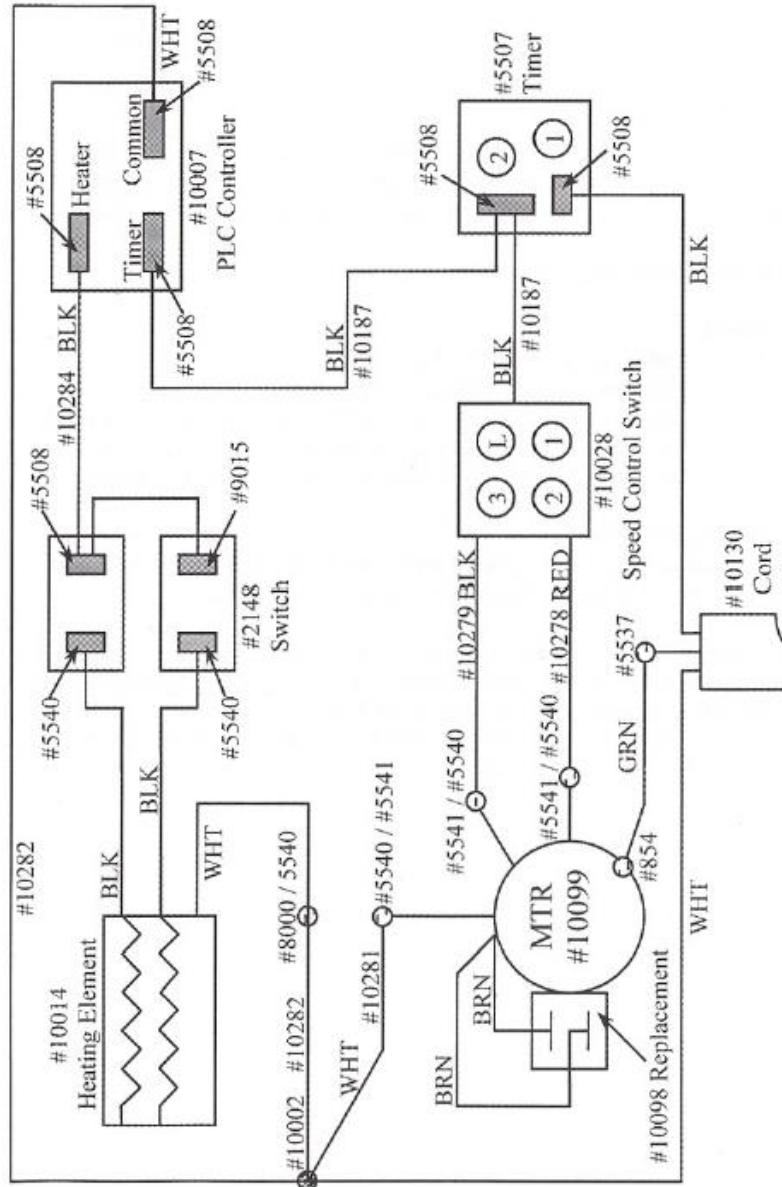


Figure 4.6: Block diagram for electrical circuits in ChallengeAir 560 dryer

Figure 4.7 shows the unmodified controls within the dryer, and Figure 4.8 shows the controls after being modified.

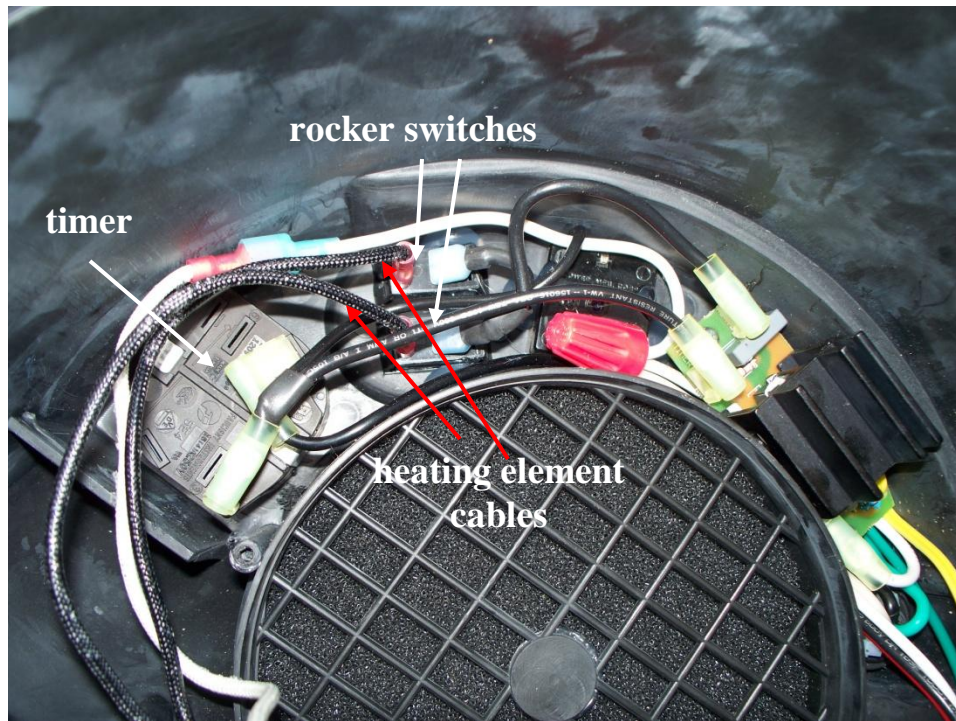


Figure 4.7: Original controls in ChallengeAir 560 dryer

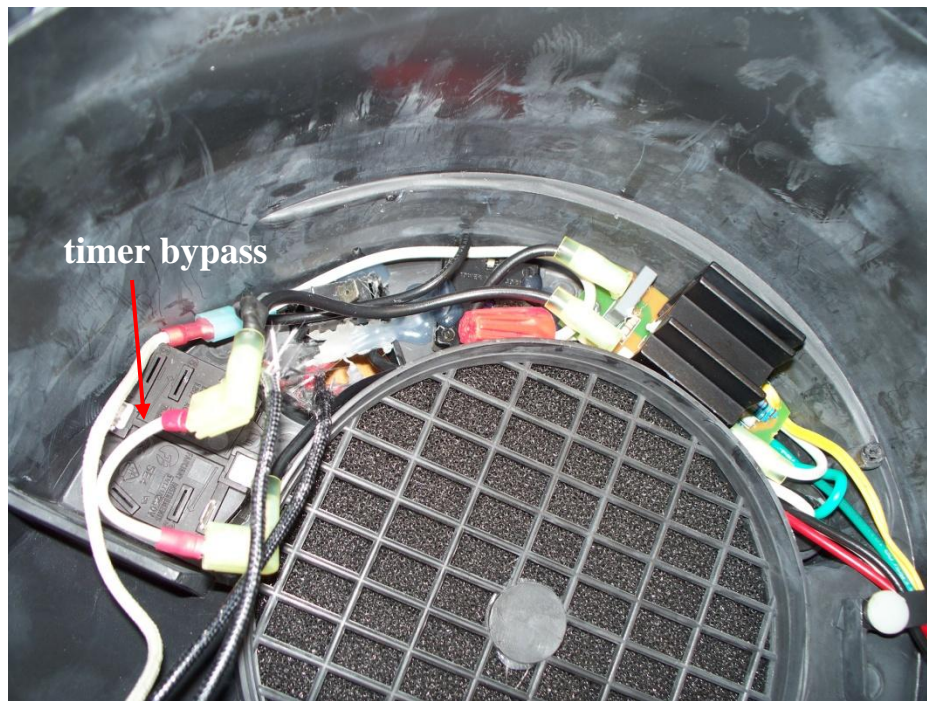


Figure 4.8: ChallengeAir 560 with modified controls

The 60-minute, rotary timer was bypassed as shown in Figure 4.8. The heating element cables were disconnected from the rocker switches and were connected to solid-state relays that would be used to power the appropriate heating elements when given a control voltage, Figure 4.9.

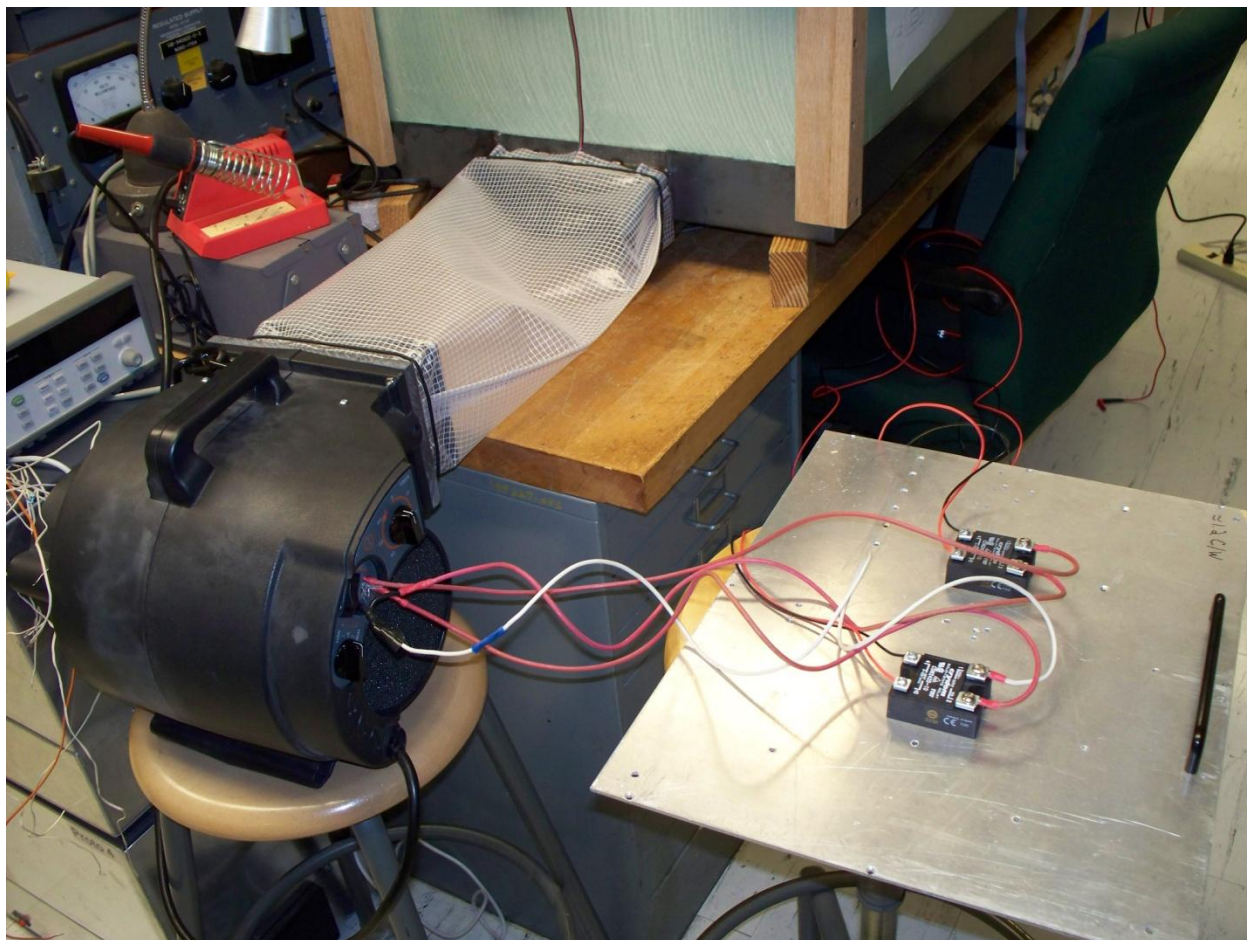


Figure 4.9: Dryer shown connected to solid-state relays for automated control

The aluminum sheet the solid-state relays are fastened to serves as a heat sink with heat dissipation at ≈ 1.2 C/W. The aluminum sheet is 1/8 in. thick and measures 17.5" x 14". The dryer is connected to the drying trailer by a 48 cm long vinyl duct. Aeration requirements were within desired specifications given by the peanut industry and are discussed further in chapter eleven, section two along with specifications for dryer operation.

CHAPTER 5

FEEDBACK CONTROL SYSTEMS

Feedback control was implemented in this system to keep the temperature of the air blown into the peanuts regulated according to given specifications. The temperature of the air at the inlet to the drying trailer is monitored continuously with a temperature sensor. At any given time, dryer control settings are adjusted automatically according to the difference between the current temperature at the inlet and the target temperature. The following sections of this chapter discuss the aspects of feedback controllers and provide a rationale as to why a feedback controller was chosen as a mechanism for temperature regulation.

5.1 Feedback Control System Background

A system has been defined as an arrangement, set, or collection of things connected or related in such a manner as to form an entirety or whole; and an arrangement of physical components connected or related in such a manner as to form and/or act as an entire unit (Distefano, 1990). A control system is defined as an arrangement of physical components connected or related in such a manner as to command, direct, or regulate itself or another system (Distefano, 1990). Control systems receive an input and produce some sort of output. The input is the stimulus, excitation or command applied to the control system, typically from an external energy source. The output is the response obtained from the control system, and it may be directly or indirectly related to the input (Distefano, 1990). Control systems are generally grouped into two categories: open-loop and closed-loop. Open-loop control systems are those in which the control action is independent of the output; however, in closed-loop control systems,

the control action exhibits dependency on the output (Nise, 2008). Closed-loop control systems are commonly referred to as feedback control systems due to the output being “fed back” as input to help govern the control action.

Distefano et al. (1990) defines feedback as the property of a closed-loop system that permits the output (or some other controlled variable) to be compared with the input to the system so that the appropriate control action may be formed as some function of the output and input. Thus, a feedback control system monitors a process continuously and influences the process in such a manner that one or more of its parameters stay within a prescribed range (Haidekker, 2011). The controlled variable or output is monitored and continuously compared with the desired variable or setpoint. The difference between the output and setpoint, known as the control deviation, is analyzed to facilitate the determination of the appropriate control action. The control action is required to drive the output variable to the established setpoint.

Figure 5.1 shows a block diagram for a closed-loop feedback system.

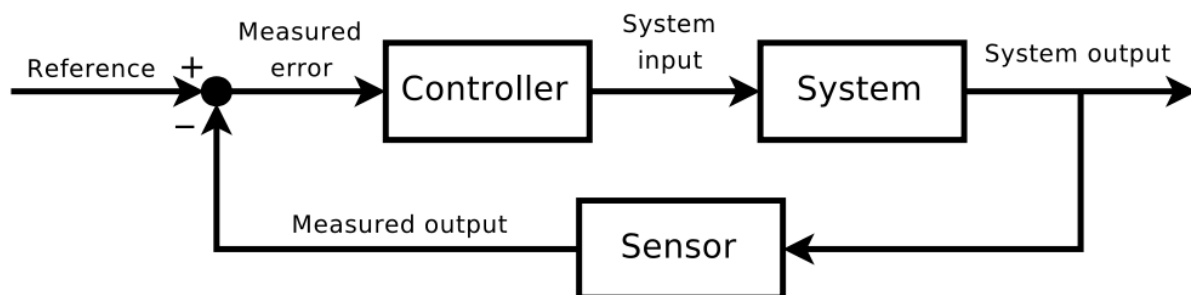


Figure 5.1: Block diagram of closed-loop feedback system

A feedback control system consists of the components shown in the block diagram in Figure 5.1, with varying terminology in some instances. The reference, or setpoint, determines the operating point of the system. It is expressed in the same units as the sensor and can be constant or

variable. The controller measures the control deviation and determines an appropriate control action. The control deviation is the difference between the setpoint and the measured output from the sensor. The controller can be classified as PID type, consisting of some type of proportional, integral and derivative error calculation. The proportional term depends on the present error, the integral term depends on the accumulation of past errors, and the derivative term is a prediction of future errors (Distefano et al., 1990; Haidekker, 2011; Nise, 2008). The system, also referred to as the process, provides a means of influencing the controlled variable (Haidekker, 2011). The sensor provides continuous measurements of the controlled variable, or system output, and converts the output to a signal which can be differentiated by the controller.

When assessing a PID controller, the equation including all terms is as follows:

$$u(t) = k_p e(t) + k_i \int_0^t e(t) dt + k_d \frac{d}{dt} e(t) \quad (5.1)$$

where $u(t)$ is the controller output, e is the error or control deviation, t is instantaneous time, k_p is proportional gain, k_i is integral gain and k_d is derivative gain. These gain parameters have to be tuned for optimal response within the system.

5.2 Feedback Control System: Closed-Loop Regulation

In this system, the setpoint, or reference, is the temperature of the ambient air in degrees Fahrenheit plus 15 °F. Therefore, the setpoint is variable and will fluctuate throughout the entire peanut drying process. The microcontroller serves as our controller. However, control is not like that of a pure, linear feedback system. Because of several control criteria in place, control will be mostly algorithmic. The process, or system, is the dryer and the air inlet to the drying trailer. The inlet air is controlled such that its temperature never exceeds the setpoint. The sensor is an LM35 temperature sensor that outputs a voltage relative to the current temperature with a relationship of 10 mV/ °C.

The block diagram for the air inlet is shown in Figure 5.2. This reflects the open-loop control of the system, in which a constant power is supplied, and the process heats until the energy supplied is equal to the energy lost to the environment. Figures 5.3 and 5.4 show the temperature response of the dryer at different heat settings with open-loop control at low and high fan speeds, respectively. Each plot in the graphs of Figures 5.3 and 5.4 shows how the temperature of the inlet air approaches the equilibrium temperature, which is different for each heat setting.

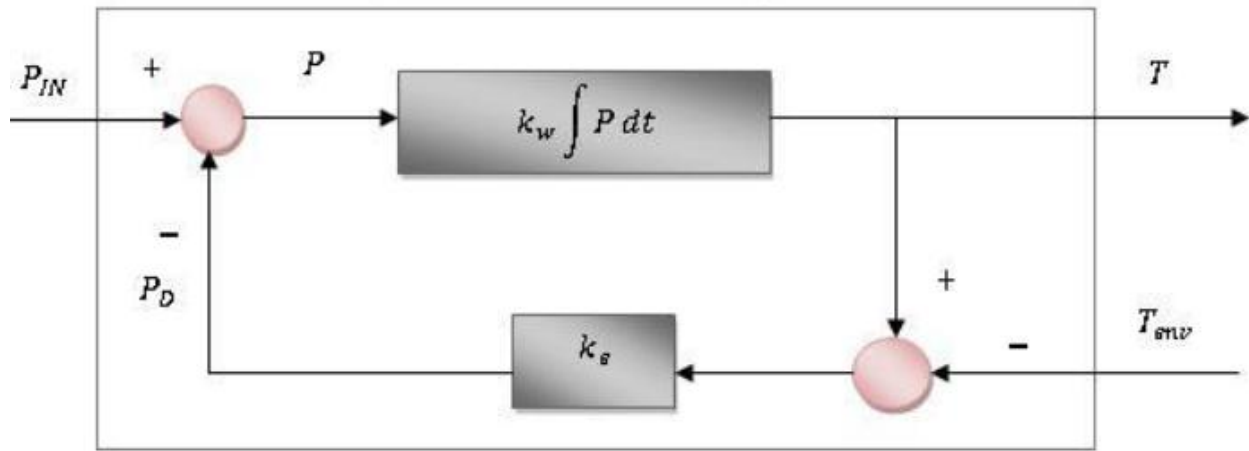


Figure 5.2: Block diagram for open-loop air inlet process

In Figure 5.2, P_{IN} is the power supplied to the system (power supplied to heating elements, more specifically), P is the heating power, k_e and k_w are process constants representing thermal conductivity and resistance properties, T is the temperature of the inlet air, T_{env} is the ambient air temperature, and P_D is the power lost to the environment. The temperature at a certain time once the constant input power P_{IN} is applied is defined as follows:

$$T(t) = T_{env} + \frac{P_{IN}}{k_e} (1 - e^{-k_w k_e t}) \quad (5.2)$$

The constant k_e can be determined by using the equilibrium temperature as follows:

$$k_e = \frac{T(t \rightarrow \infty) - T_{env}}{P_{IN}} \quad (5.3)$$

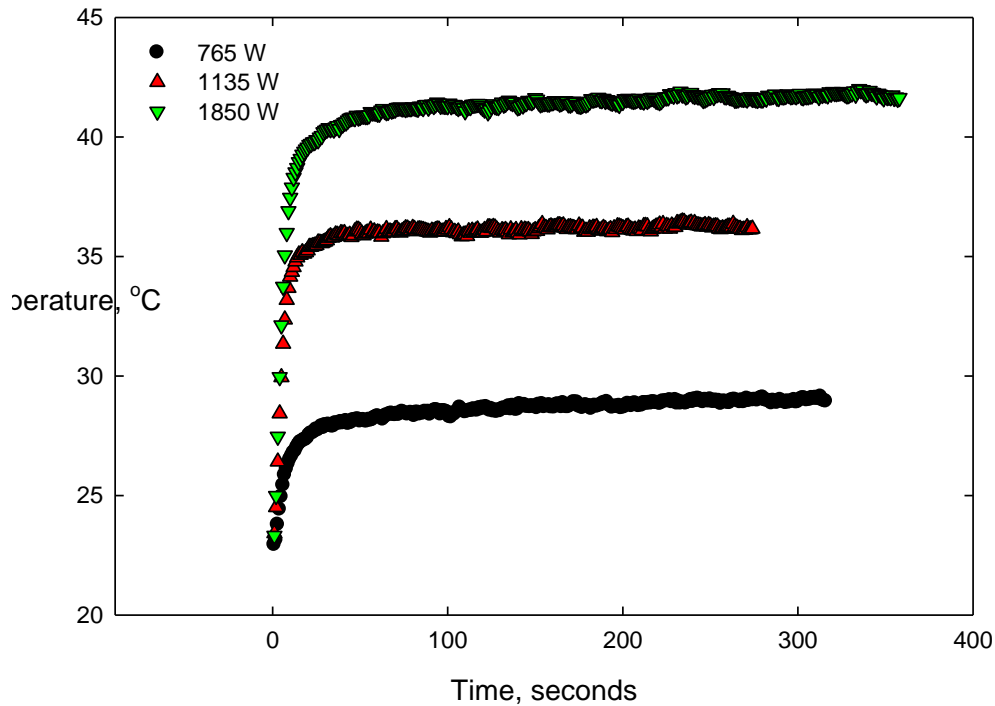


Figure 5.3: Dryer response at low fan speed

The various coefficients and constants were calculated for each fan setting, and are shown in Tables 5.1 and 5.2. The low fan setting was chosen because air velocity and flow rate were sufficient with regard to specifications given by the peanut industry. The time coefficient, τ , represents the time it takes for temperature of the process to rise 63% of the total rise to the equilibrium temperature. The coefficients in Table 5.1 show the time response and equilibrium temperatures for the three power settings at low fan speed. These values were useful in the control scheme for the dryer. The appropriate heater setting was selected by comparing the

setpoint with the equilibrium temperature for each heater setting. Heat settings were selected only if their observed equilibrium temperature was greater than the setpoint for that instance.

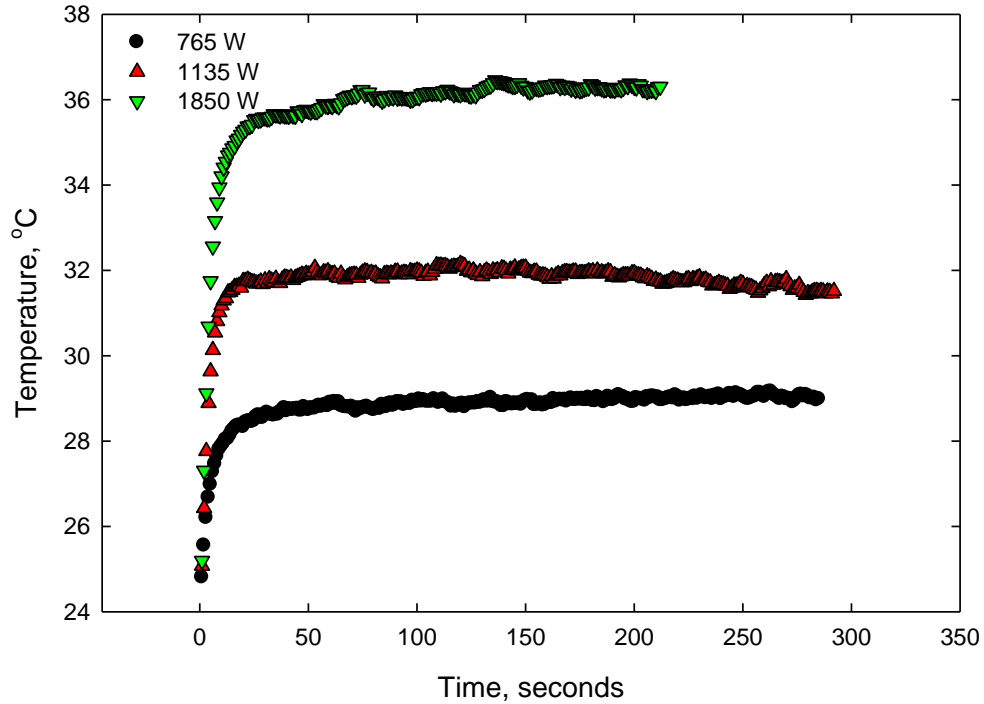


Figure 5.4: Dryer response at high fan speed

Table 5.1: Data for open-loop coefficients and constants at low fan speed

Term	Power Setting		
	765 W	1135 W	1850 W
τ , seconds	11.5	6	6.7
T_{env} , °C	22.7	22.7	22.7
$T(t \rightarrow \infty)$, °C	29	36	41.5
k_w , K/J	0.000451	0.00123	0.000955
k_e , W/K	0.00824	0.0117	0.0102
$T(t \rightarrow \infty) - T_{env}$, °C	6.3	13.3	18.8
T at τ , °C	26.67	31.08	34.54

Table 5.2: Data for open-loop coefficients and constants at high fan speed

Term	Power Setting		
	765 W	1135 W	1850 W
τ , seconds	4	3.8	4.5
T_{env} , °C	22.7	22.7	22.7
$T(t \rightarrow \infty)$, °C	29	31.7	36.3
k_w , K/J	0.00130	0.00131	0.00735
k_e , W/K	0.00824	0.00793	0.00735
$T(t \rightarrow \infty) - T_{env}$, °C	6.3	9	13.6
T at τ , °C	26.67	28.37	31.27

Although the process, or system, was defined as the plenum inlet and dryer, the bed of peanuts served as a virtual process component. Originally, the bed of peanuts was defined as the process; however, temperature gradients with bed depth made this task cumbersome. Therefore, the assumption was made that if the temperature of the air being blown into the peanuts does not exceed 15 °F above the ambient air temperature, the temperature of the bed of peanuts will not exceed 15 °F more than the ambient air temperature. To observe the heating of the peanut bed when heated air was blown into it, the dryer was set to operate with open-loop control at low fan and high heat settings. Figure 5.5 shows the resultant graph. The temperature of the inlet air is shown in comparison with the temperature distribution throughout the bed of peanuts. The seven asymptotic lines, appearing after 1000 seconds, reflect a built-in safety feature in which the heating elements are disengaged when the temperature exceeds 44.36 °C. Figure 5.5 shows that there is substantial hysteresis between the heating of the inlet air and the bed of peanuts. We also observe that the rate of heating of the peanut bed was not affected by the brief interrupts in heat caused by the safety feature.

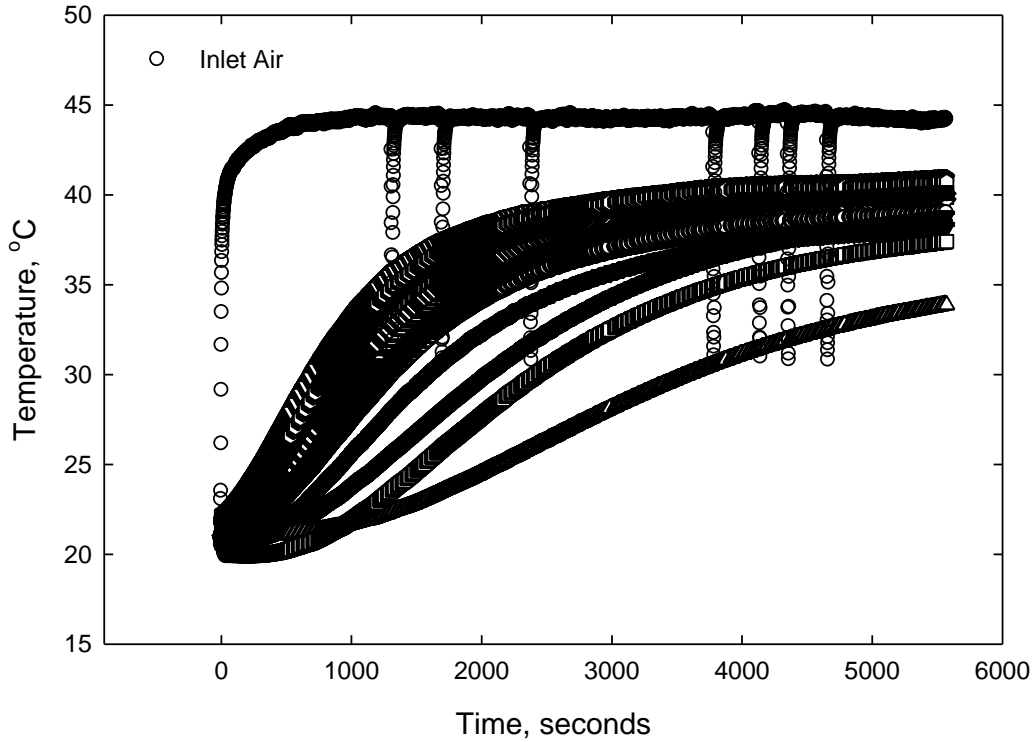


Figure 5.5: Open-loop control and temperature distribution throughout bed of peanuts

To implement closed-loop control, a controller and sensor were added to the block diagram of the process, Figure 5.6 (Haidekker, 2011). A P-controller was used, and the proportional gain is represented by k_p . The gain for the sensor, k_s is 10 mV/ °C or 0.010 V/ °C. The output of the sensor block is in volts, U_{temp} . For example, 23 °C is output as 0.23 V. Therefore, the setpoint is also defined in voltage, U_{set} , rather than degrees Celsius. This enables the calculation of the control deviation between setpoint and sensor output at the summation point. To determine temperature at a certain time with closed-loop control implemented, Equation 5.2 is redefined as:

$$T(t) = T_{env} + \left(\frac{k_p}{k_e + k_p k_s} U_{set} - \frac{k_p k_s}{k_e + k_p k_s} T_{env} \right) \left(1 - e^{-\frac{t}{\tau}} \right) \quad (5.4)$$

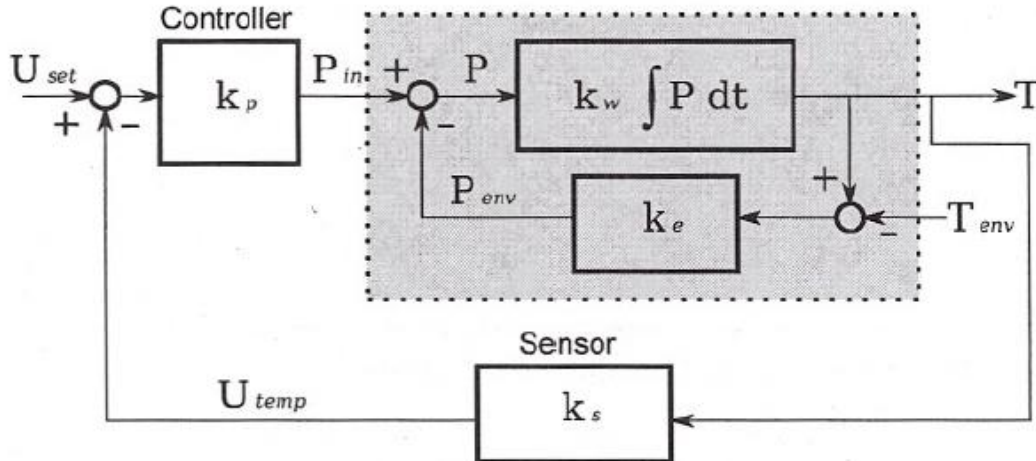


Figure 5.6: Block diagram for closed-loop control of inlet air temperature shown with P-controller

Equation 5.4 and the corresponding block diagram shown in Figure 5.6 are most applicable to a linear feedback controller. Control criteria, discussed in chapter three, set in place by the peanut industry to regulate the peanut drying process limit the linear behavior of the feedback controller used in this research. Therefore, the feedback controller is more algorithmic. Since constant power applied to a heating element results in saturation at an equilibrium temperature when $t \rightarrow \infty$, pulse width modulation (PWM) was used to vary the power. With pulse width modulation, a duty cycle is determined in which the power is turned on for a certain percentage of the time cycle. The P-controller is used in a “unity” gain setting, meaning k_p is equal to one. Therefore, referring to equation 5.1, the controller output is driven solely by the control deviation. The duty cycle is determined by the size of the control deviation; and this is after the appropriate heater setting has been selected based on open-loop evaluation previously discussed. Feedback control used within this system resembles two-point control; however, two-point control systems are nonlinear (Haidekker, 2011). The linear aspect of the feedback

controller is used in the open-loop analysis and P-controller application. Figure 5.7 shows an example of the feedback control used in this system. The pulsation caused by the pulse width modulation is reflected by the plot for the inlet air. The other plots reflect temperature distribution throughout the bed of peanuts. Therefore, feedback control was implemented successfully within the system. Control criteria were maintained throughout operation.

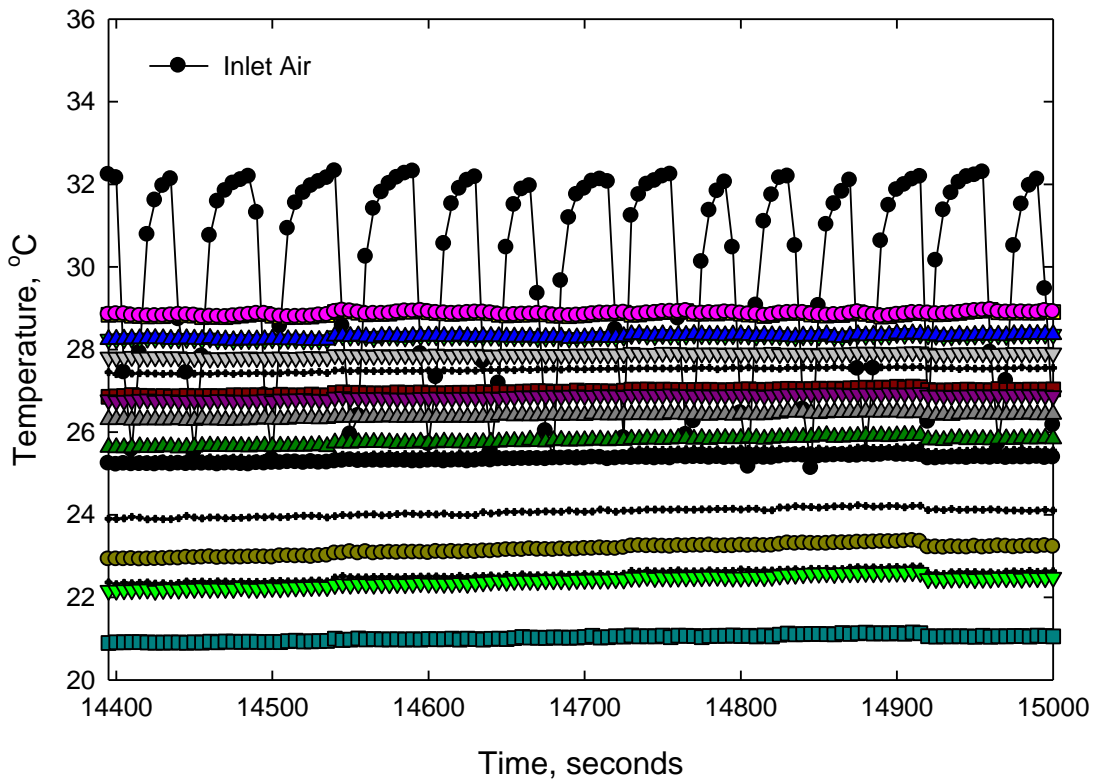


Figure 5.7: Temperature of inlet air shown in comparison with temperature distribution throughout bed of peanuts

CHAPTER 6

MICROWAVE MOISTURE SENSING

The most important input to the controller to govern the duration of the drying process is the kernel moisture content. This parameter also accounts for 20% of the final grade that peanuts receive. In the present grading process, samples of peanuts have to be extracted for kernel moisture content determination. When drying, this involves manually removing samples from the trailer, cleaning the samples, shelling the samples, and then proceeding with the kernel moisture content determination. Therefore, a nondestructive method for kernel moisture content determination is imperative for this application.

6.1 Nondestructive Testing

Nondestructive testing is so attractive because of its potential to automate control analyses, reduce analytical costs, improve processing, minimize human labor, and increase product quality to meet standards and regulations as well as customer satisfaction (Irudayaraj and Reh, 2008). Implementation of nondestructive testing is more feasible now than in earlier years because of improvements in technology and price reductions in certain components.

When nondestructive testing equipment is applied in process control, its use is either direct (online) or indirect (off-line). Online implementations can be broken down into either direct or bypass measurements. In direct measurements, the process is not affected by the testing equipment, and the product flows normally through the process line. However, in bypass measurements, the equipment is placed in a bypass loop where the product is redirected in order to perform the measurement. This is necessary in applications where it is not feasible to use the

instrument within the existing process line. The alternatives to online analysis are off-line, at-line, or near-line; all three of which involve a sampling procedure from the process line to the instrument. At-line and near-line analyses allow for adaptation to the process conditions without actually being in the process. The equipment is well defined for the application and remains on site for tests when needed. Off-line analysis is usually done with standard laboratory equipment and requires sampling and transport of the product (Irudayaraj and Reh, 2008). Such sampling injects a risk of error, in the quality of the analytical result and in the products undergoing physical modifications before being measured.

Presently, the determination of kernel moisture content during peanut drying is determined with off-line analysis, in a destructive manner. Peanuts sampled for kernel moisture content determination are usually discarded. In the application described in this dissertation, the moisture sensor was implemented directly within the drying trailer. Therefore, the implementation was online, and the measurements were direct, resulting in no effect on the existing process.

6.2 Indirect Methods from Reference Methods

Direct or primary methods measure the property of interest of a sample. These methods are used as reference methods because of their accuracy and acceptance as standards in the research realm. The drawback with primary methods is that they may be complicated and time consuming. Also they sometimes require expensive and sophisticated instruments and experienced personnel. These drawbacks decrease the feasibility of implementing primary methods in production lines or other real-life applications (Irudayaraj and Reh, 2008).

To avoid such drawbacks, other methods are used to quantify the property of interest of a sample utilizing a simpler implementation. These methods are referred to as indirect or

secondary methods because they do not necessarily measure the property of interest. Instead, they measure an entity that has a dependence on the extent of the property of interest. These methods usually work with simpler and less expensive equipment and are easier to implement and carry out. Another usual benefit from indirect methods is time gain in analysis (Irudayaraj and Reh, 2008).

Since the indirect method does not measure the property of interest, it needs a correlation between the entity it measures and that property. In this process, the property of interest of a sample is measured first using a direct method. This will serve as the reference, and the resulting values are referred to as “true” values. Then, samples with known properties are measured with the indirect method. The values obtained here are then related to the true values. The indirect and true values are plotted to yield a regression curve; this is the line of calibration (Irudayaraj and Reh, 2008). After the calibration is established, samples of unknown properties are measured with the indirect method to check its precision. These values are referred to as predicted values. The accuracy and performance of the indirect method is fully dependent on the correctness of the direct method. A good calibration to an inaccurate direct method is just as detrimental as a bad calibration.

For this application, the property of interest was the kernel moisture content. The reference method for kernel moisture content determination consists of drying peanut kernels in a forced-air, convection oven for 6 hours at 130 °C (ASAE, 2002). Upon completion of drying, the dry weight of the kernels is measured, and the wet basis moisture content, in percent, is calculated as:

$$M = \frac{m_w}{m_w + m_d} \times 100 \quad (6.1)$$

where m_w is the mass of the water and m_d is the dry mass of the material.

In the existing process, kernel moisture content is determined off-line by a meter using a secondary method, the GAC2100 grain analysis computer manufactured by DICKEY-john®. The microwave moisture sensor described in this dissertation also uses a secondary method. It measures the dielectric properties of the peanuts, and moisture is determined from a predetermined correlation between the dielectric properties and the moisture content as determined by the oven-drying method (Nelson et al., 1998; Trabelsi et al., 1998; Trabelsi et al., 1999b; Trabelsi and Nelson, 1998).

6.3 Microwaves

Usually, when microwaves are mentioned, the household kitchen appliance, the microwave oven, comes to mind. Microwave ovens have applications in everyday use for warming food. Within a microwave oven, a magnetron is used to generate microwaves at a frequency of approximately 2.45 GHz. Microwaves at this frequency are ideal because they are absorbed by water, fats and sugars; and they are not absorbed by most plastics, glass or ceramics (Metaxas, 1996). In these applications, relatively high power levels, ranging from 700 – 1500 Watts are used. These waves penetrate food and cause what is known as dielectric heating (Pozar, 1993). In this process, the molecules within the food are excited causing motion which results in heat.

Microwaves are electromagnetic waves with frequencies between 0.3 GHz and 300 GHz and wavelengths ranging from 1 mm to 1 m. Figure 6.1 shows the electromagnetic spectrum. The frequency range for microwaves can be divided into three types of signals: ultra-high frequency (UHF: 0.3 – 3 GHz), super high frequency (SHF: 3 – 30 GHz), and extremely high frequency (EHF: 30 – 300 GHz). Microwaves have useful applications in communications, remote sensing, navigation, and power generation and transmission (Pozar, 1993).

Microwaves can be successfully used to indirectly determine physical properties of granular materials and oilseeds such as wheat, barley, soybean, corn and peanuts and other materials such as cotton, biomass and poultry meat (King, 1997; Nelson and Trabelsi, 2008; Trabelsi and Nelson, 2004a; Trabelsi et al., 2008d). In such applications, the material is unaffected because low power microwaves (< 30 mW) are used. This is substantially lower than levels used in the typical microwave oven. Therefore, no dielectric heating occurs during measurements.

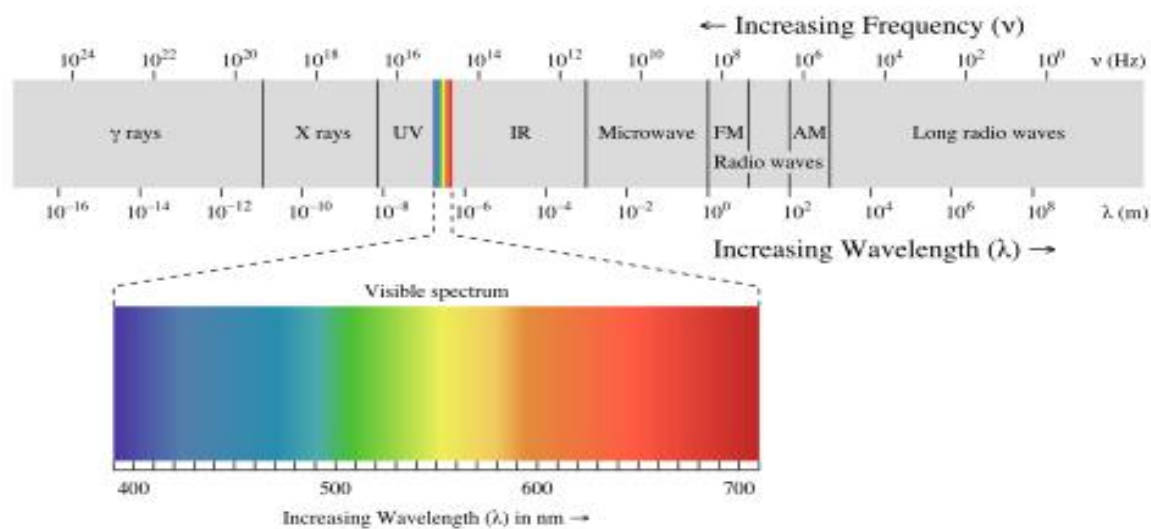


Figure 6.1: Electromagnetic spectrum

6.4 Microwave Measurement Methods

Microwave sensors emit microwaves which propagate through the material of interest when measurements are taken. As microwaves pass through the material, the following effects are observed:

- the material absorbs part of the power, causing the wave to be attenuated,

- the material changes the wavelength and the velocity of propagation, causing the wavefront to bend, phase angle to change, and the signal to be delayed,
- and the material changes the wave impedance, causing the wave to be reflected (Nyfors and Vainikainen, 1989).

Such effects depend on the permittivity and permeability of the material, which depend on physical properties of the material. Depending on application, material and sample size, the type of microwave sensor can be chosen to optimize the measurement procedure. The following methods are most common for measurements of dielectric properties of materials: transmission, reflection, and resonator. As described in the rest of this section, several techniques can be used for such measurements (Bussey, 1967; Nelson, 1999; Nelson, 2010; Von Hippel, 1954).

Transmission methods include coaxial air-line, hollow metallic waveguide, surface waveguide and free-space (Chen et al., 2004). Such methods can be classified as having open or closed structures. Open-structure techniques include free-space transmission measurements and open-ended waveguide measurements (Kraszewski, 1980). Closed-structure techniques include waveguide and coaxial-line transmission measurements and resonant cavities.

Reflection methods measure the signal reflected back from an object. The magnitude and phase of the reflection coefficient can be used to determine material properties, either with a contacting sensor or from a distance. The scattering properties of the material can be used to measure surface roughness and orientation (Nyfors and Vainikainen, 1989). The reflection coefficient as a function of frequency can be used to measure layer thicknesses of laminated materials.

Reflection methods include open-ended transmission line, coaxial-line, waveguide, and free-space (Chen et al., 2004; Nyfors and Vainikainen, 1989). Closed-structure methods include

short-circuited waveguide and coaxial-line reflection measurements. Nelson (2010) discussed use of the short-circuited line technique to measure dielectric properties in cereal grain. Open-structure methods include open-ended coaxial-line reflection measurements. The open-ended coaxial probe is a common contacting sensor used in the reflection measurements.

In resonator methods, the waves are bouncing back and forth, either between two reflectors or reflecting discontinuities in a transmission line (Nyfors and Vainikainen, 1989). Resonant frequencies are those at which the waves combine to form a standing wave pattern. These frequencies are dependent upon the size of the sensor (wavelengths) and are affected by the real parts of the relative complex permittivity, ϵ' , and the relative complex permeability, μ' . The rate of decay of the waves is affected by the imaginary parts of the relative complex permittivity, ϵ'' and permeability, μ'' .

Advantages of resonator methods are their versatility in measurement principle and high measurement accuracy. Resonator methods include hollow cavity, open and closed coaxial surface-wave, strip, two-conductor line, slotline and split-cylinder-cavity.

Free-space transmission methods are considered to have the most straightforward construction. They usually consist of a transmitter, a receiver, and a pair of antennas. The material being measured is placed between the antennas, causing attenuation of the amplitude of the microwave signal and change of the phase (Nyfors and Vainikainen, 1989). Generality and simplicity are the major advantages of transmission methods. However, such methods require a relatively large sample of material to achieve sufficient sensitivity and reduce the influence of reflections.

6.5 Microwave Moisture Sensor Measurement Principle

For any particular application, the appropriate measurement technique depends on the size of the sample of material, physical and electrical nature of the material, frequency of interest, implementation of sensor, and the degree of accuracy required. For this research, the free-space transmission method was used because of its simplicity, lack of requirements for special sample preparation, and its ability to provide nondestructive, rapid measurements that in many cases require no contact with the sample. Research has shown that free-space dielectric based sensing systems operating at microwave frequencies can be used for simultaneous determination of moisture content and bulk density and moisture content determination independent of density (Trabelsi et al., 2009c; Trabelsi and Nelson, 1998; Trabelsi and Nelson, 2004b; Trabelsi and Nelson, 2006a; Trabelsi et al., 2008c).

Accurate measurements of complex permittivity, ϵ , can lead to the determination of physical properties such as bulk density and moisture content in materials (Trabelsi and Nelson, 2006a). The relative complex permittivity, $\epsilon = \epsilon' - j\epsilon''$, represents the wave-matter interaction. The dielectric constant, ϵ' , describes the ability of the material to store energy, and the dielectric loss factor, ϵ'' , describes the ability of the material to dissipate electric-field energy. Dielectric properties were successfully used to determine physical properties of cereal grain and oilseed (Nelson, 1973). Dielectric properties are dependent on frequency, bulk density, moisture content and temperature (Hasted, 1973; Nelson, 1982; Trabelsi et al., 2008a). For moisture determination from dielectric properties, measurements can be performed at a fixed frequency, and temperature can be measured easily with inexpensive thermocouples. The effect of density can be accounted for by determination by gravimetric means; and they can be eliminated through the definition

and use of density-independent calibration functions (Meyer and Schilz, 1980; Trabelsi et al., 2009c; Trabelsi and Nelson, 1998).

Free-space transmission measurements are made to determine the scattering transmission coefficient S_{21} for microwaves traversing a layer of material. The principle of the measurement technique is shown in Figure 6.2. A material of thickness, d (cm), is placed between a transmitting and receiving antenna. The electric field of the incident wave is E_i . At the air-material interface, some of the incident wave energy enters the sample, and some is reflected, E_r . The reflection coefficient, Γ , is described as the ratio of the electric field of the reflected wave, E_r , to that of the incident wave, E_i . Within the material, some of the energy is absorbed, and some is transmitted, E_t . The transmission coefficient, τ , is described as the ratio of E_t to E_i . Measurements based on these principles yield the dielectric properties, ε' and ε'' ; and from these properties, physical properties such as moisture content and bulk density can be determined (Trabelsi et al., 1998; Trabelsi and Nelson, 2004a; Trabelsi and Nelson, 2004b). Figures 6.3 and 6.4 show free-space transmission measurement systems used throughout this study.

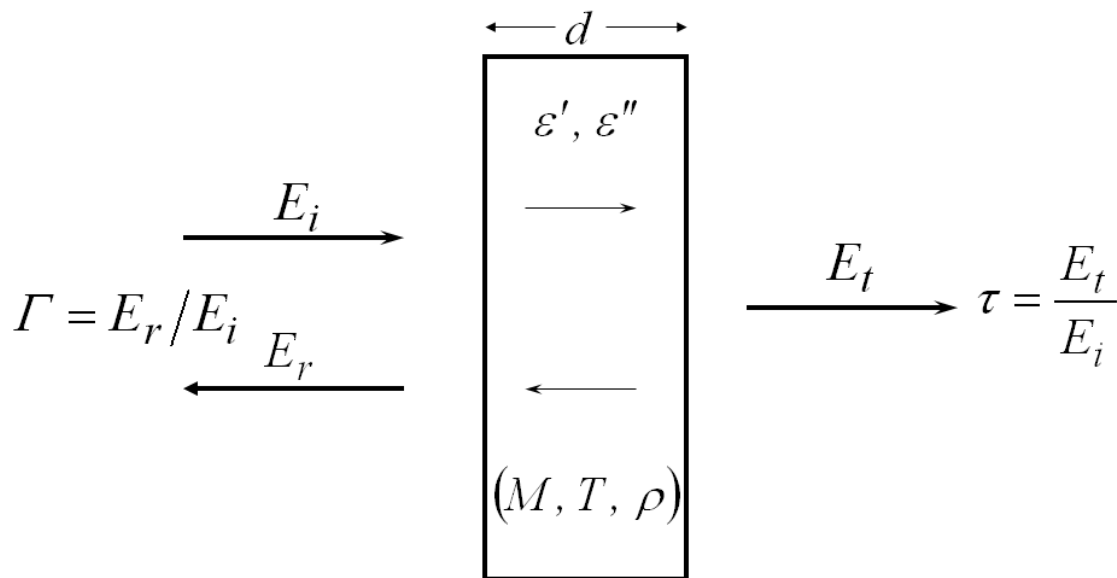


Figure 6.2: Free-space transmission method measurement principle

The measured scattering transmission coefficient can be expressed as:

$$S_{21} = \frac{(1-\Gamma^2)\tau}{1-\Gamma^2\tau^2} \quad (6.2)$$

The reflection coefficient, Γ , is defined as:

$$\Gamma = \frac{1-\sqrt{\varepsilon}}{1+\sqrt{\varepsilon}} \quad (6.3)$$

where ε is the complex permittivity. The transmission coefficient, τ , is defined as:

$$\tau = e^{-j\frac{\omega}{c}\sqrt{\varepsilon\mu}d} \quad (6.4)$$

where ω is angular frequency, c is the speed of light, d is sample thickness, and μ is the relative complex permeability, which has a value of 1 for nonmagnetic materials.

The scattering transmission coefficient, S_{21} , is the complex resultant from the measurements. From measurement of the modulus, $|S_{21}|$, and the argument of S_{21} , the attenuation, A , and phase shift, ϕ are calculated as follows:

$$A = 20 \log|S_{21}| \quad (6.5)$$

$$\phi = \text{Arg}(S_{21}) - 2n\pi \quad (6.6)$$

where n is a term that is determined to resolve the phase ambiguity when the thickness of the material is greater than the wavelength in the material (Trabelsi et al., 2000). The attenuation and phase shift are then used to calculate the attenuation constant, α , phase constant, β , and free-space phase constant, β_0 :

$$\alpha = \frac{A}{d}, \quad \beta = \frac{\phi}{d} + \beta_0, \quad \beta_0 = \frac{2\pi}{\lambda_0} \quad (6.7)$$

where λ_0 is the free-space wavelength. Therefore, using these three constants, the dielectric constant and loss factor are given as:

$$\epsilon' = \left(\frac{\beta - \alpha}{\beta_0} \right)^2 \quad \epsilon'' = \frac{2\alpha\beta}{\beta_0^2} \quad (6.8)$$



Figure 6.3: Free-space measurement system with vector network analyzer

Figure 6.3 shows the fundamental research system consisting of the vector network analyzer (VNA) and horn-lens antennas. This system has been used to provide a foundation on complex permittivity measurements taken at microwave frequencies (Trabelsi and Nelson, 2003a). The progression toward a more portable, cost-effective system is shown in Figure 6.4 as one of the earlier versions of the microwave moisture meter.

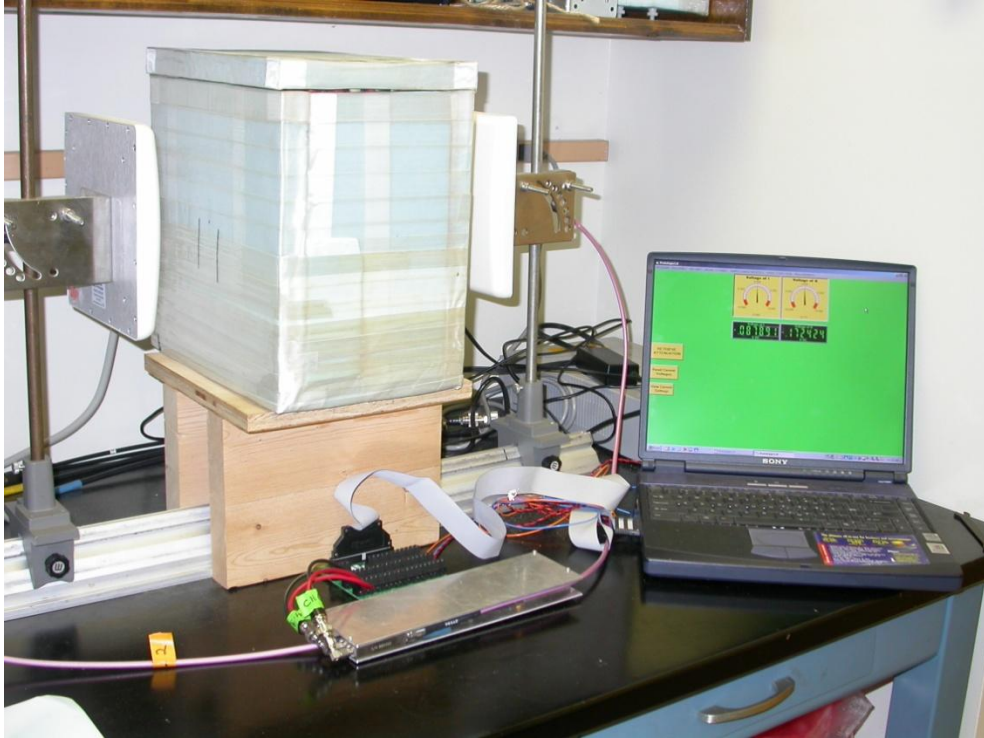


Figure 6.4: Laptop-controlled free-space measurement system using microwave components

When measurements are taken with the VNA, a response-type thru calibration is performed while an empty sample holder is placed between the two antennas (Trabelsi and Nelson, 2003a). Next, the sample holder is filled with the material being measured and placed again between the antennas. Then, the VNA sweeps the selected frequencies and outputs the modulus and argument of the scattering transmission coefficient, S_{21} , to the controlling computer, and the dielectric properties are calculated as explained earlier in this section.

When measurements are taken with the microwave meter, either as pictured in Figure 6.4 or a newer version, Figure 6.5, two voltages are measured from electronic circuits while an empty sample holder is placed between the antennas. These voltages are referred to as the reference voltages. After the sample holder has been filled with the material of interest, it is replaced between the antennas, and the two voltages are measured again. Using the two sets of

voltages, the attenuation and phase shift produced by the material are determined, and from these values the dielectric properties are calculated as explained earlier.



Figure 6.5: Enclosed version of microwave moisture meter

6.6 Peanut Moisture Content Determination (Unshelled, Shelled, & In-shell)

In this study, the main parameter of interest is the peanut kernel moisture content; and there is great concern with its determination while the peanut remains unshelled. This section will systematically address moisture content determination in peanut pods (unshelled), peanut kernels (shelled), and kernels while still in the shell. Figure 6.6 shows peanuts in their different forms. By using the dielectric properties of the peanuts, regardless of form, moisture content can be determined with appropriate calibration functions (Trabelsi et al., 1998; Trabelsi et al., 2001a; Trabelsi and Nelson, 1998; Trabelsi and Nelson, 2004a; Trabelsi and Nelson, 2004b).

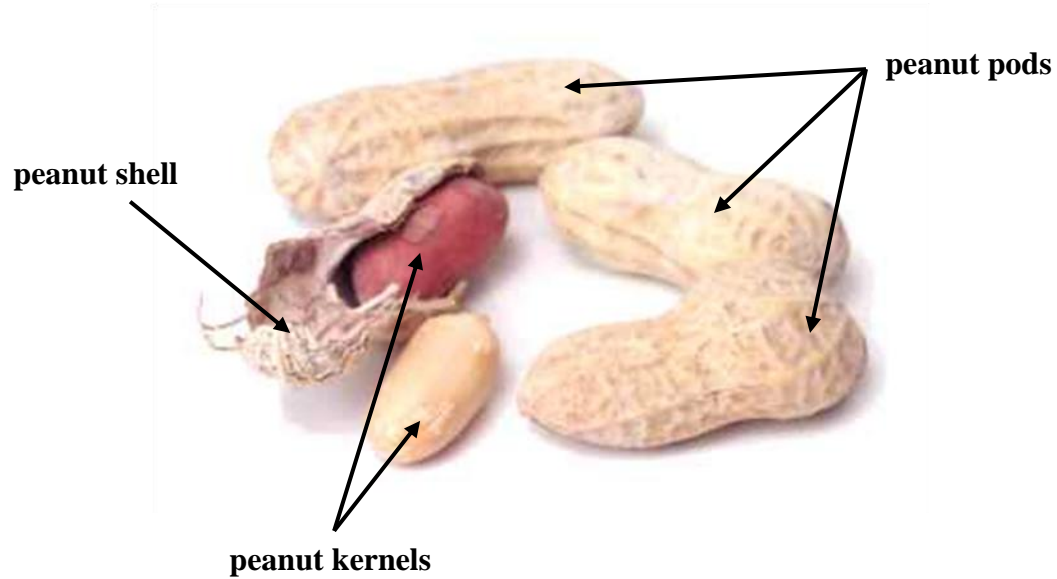


Figure 6.6: Peanuts shown in different forms

Moisture content determination in peanuts, pods or kernels, is possible by using a correlation between moisture content and a permittivity-based, density-independent calibration function, ψ (Trabelsi et al., 1998; Trabelsi et al., 2001a; Trabelsi and Nelson, 1998; Trabelsi and Nelson, 2004b). This calibration is based on the principle of energy distribution between stored and dissipated electric energy and the complex-plane representation of the relative complex permittivity divided by bulk density (Trabelsi et al., 1997; Trabelsi et al., 1999a; Trabelsi et al., 1999b; Trabelsi et al., 2001a). It is defined as:

$$\psi = \sqrt{\frac{\varepsilon''}{\varepsilon' (a_f \varepsilon' - \varepsilon'')}} \quad (6.9)$$

where ε' is the dielectric constant, ε'' is the dielectric loss factor, and a_f is a frequency-dependent coefficient determined from the slope of the regression line in the complex-plane representation of the dielectric properties, each divided by bulk density.

The coefficient a_f is determined from the complex-plane representation (Trabelsi et al., 1997; Trabelsi et al., 1998). Figure 6.7 provides an example of the complex-plane graphs for GA Runner type peanuts (kernels and pods) measured with the microwave moisture meter at 5.8 GHz and 23 °C.

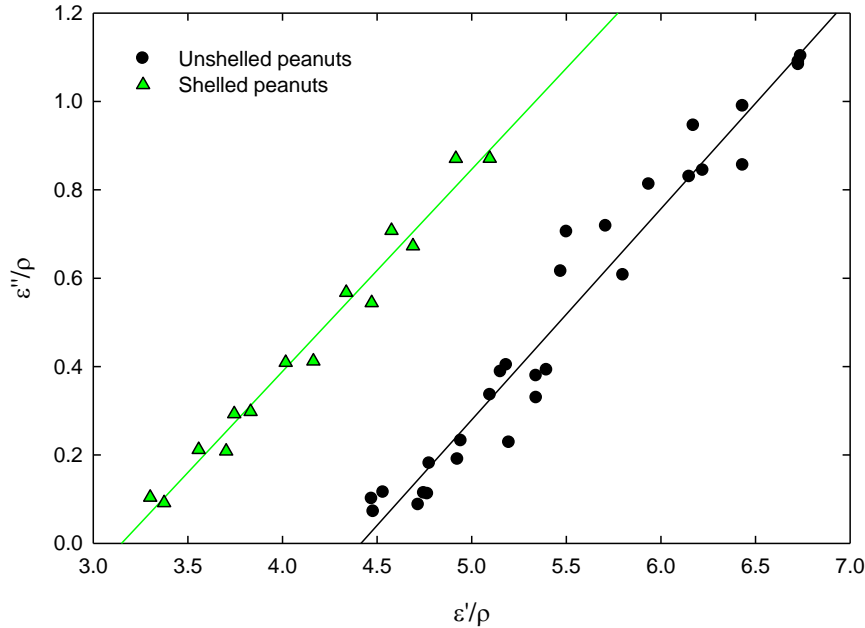


Figure 6.7: Complex-plane representation for kernels and pods

The data points along each regression line represent samples of different moisture contents, and the moisture content increases with increasing values of ϵ' and ϵ'' along the regression lines. The values of a_f for kernels and pods as shown in Figure 6.7 are 0.4573 and 0.4776, respectively. The dielectric properties for each sample along with the calculated value of a_f are used to calculate ψ . Figure 6.8 shows the variation of ψ with moisture content for the same set of GA Runner type kernels and pods used for the complex-plane representation.

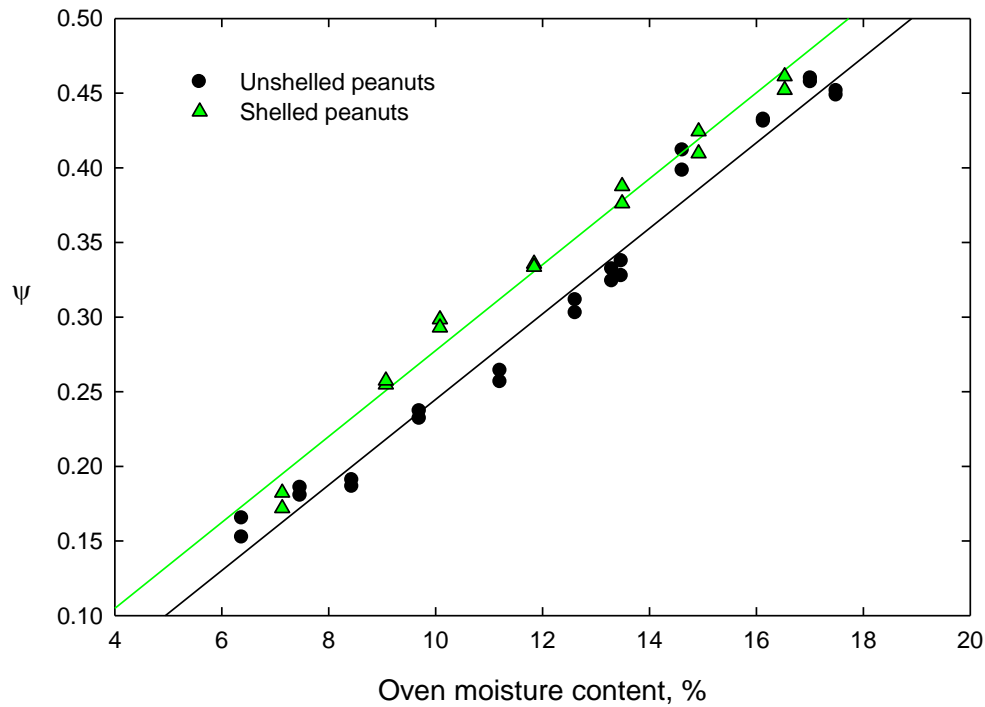


Figure 6.8: Variation of ψ with moisture content for kernels and pods

A linear trend is observed in the correlation between ψ and moisture content for kernels and pods. Therefore, a linear regression of the following form is used to correlate ψ with moisture content:

$$\psi = AM + B \quad (6.10)$$

Equation 6.10 can be rearranged to solve for moisture content, M , as follows:

$$M = \frac{\psi - B}{A} \quad (6.11)$$

The values for the coefficient of determination, r^2 , of the regressions for kernels and pods observed in Figure 6.8 are 0.98 and 0.97, respectively. Therefore, the moisture content of kernel and pod samples are determined routinely with a standard error of performance of approximately 0.3%.

The regressions in Figure 6.8 have similar slopes (coefficient A in equations 6.10 and 6.11); 0.02879 for kernels and 0.02865 for pods. This observation provides a means for determination of moisture content in peanut kernels from dielectric measurements on peanut pods (Trabelsi et al., 2009b; Trabelsi et al., 2010; Trabelsi and Nelson, 2006a). The calibration function ψ can be calculated from the dielectric properties and a_f value of the pods, and the kernel moisture content can be solved for by equating the pod calibration function to the kernel calibration function as follows:

$$\psi_p = \psi_k \quad (6.12)$$

$$\psi_p = A_p M_p + B_p = A_k M_k + B_k \quad (6.13)$$

$$M_p = \frac{\psi_p - B_p}{A_p} \quad (6.14)$$

$$M_k = \frac{A_p M_p + B_p - B_k}{A_k} \quad (6.15)$$

Equation 6.15 is a kernel moisture content calibration equation. It provides kernel moisture content from measurements on unshelled peanut pods. Thus, a method for in-shell determination of kernel moisture content is shown (Trabelsi et al., 2009b; Trabelsi et al., 2010; Trabelsi and Nelson, 2006a).

For moisture content determination previously described, the temperature is assumed to be constant. Therefore, no term was included for temperature compensation. However, since temperature is a factor that affects dielectric properties, it needs to be measured and compensated for in conditions where temperature can fluctuate (Nelson, 1982; Neslon and Bartley, 2002; Trabelsi et al., 2008a; Trabelsi et al., 2009a; Trabelsi and Nelson, 2006a; Trabelsi and Nelson,

2006c). A multiple linear regression was performed to correlate ψ to moisture content and temperature of kernels and pods. Figure 6.9 shows a graph in which the regressions for kernels and pods are shown together to observe the parallel trend between them. This same trend was also observed in the two-dimensional assessment. Because of this trend, kernel moisture content can be determined in-shell with temperature compensation. Equations 6.16 – 6.18 show the calculation of kernel moisture content with the inclusion of the term for temperature in the calibration equation.

$$\psi_p = A_p M_p + B_p T + C_p = A_k M_k + B_k T + C_k \quad (6.16)$$

$$M_p = \frac{\psi_p - B_p T - C_p}{A_p} \quad (6.17)$$

$$M_k = \frac{A_p M_p + (B_p - B_k) T + C_p - C_k}{A_k} \quad (6.18)$$

In-shell determination of kernel moisture content is possible in settings where the temperature will remain constant and in other settings where temperature is bound to fluctuate. Such capability allows for real-time monitoring of kernel moisture content in samples of unshelled peanuts.

The microwave moisture meter (Figure 6.5) was field-tested for the 2008, 2009 and 2010 peanut harvest seasons. During the 2009 and 2010 harvest seasons, the microwave meter was included in an unbiased test in which its moisture content prediction and that of the two official moisture meters were compared with the moisture content as determined with the oven-drying reference method (ASAE, 2002). In the 2010 harvest season, peanut pod samples of different varieties were shipped from 10 different states for moisture content determination. Kernel

moisture content was determined from measurements on peanut pod samples. After analyzing the data for 543 measured samples, the standard error of performance was 0.4%. In Figure 6.10, the predicted kernel moisture content is plotted against the reference moisture content determined by oven drying. The solid diagonal line in the graph shows the ideal relationship between the predicted and reference values of moisture content. Figure 6.11 shows a distribution of the temperatures of the samples.

Results showed that the performance of the microwave moisture meter was as good as if not better than the two official moisture meters. The microwave meter provided the advantage of not having to shell the peanuts to evaluate kernel moisture content.

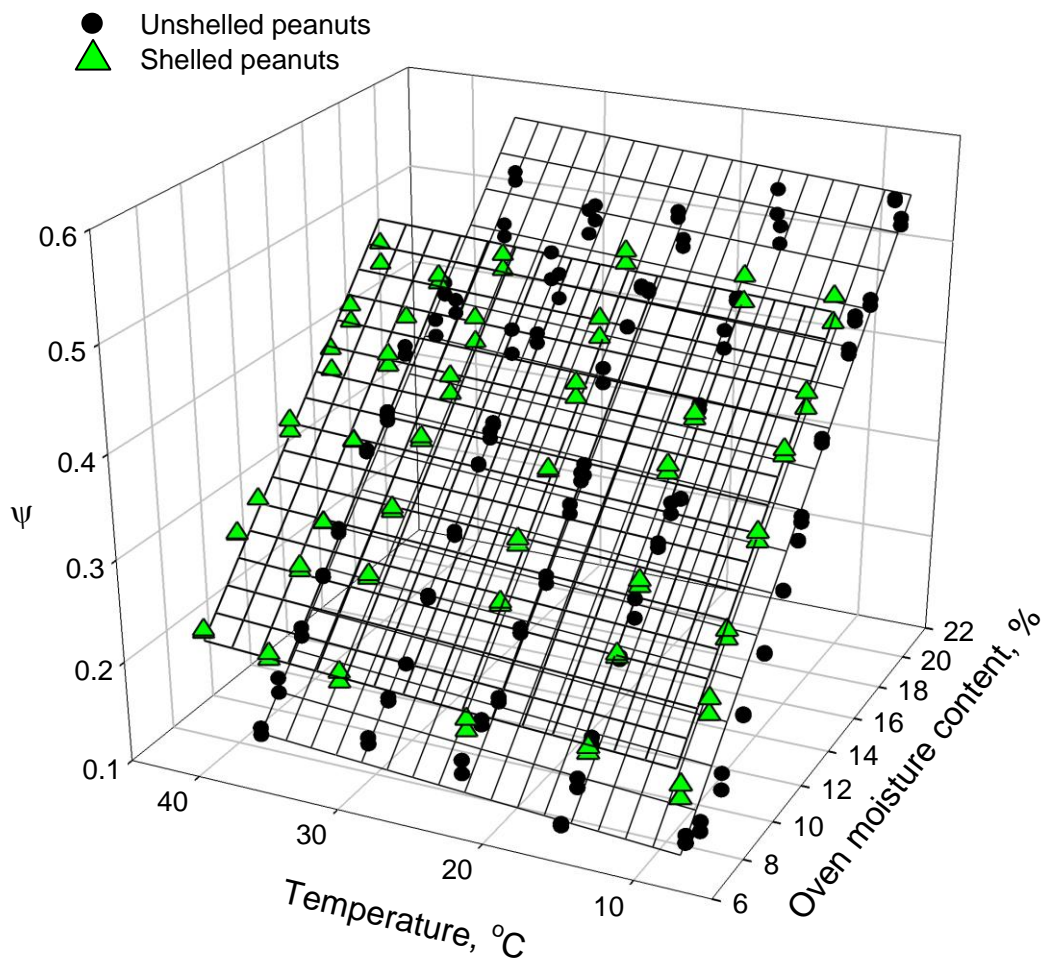


Figure 6.9: Variation of ψ with moisture content and temperature for kernels and pods

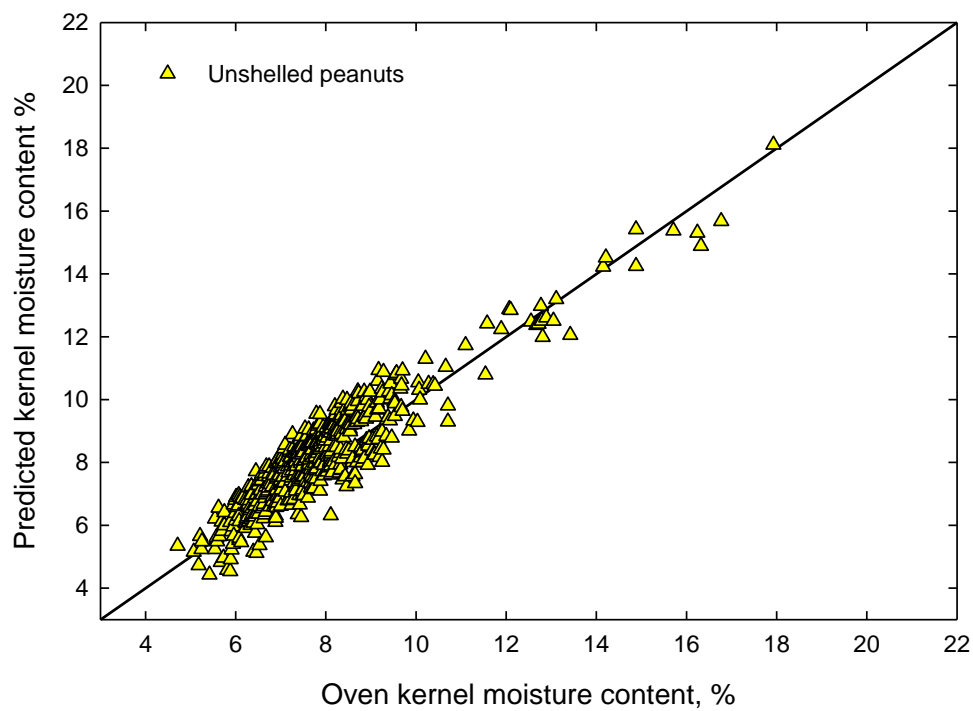


Figure 6.10: Predicted kernel moisture content versus reference moisture determined by oven drying

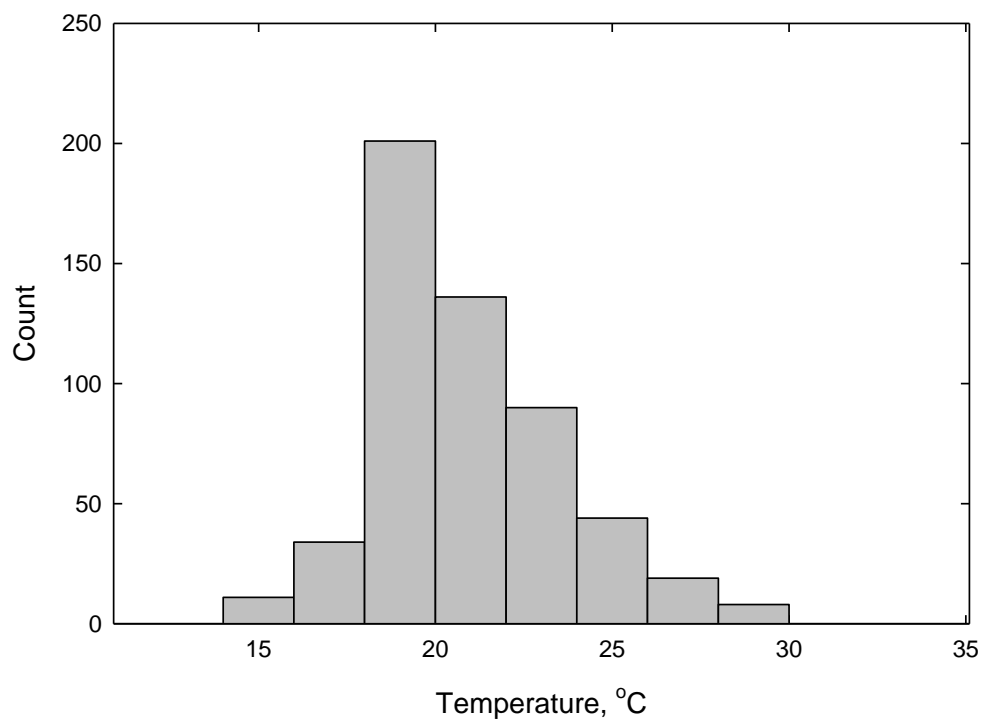


Figure 6.11: Temperature distribution of peanut pod samples

CHAPTER 7

SOFTWARE IMPLEMENTATION

Original code was written to facilitate the automated control of the peanut drying process. The software was written in C programming language and was created in Paradigm Integrated Development Environment (IDE). This IDE was provided with the microcontroller used in this system, the SensorCore manufactured by Tern, Inc. This microcontroller is also the one used by the microwave moisture meter (Lewis and Trabelsi, 2011a; Lewis and Trabelsi, 2011b). To avoid the addition of another microcontroller, the software for the entire system to control the drying process was implemented on the microcontroller already used by the microwave meter.

7.1 Summary of Program Execution

The code was written in the creation of an independent, monitoring-type software requiring minimal user interaction. When the software is initialized, the user is asked to enter the target kernel moisture content. After this interaction with the user, the software requires no further input. The target kernel moisture content can also be embedded within the code as a constant so that no user input is required. The software sweeps the sensor network, and the temperatures, relative humidity, and initial pod and kernel moisture content are all calculated. The initial control action for the dryer is determined by using the initial kernel moisture content, relative humidity, and temperature of the ambient air.

Once the drying process has begun, the software continuously monitors the specified conditions through the acquisition of data from the sensor network. Appropriate control actions for the dryer are determined from the assessment of these data. These control actions include

heating element selection, termination of aeration, and the appropriate duty cycle to yield required power. The microcontroller has a digital-to-analog converter (DAC) that can output voltages up to 4.09 V. The two channels of the DAC are used to switch the solid-state relays, providing power to the heating elements individually or simultaneously. The software uses a pulse-width-modulation (PWM) algorithm to vary the power, based on air temperature needed at the inlet to the plenum.

7.2 Modular Programming

The software was developed in modular format and was divided into five classes: `bitmap`, `dry_monitor`, `data_acquisition`, `calculations`, and `data_out`. The classes are listed in order of execution. The `bitmap` class is only executed upon initialization; however, the other classes loop for the duration of the drying process. A flowchart of event execution is shown in Figure 7.1

The `bitmap` class controls the scrolling bitmap images for the USDA and ARS logos. These images are displayed when the microcontroller is turned on initially or reset. The `dry_monitor` class controls the constant and real-time monitoring of the sensors within the sensor network. It initiates the acquisition of the data from the sensors and facilitates the display of the measured parameters on the graphical LCD. The `data_acquisition` class executes the acquisition of data and the conversion of data from analog to digital to float values that can be manipulated in calculations or displayed by other classes.

The `calculations` class uses the voltages acquired from the microwave meter to calculate the dielectric properties of the sample. Coded algorithms are then used to determine the moisture content from the dielectric properties (Lewis and Trabelsi, 2011a; Lewis and Trabelsi, 2011b; Trabelsi et al., 1998). The voltages acquired from the temperature sensors are used to calculate the temperature in degrees Celsius based on of 10 mV/ °C.

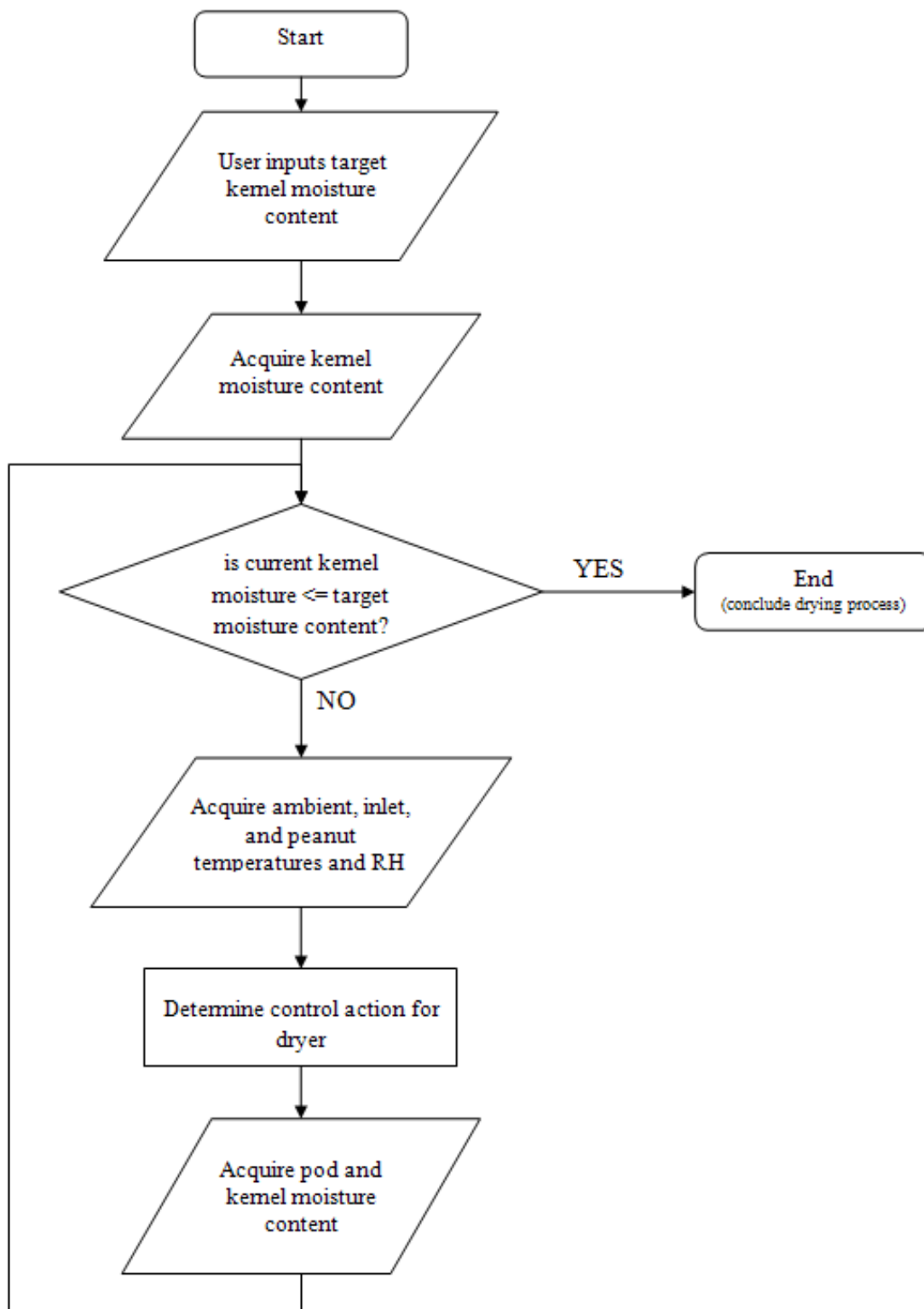


Figure 7.1: Flowchart for main program execution

The voltage acquired from the relative humidity sensor is used to determine RH using the equation shown in Figure 8.2. It is also in this class that the control action for the dryer is determined. Output from the feedback controller and other control criteria are used to determine whether both heating elements are turned on, both are turned off, or either is turned on individually. The ambient air temperature ($T_{ambient}$) and the air temperature at the plenum inlet (T_{inlet}) are converted to degrees Fahrenheit to perform all assessments since drying control criteria were established in degrees Fahrenheit.

The data_out class controls the on-off and high-low output to the heating elements to control the temperature of the drying air. Pins of the microcontroller are configured such that digital values can be output as analog to the appropriate channels. The five classes work together to provide automated control of the drying process. Atmospheric conditions are monitored in real-time, and thus, drying parameters are controlled in real-time. Real-time monitoring of kernel moisture content allows the user to know the moisture content of the bed at all times.

CHAPTER 8

DATA ACQUISITION

This system uses a sensor network to measure atmospheric conditions as well as conditions within the drying system in real-time. Data are acquired from these sensors via an analog-to-digital converter (ADC). The sensor network, with consistent data acquisition, establishes a real-time system for monitoring the drying process. The following sections of this chapter discuss the sensor network used in this system and how data were acquired from it. A rationale is given as to why a sensor network was chosen as the mechanism for data acquisition.

8.1 Sensor Network

The following two definitions have been used to describe sensor networks. The first definition was given by Dr. Jim Kurose and Dr. Victor Lesser, professors at the University of Massachusetts; both were instructors for the sensor network class (CSCI 791L) for the fall semester of 2003. They describe a sensor network as "... a sensing, computing and communication infrastructure that allows us to instrument, observe, and respond to phenomena in the natural environment, and in our physical and cyber infrastructure". The second definition describes a sensor network as a computer network consisting of spatially distributed autonomous devices using sensors to cooperatively monitor physical or environmental conditions, such as temperature, sound, vibration, pressure, motion or pollutants, at different locations (Haenselmann, 2006). The two definitions emphasize the usefulness of sensor networks in regard to gathering and processing information from the surrounding environment.

The sensor network in this system was used to measure five parameters from the atmosphere and the drying system: temperature of the ambient air, temperature of the air at the inlet to the air plenum of the drying trailer, temperature of the drying peanuts at the location of the microwave moisture sensor, relative humidity of the ambient air, and kernel moisture content of the drying peanuts. The sensor network consisted of five sensors: three LM35 (TO-46 metal can) temperature sensors, an HIH-4000-001 relative humidity sensor, and a microwave moisture meter for in-shell peanut kernel moisture content determination, developed within USDA ARS.

The LM35 temperature sensor outputs a voltage that increases linearly with the increase of temperature. It outputs 10 mV/ °C and was chosen because its range of output fits within the input range of the ADC of the microcontroller (0 to 2.5 V). The TO-46 metal can and the TO-92 plastic package versions of the LM35 were tested, and better response was observed using the TO-46 version. To measure the ambient air temperature, one LM35 was mounted on a breadboard. Extensions were made for the other two temperature sensors because of their required location. Their pins were soldered to 22-gauge wire, and a plastic sleeve was installed over the solder connections to make the sensor more rigid. The sensor used to measure the temperature of the drying peanuts was given a 35-cm extension, and the sensor used to measure the temperature of the inlet to the air plenum was given a 1.7-m extension. Figure 8.1 shows a picture of the modified sensors.

The HIH-4000-001 sensor was mounted on a breadboard to measure the relative humidity of the ambient air. It outputs a voltage that increases linearly with increase in relative humidity. The data sheet for the sensor provided measured voltages at various levels of relative humidity. The data was graphed, and a linear regression was performed to generate an equation to calculate relative humidity. Figure 8.2 shows the regression and the resulting equation.

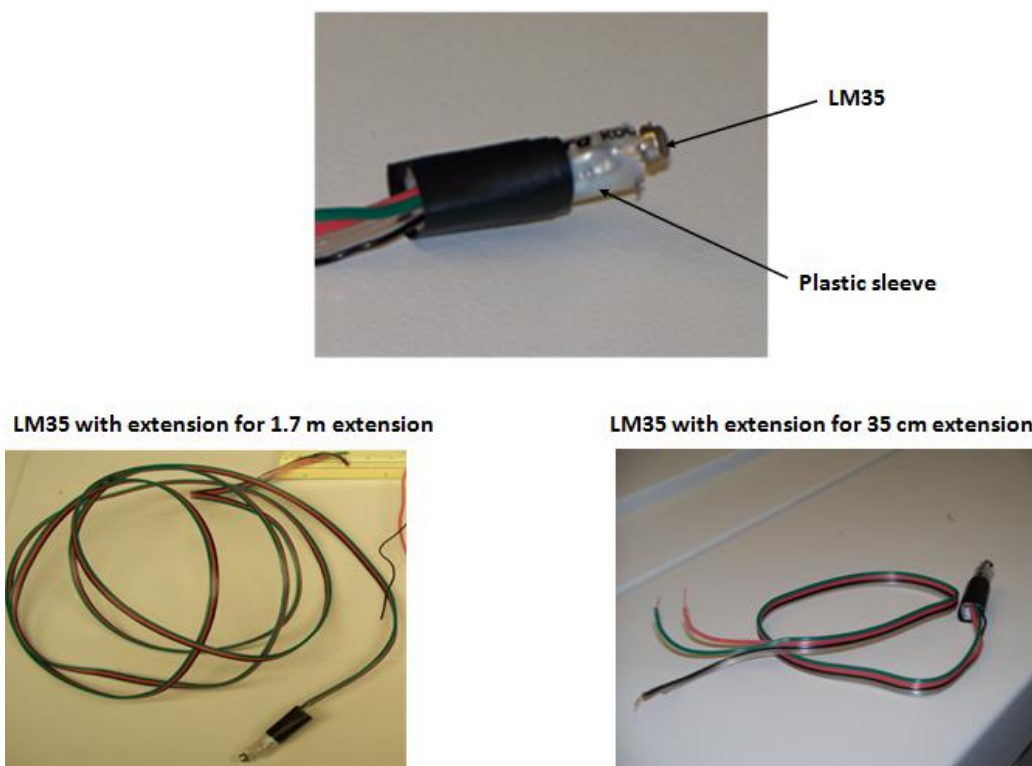


Figure 8.1: Modified LM35 temperature sensors

The microwave moisture sensor was modified so that the antennas could be mounted within the drying trailer. A wooden mount was made such that the antennas were appropriately aligned and there was a distance of 29 cm between them, measuring from the back of each antenna. The distance between the antennas allowed for the material of interest to be placed between the antennas so that there was one wavelength distance between the material and either antenna. This is within the design specifications for the microwave moisture meter. Its enforcement prevents samples from being in the immediate near-field of the antennas. For the operating frequency of the microwave meter, one wavelength is equal to 5.16 cm. To create the needed separation between antenna and material, 2" (5.08 cm) thick polystyrene sheathing was inserted in front of each antenna. The sheathing had no effect on the measurements since its dielectric constant is similar to that of air (polystyrene sheathing - 1.03 versus air - 1.0006).

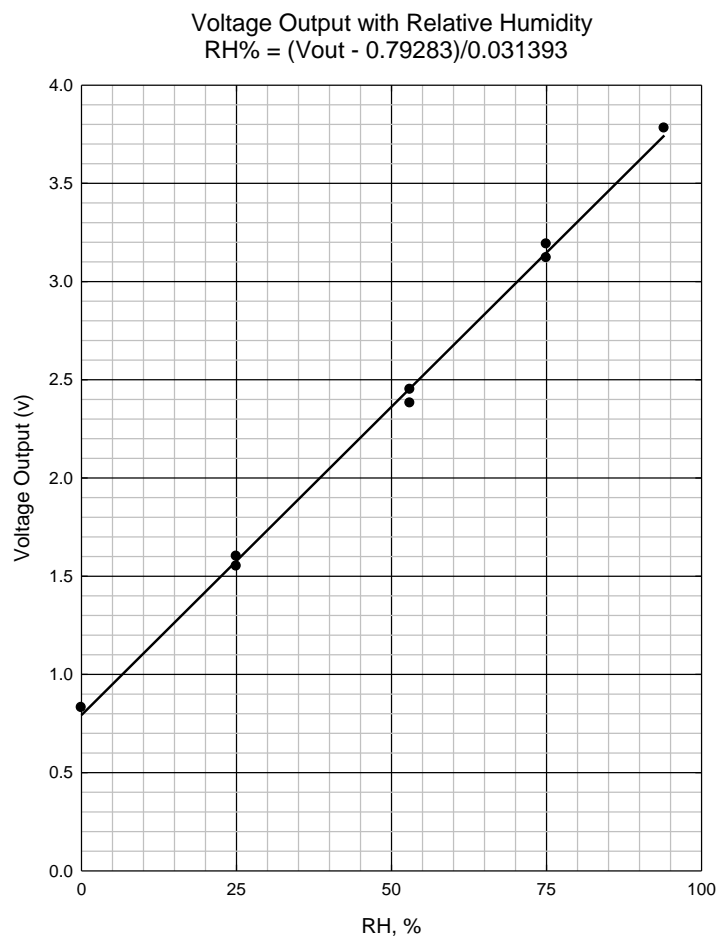


Figure 8.2: Linear regression for determination of relative humidity

Figure 8.3 shows the antennas mounted within the drying trailer. The mount was designed so that the bottom of the antennas was 4 cm from the perforated, metallic floor. Testing revealed that at that height, the microwaves from the antennas were not affected by the metal floor. This height above the metallic floor resulted in the top of the antennas being 6.7 cm below the top of the trailer.

Special circuitry was added to condition the voltage outputs from the microwave meter so they could be read correctly by the ADC. From previous measurements, an output range of $-/+ 1$ V was defined for the microwave meter. However, the ADC had a unipolar input range of 0 to

2.5 V. Therefore, a level shifter circuit was implemented to shift the bipolar output range of the microwave meter to a unipolar range accepted by the ADC. The level shifter added 1 V to the output, shifting the -1 to 1 V range to a 0 to 2 V range. Appropriate adjustments were made within the software. This implementation is discussed in more detail in chapter ten, section two.



Figure 8.3: Antennas for microwave meter mounted within drying trailer

The five sensors were implemented together in the creation of a sensor network. The sensor network was used to gather data from the drying process and the atmosphere. Acquired data were used to facilitate decision making and govern control of air temperature and drying duration. The sensor network provided a real-time monitoring system for the peanut drying process.

CHAPTER 9

**ANALYSIS OF STABILITY AND TYPE INDEPENDENCE OF THREE DENSITY
INDEPENDENT CALIBRATION FUNCTIONS FOR MICROWAVE MOISTURE
SENSING IN SHELLED AND UNSHELLED PEANUTS¹**

¹ Lewis, M.A, S. Trabelsi, S.O. Nelson, and E.W. Tollner. Accepted by *Transactions of the ASABE*.
Reprinted here with permission of the publisher

Abstract

A microwave dielectric method was used for nondestructive and rapid determination of moisture content in shelled and unshelled peanuts of various types from transmission measurements of their relative complex permittivities in free space at 23 °C between 5 and 15 GHz. Moisture content was estimated, independent of bulk density, with three density-independent calibration functions and compared to standard oven moisture determinations: two of these functions are permittivity-based, and the other is expressed in terms of attenuation and phase shift. The effectiveness and stability of these three functions for type independence were evaluated over broad ranges of frequency, moisture content and bulk density. While the performance of each function with individual type calibrations was reaffirmed, statistical analysis also showed high coefficients of determination in predictions with the combined type-independent calibrations. Therefore, with microwave moisture sensing technology, calibration equations can be used to accurately predict moisture content in peanuts with insensitivity to type; which is a characteristic lacking in today's commercial moisture meters.

9.1 Introduction

The use for peanuts has changed drastically since their origin in South America approximately 3500 years ago (American Peanut Council, 2007). Upon their introduction to North America in the 1700's, they were merely used as food for swine (University of Georgia, 2003). However, since that time, the commercial growth of peanuts has increased substantially; and today, peanuts and peanut-based products constitute an important group of food products available in the market place. Peanuts are categorized into four types, which are distinguished by their growth location, branching habit and branching length (Virginia-Carolina Peanut Promotions, 2007). The four types are Runner, Virginia, Spanish and Valencia. Despite their differences, the same routines are followed for all types in planting, harvesting, and processing.

In today's agricultural market, farming, handling, and processing of peanuts require rapid testing methods for peanut characterization. Accurate and efficient determination of physical properties such as moisture content is essential in the grading process. Research has shown that dielectric properties can be successfully used to determine physical properties of cereal grain and oilseed (Nelson, 1973). Free-space dielectric-based sensing systems operating at microwave frequencies can be used for moisture content determination independent of bulk density (Trabelsi and Nelson, 2004a). Such measuring systems are advantageous because they provide nondestructive, rapid measurements and in most cases require no contact with the material being measured.

Accurate and effective microwave measurements of complex permittivity, ϵ , can lead to the determination of physical properties such as moisture content in materials (Trabelsi and Nelson, 2006b). The relative complex permittivity, $\epsilon = \epsilon' - j\epsilon''$, influences the wave-matter interaction and can be considered as the electrical signature of a given material (Trabelsi et al.,

1999a). The dielectric constant ϵ' and the dielectric loss factor ϵ'' are indicative of the capability of a material to store electric energy and dissipate electric energy, respectively. Dielectric properties are dependent on frequency, bulk density, moisture content and temperature (Nelson, 1982; Trabelsi et al., 2008a; Trabelsi and Nelson, 2004b). Frequency can be fixed in measurements, and temperature can be measured, leaving bulk density and moisture content as parameters of interest. The dielectric constant and loss factor have been observed to increase with moisture content and bulk density (Trabelsi et al., 2008a). The effects of density can be accounted for by its determination by gravimetric means; and the effects of density can be eliminated through the definition and implementation of density-independent calibration functions (Meyer and Schilz, 1980; Trabelsi et al., 2009c; Trabelsi and Nelson, 1998). Gravimetric determinations of density are feasible in static measurement processes. However, in dynamic on-line processes, determination of density through a gravimetric means is impractical, especially in cases where the density of the material lacks homogeneity (Irudayaraj and Reh, 2008).

This paper discusses the performance and stability of three density-independent moisture calibration functions for shelled and unshelled peanuts (peanut kernels and pod peanuts, respectively) as frequency increases from 5 to 15 GHz in the assessment for the feasibility of type-independent moisture content determination.

In today's grading processes for various commodities, existing moisture meters, operating at lower frequencies in the radio-frequency range, require a separate calibration for each type of a specific grain or oilseed. However, at microwave frequencies, complex-permittivity measurements on peanuts are unaffected by type (Lewis et al., 2009; Lewis et al., 2010). This provides for moisture content determination without the need for consideration of

peanut type. To this end, three density-independent calibration functions (Trabelsi and Nelson, 1998; Trabelsi and Nelson, 2004a) were evaluated for their type-independence to assess the feasibility of moisture content determination insensitive to peanut type. A moisture meter with such provisions would save time and eliminate erroneous type selection during the peanut grading process. The coefficients for each calibration equation, for individual peanut types and for all types combined, along with standard errors of calibration are given and discussed.

9.2 Materials and Methods

Sample Preparation

For this study, three types of peanuts, including two varieties of the Runner type, were used. One variety was Georgia grown peanuts, while the other variety, having a high-oleic-acid content, was grown in Texas. Peanuts with a high-oleic-acid content are more stable with respect to lipid oxidation during heating, thus having longer shelf life (Chung et al., 2002). Therefore, the peanut types measured included GA Runner and TX Runner (high-oleic), Valencia, and Virginia unshelled (pods) and shelled (kernels).

Pod peanut samples consisted of approximately 5 kg, and the kernel samples consisted of approximately 7 kg. For each peanut type and variety measured in this experiment, five to eight pod and kernel samples were conditioned to different levels of moisture content to cover a range from 6% to 18% in increments of about 2%. Moisture content was increased in samples by spraying them with a fine mist of distilled water, using an Ortho¹ Heavy Duty sprayer. The samples were then stirred for approximately five minutes to ensure that the water was evenly distributed. The quantity of water (grams) added, m_{wa} , to each sample was proportional to the

¹ Mention of company or trade names is for descriptive purposes only and does not imply endorsement by the U.S. Department of Agriculture or The University of Georgia

difference in its initial moisture content M_i and the desired moisture content M_d and was calculated as:

$$m_{wa} = m_s \left(\frac{M_d - M_i}{100 - M_d} \right) \quad (9.1)$$

where m_s is the mass of the sample in grams, M_d is the desired moisture content of the sample in percent, and M_i is the initial moisture content in percent. To obtain the initial moisture content of each sample, subsamples were extracted (three 15 g subsamples for kernels and two 100 g subsamples for pods) for moisture content testing according to the specifications of the ASAE Standards (ASAE, 2002). The subsamples were oven-dried for 6 hours at 130 °C. Upon completion, moisture content (%) was calculated on the wet basis as follows:

$$M(\%) = \frac{m_w}{m_w + m_d} \times 100 \quad (9.2)$$

where m_w is the mass of the water and m_d is the dry mass of the material.

After the water was added to all samples and all were stirred, the samples were sealed in plastic bags and stored for a minimum of 72 hours at 4 °C for equilibration. Before each set of microwave measurements was performed, samples to be used were allowed to equilibrate at room temperature in sealed bags for a minimum of 12 hours.

9.3 Free-Space Complex Permittivity Measurements

The free-space-transmission technique is one of several techniques that can be used for complex permittivity measurements (Bussey, 1967; Von Hippel, 1954). It was chosen for these measurements because it is rapid, nondestructive, and requires no contact with the sample in most cases. For this research, free-space-transmission measurements were made to determine the scattering transmission coefficient S_{21} for microwaves traversing a layer of peanuts (Trabelsi et al., 1999a; Trabelsi and Nelson, 2003a). The attenuation, ΔA , and phase shift, $\Delta \Phi$, caused by

each sample were measured with an 8510C Hewlett-Packard vector network analyzer (VNA). The dielectric properties ϵ' and ϵ'' were determined from these measured parameters. The measurement system consisted of two horn-lens antennas connected to the VNA with high quality coaxial cables. The antennas faced each other directly, 37 cm apart, and were kept in alignment with a wooden antenna supporting stand. Figure 9.1 shows the measurement system.



Figure 9.1: Free-space measurement system with pod sample shown

Measurements were conducted in a room providing stable temperature at 23 °C and relative humidity control. Measurement equipment was given an hour to warm up before measurements. A response thru-type calibration was performed on the VNA with an empty Styrofoam sample holder of rectangular cross section placed between the antennas (Trabelsi and Nelson, 2003a). Styrofoam sheet fillers were placed in the sample holder to change the thickness of the sample. After calibration, the material, whether kernels or pods, was poured into the sample holder and placed between the horn lens antennas for the measurements. During

calibration and measurements, the sample holder was placed in the same location between the antennas. The measurement procedure was fully automated and controlled remotely by a desktop computer connected to the VNA via GPIB interface. The computer also provided data storage for acquired parameters and calculations. For each sample, measurements were performed at three different bulk densities ranging from loosely packed to compact by settling the sample with repeated impact of the sample holder on a solid work bench. Upon the completion of measurements, subsamples were extracted from each sample for moisture content determination by the oven drying reference method (ASAE, 2002).

From the measured transmission scattering parameter S_{21} for each sample, the dielectric properties were calculated from the modulus, $|S_{21}|$, and argument φ of S_{21} , assuming that a plane wave is propagating through a low-loss material, ($\varepsilon'' \ll \varepsilon'$) (Trabelsi and Nelson, 1998) as follows:

$$\varepsilon' = \left[1 - \frac{(\varphi - 360n) c}{360d f} \right]^2 \quad (9.3)$$

$$\varepsilon'' = \frac{-20 \log |S_{21}| c}{8.686 \pi d f} \sqrt{\varepsilon'} \quad (9.4)$$

where f is the frequency in Hz, d is the thickness of the layer of material (expressed in meters), c is the speed of light (m/s), and n is an integer to be determined that addresses phase ambiguity (Trabelsi et al., 2000). The dielectric properties represent average values for the air-material mixture. Table 9.1 summarizes the physical characteristics and the measurement data of the kernel and pod samples used in this study.

Table 9.1: Ranges of physical characteristics and measurement data of kernel and pod samples used for calibration

Peanut form	Moisture content range, %	Density, g/cm³	Attenuation, dB	Phase Shift, degrees	ϵ'	ϵ''
Kernels	6.1 – 18.0	0.524 – 0.738	5.4 – 17.7	-616.2 – -264.3	2.1 – 3.6	0.10 – 0.99
Pods	6.9 – 18.4	0.211 – 0.370	2.6 – 14.8	-383.9 – -168.7	1.3 – 2.0	0.04 – 0.33

Density Independence

As mentioned earlier, density is one of many factors that have an effect on the dielectric properties of a material. However, in the three following functions, the effect of density has been eliminated, making the determination of density unnecessary for moisture content determination. Two of the three density-independent calibration functions are permittivity based, and the third is expressed in terms of attenuation and phase shift. The functions are referred to as ψ_1 , ψ_2 , and ψ_3 . The first function ψ_1 is based on the distribution of stored and dissipated electric energy in the material, and the same function predicted moisture well for cereal grain and oilseed (Trabelsi et al., 1998; Trabelsi et al., 2001b). It is defined as

$$\psi_1 = \sqrt{\frac{\epsilon''}{\epsilon'(a_f \epsilon' - \epsilon'')}} \quad (9.5)$$

where a_f is the slope of the regression line in the complex-plane representation of the dielectric properties, each divided by bulk density. The complex-plane representation is used for the determination of a_f and ψ_1 (Nelson and Trabelsi, 2004). Figure 9.2 provides examples of the complex-plane plots for peanuts (kernels and pods).

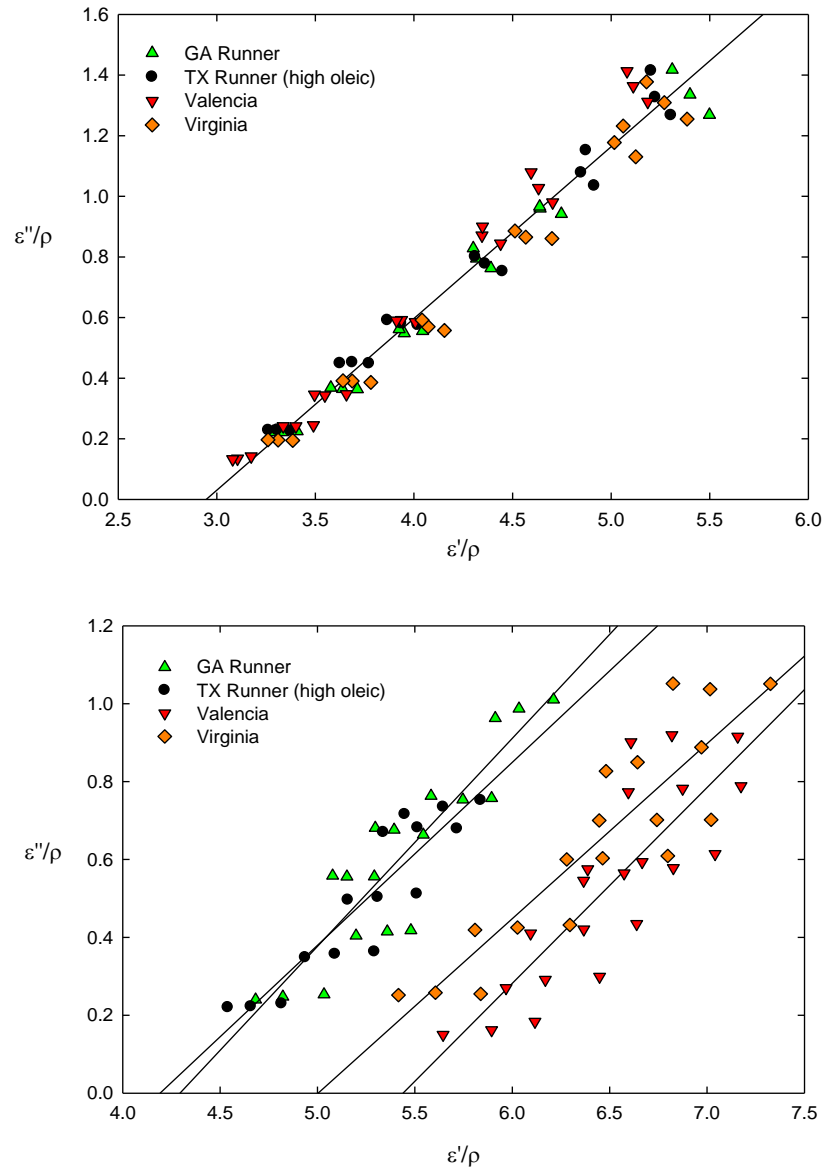


Figure 9.2: Complex-plane representation of dielectric properties of kernels (upper) and pods (lower) of indicated peanut types at 6 GHz and 23 °C

Reflecting on the equation for the complex permittivity, $\epsilon = \epsilon' - j\epsilon''$, note that in both graphs the real part, the dielectric constant, is graphed on the x-axis, and the imaginary part, the loss factor, is graphed on the y-axis. Both properties are divided by bulk density, ρ . The upper graph shows that the kernel data in the complex-plane representation of the dielectric properties of all four lots

of kernels were fitted satisfactorily with a single linear regression, resulting in a slope a_f value of 0.5666. The lower graph shows that a linear regression was performed for each of the four lots of pods. The a_f values are as follows: GA Runner, 0.5340; TX Runner, 0.4697; Valencia, 0.5028; and Virginia, 0.4494. Both, the differences in scale and lower values for the loss factor contribute to an apparent greater scatter of points in the plot for pods compared to that for the kernels.

The second function ψ_2 is based on the ratio between attenuation and phase shift. It is noted as the first density-independent function to be expressed in terms of the dielectric properties (Jacobsen et al., 1980). It is defined as

$$\psi_2 = \frac{\varepsilon''}{\varepsilon' - 1} \quad (9.6)$$

The third function ψ_3 is based on the realization that although the attenuation and phase shift of a wave traversing the material are density-dependent, the ratio of the two is density-independent (Kraszewski and Kulinski, 1976). It is represented in terms of attenuation and phase shift as well as the modulus and argument of the transmission scattering coefficient S_{21} . It is defined as

$$\psi_3 = \frac{\Delta A}{\Delta \phi} = \frac{20 \cdot \log |S_{21}|}{\varphi - 2\pi \cdot n} \quad (9.7)$$

where ΔA is attenuation, $\Delta \phi$ is phase shift, $|S_{21}|$ is the modulus of S_{21} , φ is the argument of S_{21} , and n is an integer determined to address the problem of phase ambiguity. The denominator of equation 9.7, which also appears in the numerator of equation 9.3, refers to the determination of the corrected phase, which is necessary when the sample thickness is greater than the wavelength in the sample material. The phase ambiguity problem is solved by a technique which involves measuring the phase shifts at two frequencies (Trabelsi et al., 2000).

These three density-independent calibration functions were analyzed for their stability in regard to different peanut types and for their type independence at frequencies from 5 to 15 GHz.

Type Independence

Among the different types of peanuts, there are structural and compositional differences, whether they are shelled or unshelled. Figure 9.3 provides an illustration of the structural differences observed in the peanut samples used in this study. Although not shown here, Spanish type peanuts are similar in structure to Runner type peanuts when unshelled. The pods average 2 to 2.5 cm in length; however, Spanish type peanuts have smaller kernels. Virginia type peanuts are known for their large size. The pods average 4 to 5.5 cm in length, and they have large kernels, giving the pod a large diameter (17 to 19 mm). Valencia type peanuts are known for their elongated pods which may be over 6 cm long and contain three or four kernels. The kernels are relatively small, giving the pod a smaller diameter (14 to 16 mm). As far as compositional differences, Spanish type peanuts are naturally higher in oil content than the other types (American Peanut Council, 2007). The TX Runner type peanuts used in this study have been genetically bred to increase their oleic oil content.

The evaluation of the feasibility of type-independent moisture content determination in peanuts is of great importance to the peanut industry. Presently used moisture meters have limitations such as moisture calibrations that are not transferable across different instruments and the need for different calibrations for each kind of grain or oilseed, and in most cases, different types. This adds complexity to grading instrumentation and introduces errors due to the wrong material type being selected during moisture analysis. These limitations result from the use of frequencies in the 1 to 20 MHz range, where the influence of ionic conduction comes into play.

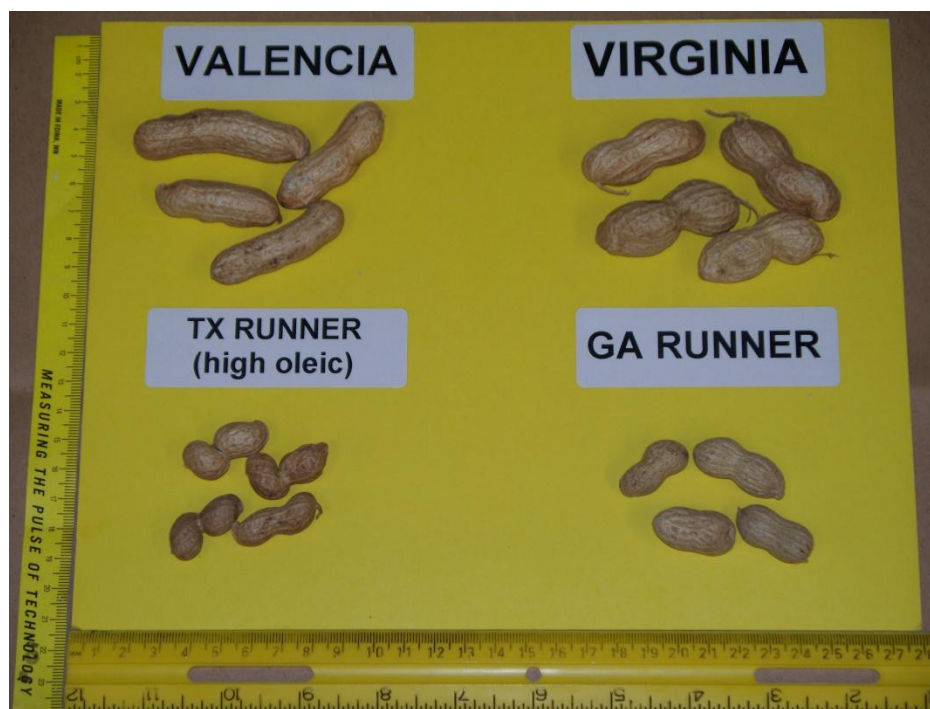


Figure 9.3: Structural differences shown for various peanut types

At these lower frequencies, the dielectric properties of grain and oilseed can be affected by factors such as kernel size, composition, type, growing location, or seasonal variation (Nelson, 1982). However, complex permittivity measurements for peanuts at microwave frequencies are unaffected by variations due to ionic conduction and are minimally affected by type and growing location (Lewis et al., 2009; Lewis et al., 2010). Type-independent moisture content determination is not just a recent observation for peanuts. It has been observed for years from complex permittivity measurements at microwave frequencies for materials such as soybean, corn and wheat (Trabelsi et al., 1998; Trabelsi and Nelson, 1998; Trabelsi and Nelson, 2004a).

9.4 Results and Discussion

When any of the three density-independent calibration functions is graphed versus moisture content, a linear trend is observed in which the function increases linearly with moisture content. An example of such observation is shown in Figure 9.4.

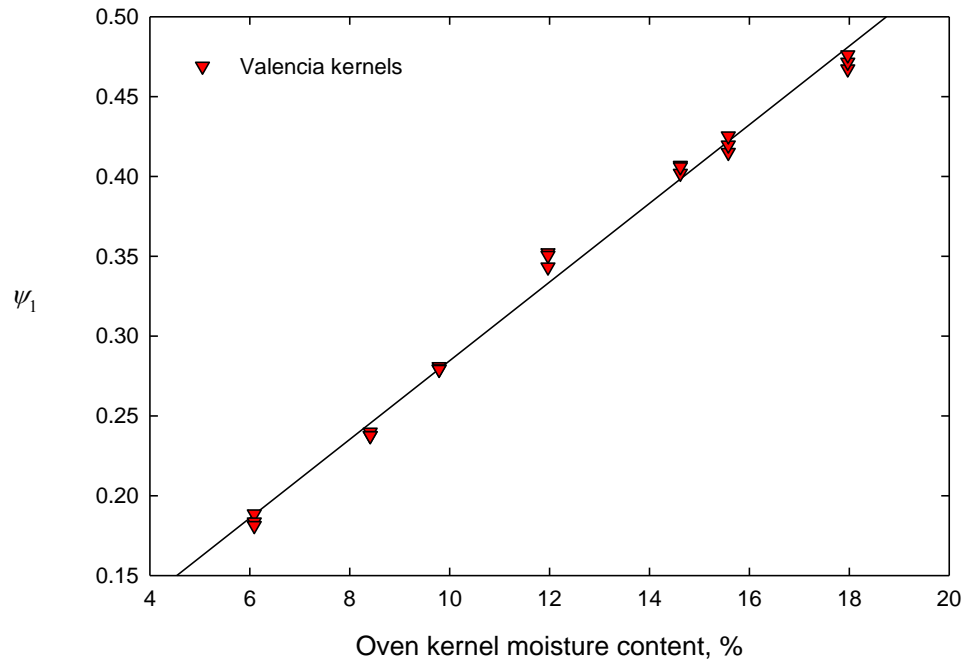


Figure 9.4: Variation of ψ_1 with kernel moisture content for Valencia type kernels measured at 6 GHz and 23 °C

Therefore, in all cases, a linear regression of the following form can be used to correlate ψ with moisture content:

$$\psi = AM + B \quad (9.8)$$

Equation 9.8 can be rearranged to solve for moisture content, M , as follows:

$$M = \frac{\psi - B}{A} \quad (9.9)$$

For each linear regression, the coefficient of determination (r^2), which serves as a measure of the strength of the correlation, and the standard errors of calibration (SEC) were calculated. The SEC is defined as:

$$SEC = \sqrt{\frac{1}{n-p-1} \sum_{i=1}^n (\Delta M_i)^2} \quad (9.10)$$

where n is the number of samples, p is the number of variables in the regression equation with which the calibration is performed, and ΔM_i is the difference between the predicted moisture content and the moisture content determined by the standard method for the i^{th} sample.

Moisture Content Determination for Individual Types

Before focusing on capabilities for type-independent moisture content determination in peanuts with functions ψ_1 , ψ_2 , and ψ_3 , the stability of the functions for individual types was examined. Measurements were taken to assess the performance of the calibration functions when applied to individual peanut types. Figures 9.5 and 9.6 show the linear regressions observed in each peanut type as ψ_1 was correlated with moisture content. The same behavior was observed for ψ_2 and ψ_3 . Tables 9.2 and 9.3 provide regression coefficients, r^2 values, and SEC values for the three functions for individual peanut-type kernels and pods, respectively.

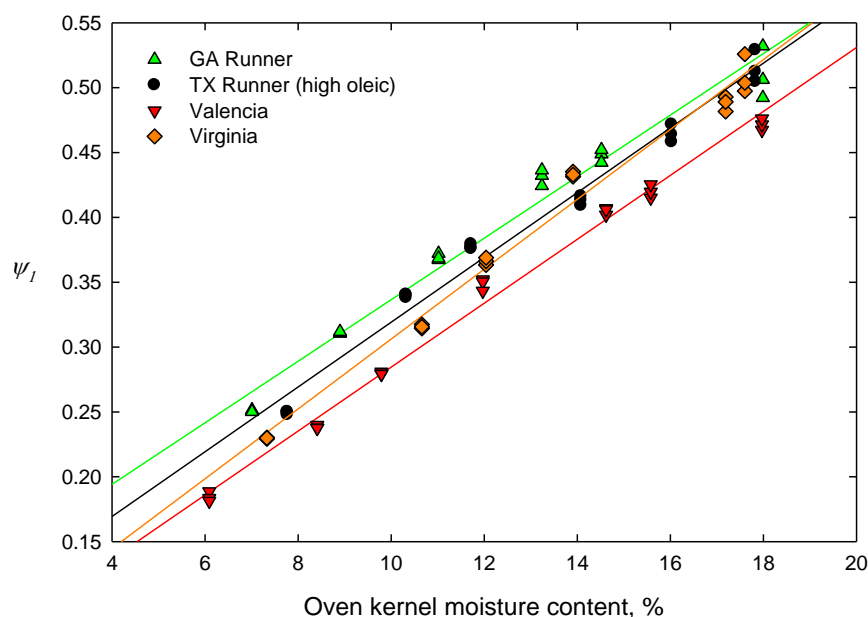


Figure 9.5: Variation of ψ_1 with moisture content for kernels of indicated types measured at 6 GHz and 23 °C (shown with individual calibrations)

Table 9.2: Regression statistics corresponding to equations (9.8) and (9.10) for moisture content prediction for kernels of specified peanut types at 6 GHz and 23 °C.

Peanut Type (kernels)	Density-Independent function	A	B	r^2	SEC, % m.c.
GA Runner	ψ_1	0.02373	0.09920	0.97	0.630
	ψ_2	0.02203	-0.01947	0.97	0.653
	ψ_3	0.002399	0.0005496	0.96	0.790
TX Runner (high oleic)	ψ_1	0.02497	0.06947	0.98	0.498
	ψ_2	0.02365	-0.04718	0.98	0.484
	ψ_3	0.002572	-0.002378	0.97	0.582
Valencia	ψ_1	0.02464	0.03813	0.99	0.360
	ψ_2	0.02607	-0.08261	0.99	0.347
	ψ_3	0.002879	-0.007144	0.99	0.449
Virginia	ψ_1	0.02694	0.03686	0.98	0.485
	ψ_2	0.02564	-0.07637	0.98	0.511
	ψ_3	0.002857	-0.006230	0.98	0.576

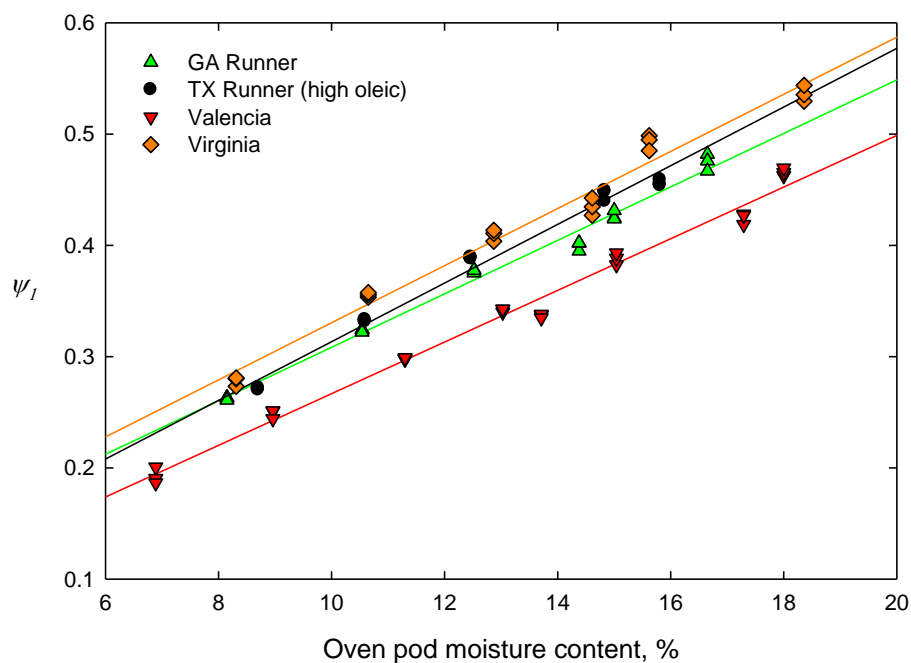


Figure 9.6: Variation of ψ_1 with moisture content for pods of indicated types measured at 6 GHz and 23 °C (shown with individual calibrations)

Table 9.3: Regression statistics corresponding to equations (9.8) and (9.10) for moisture content prediction of pods of specified peanut types at 6 GHz and 23 °C.

Peanut Type (pods)	Density-Independent function	A	B	r^2	SEC, % m.c.
GA Runner	ψ_1	0.02403	0.06802	0.98	0.351
	ψ_2	0.02122	-0.02495	0.98	0.473
	ψ_3	0.002565	-0.0004200	0.97	0.560
TX Runner (high oleic)	ψ_1	0.02637	0.04974	0.98	0.340
	ψ_2	0.02124	-0.03968	0.97	0.472
	ψ_3	0.002639	-0.002970	0.96	0.558
Valencia	ψ_1	0.02322	0.03447	0.98	0.437
	ψ_2	0.02348	-0.04790	0.99	0.419
	ψ_3	0.003005	-0.004098	0.98	0.426
Virginia	ψ_1	0.02566	0.07379	0.98	0.511
	ψ_2	0.02077	-0.01343	0.96	0.707
	ψ_3	0.002643	0.0002958	0.95	0.800

These results confirm that all three calibration functions can be used successfully to determine moisture content in peanut pods and kernels of all types with high coefficients of determination. The data in Tables 9.2 and 9.3 confirm that the regressions observed in Figures 9.5 and 9.6 exist for all functions in all peanut types. The entire study was performed with measurements ranging from 5 to 15 GHz at 1 GHz intervals. The efficiency of the three calibration functions for moisture content determination in peanuts of various types was observed over a broad range of frequencies. However, at higher frequencies, > 11 GHz for kernels and > 12 GHz for pods, the strength of the correlation between the calibration functions and moisture content tends to decline. Reasons for this decline include the effects of scattering, since, at higher frequencies, the wavelength is shorter than the length of a peanut pod.

Type-Independent Moisture Content Determination

The efficiency of moisture content determination for kernels and pods of all individual peanut types with the three density-independent calibration functions has been shown. The three functions were next evaluated with all peanut types combined and were again observed to correlate well with moisture content, having high coefficients of determination. Figures 9.7 and 9.8 show the linear trends observed for all peanut types combined, kernels and pods, for the three calibration functions. Table 9.4 provides the regression statistics for the graphs shown in Figures 9.7 and 9.8. A validation set of samples for each peanut type discussed was used to test the accuracy of type-independent moisture content determination for each of the three density-independent calibration functions. The moisture content of each sample in the validation set was calculated by using measured parameters to calculate the appropriate ψ and Equation 9.9 with coefficients shown in Table 9.4. Performance of each calibration function in moisture content determination was evaluated by calculating the standard error of performance (*SEP*) which is defined as:

$$SEP = \sqrt{\frac{1}{N-1} \sum_{i=1}^N (\Delta M_i - M)^2} \quad (9.11)$$

$$M = \left(\frac{1}{N}\right) \sum_{i=1}^N \Delta M_i \quad (9.12)$$

where N is the number of samples and ΔM_i is the difference between the predicted moisture content and the moisture content determined by the standard method for the i^{th} sample. Values for SEP for each corresponding calibration function (kernels and pods) are listed in Table 9.4.

Data in Table 9.4 show that type-independent moisture content determination in peanuts is feasible with all three calibration functions. When the r^2 and SEC values from Tables 9.2 and 9.3 are averaged and compared with those values of Table 9.4, results show that minimal accuracy is lost when converting from a calibration for an individual peanut type to one that includes all types. The statistical results shown in Tables 9.2 – 9.4 justify the use of one type-independent calibration function instead of four calibration functions for individual types.

The data corresponding to the SEP values listed in Table 9.4 can be observed graphically in Figures 9.9 and 9.10 for kernels and pod peanuts, respectively. The predicted moisture content, determined from each function, is plotted against the reference moisture content determined by oven drying for each calibration function. The solid diagonal line in the graphs shows the ideal relationship between the predicted and reference values of moisture content. Table 9.5 summarizes the physical characteristics and the measurement data for the kernel and pod samples used in the validation.

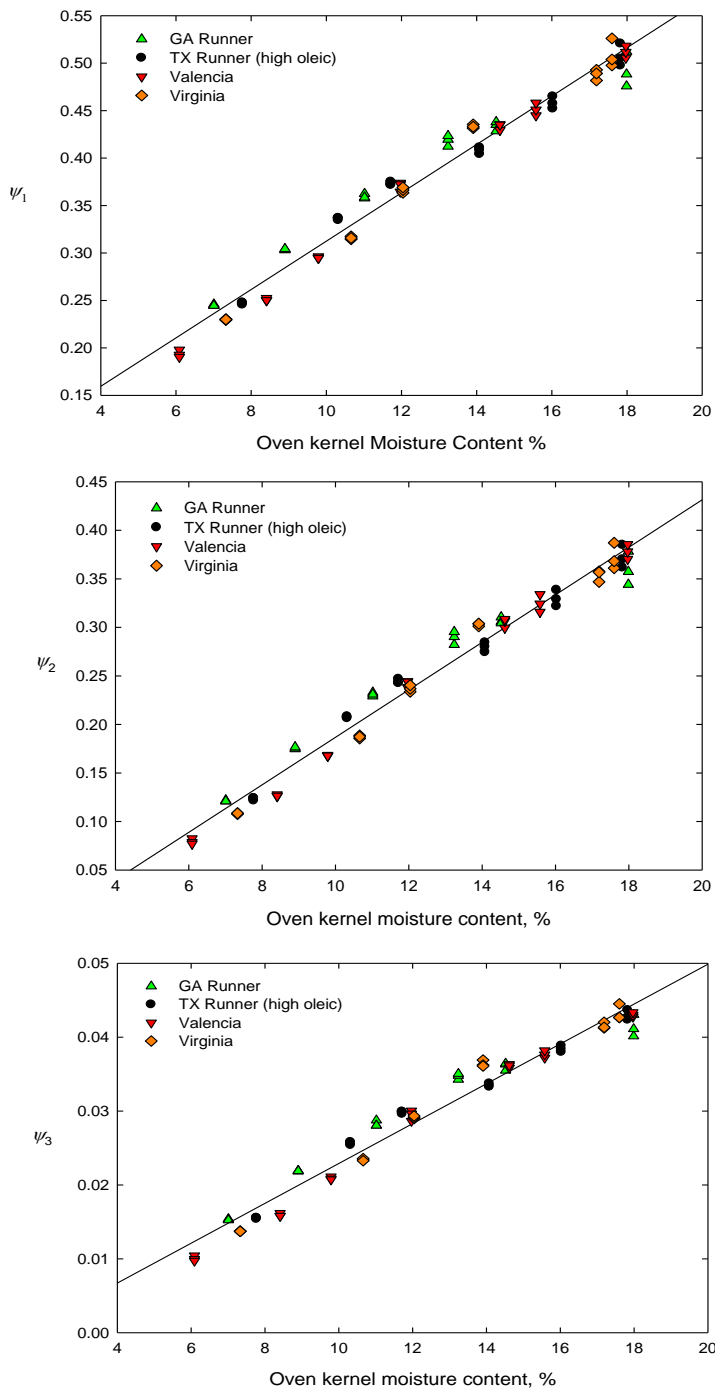


Figure 9.7: Variation of ψ_1 , ψ_2 , and ψ_3 with moisture content for kernels of combined indicated types at 6 GHz and 23 °C

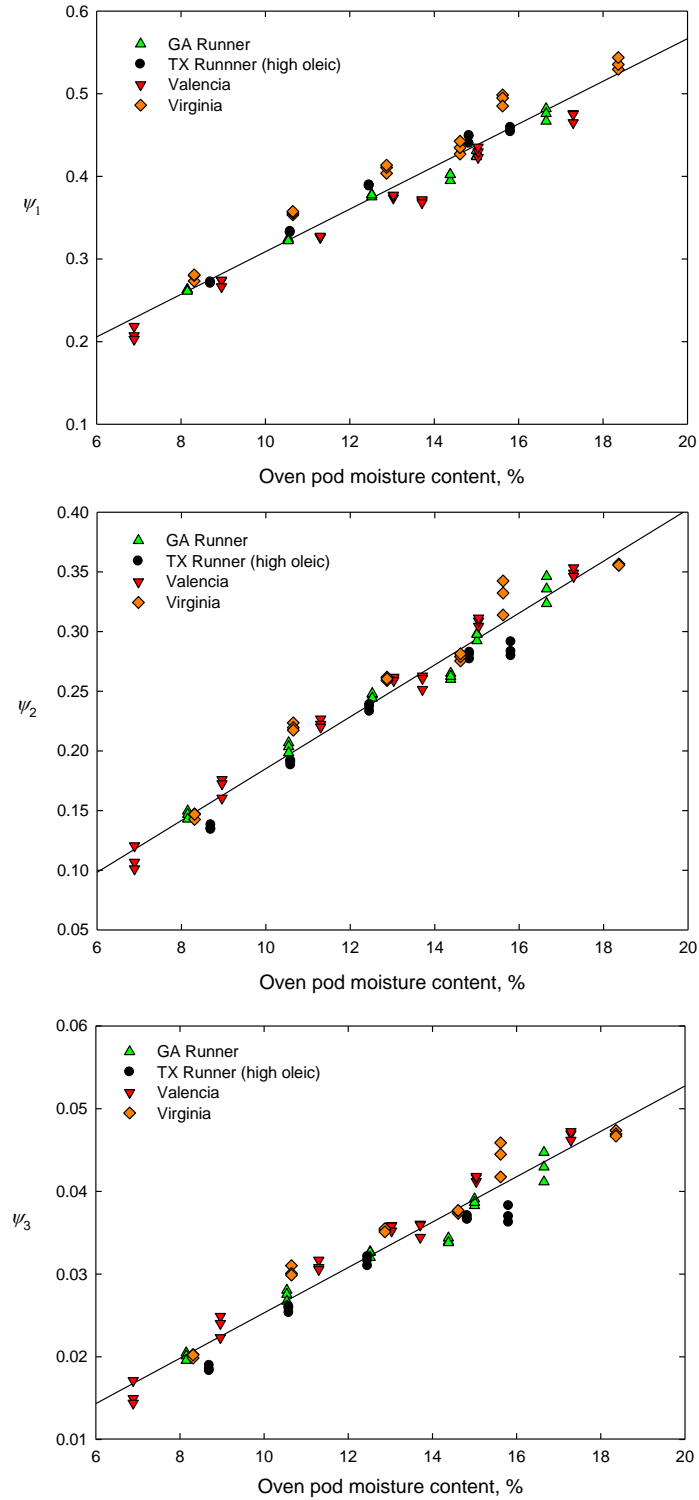


Figure 9.8: Variation of ψ_1 , ψ_2 , and ψ_3 with moisture content for pods of combined indicated types at 6 GHz and 23 °C

Table 9.4: Regression statistics corresponding to equations (9.8), (9.10) and (9.11) for type-independent moisture content determination for peanut kernels and pods at 6 GHz and 23 °C.

Peanut form	Moisture content range, %	Density-independent function	A	B	r^2	SEC, % m.c.	SEP, % m.c.
Kernels	6.1 – 18.0	ψ_1	0.02548	0.05755	0.98	0.587	0.264
		ψ_2	0.02447	-0.05796	0.98	0.578	0.282
		ψ_3	0.002697	-0.004075	0.97	0.678	0.283
Pods	6.9 – 18.4	ψ_1	0.02579	0.05082	0.95	0.706	0.298
		ψ_2	0.02173	-0.03206	0.96	0.609	0.296
		ψ_3	0.002744	-0.002132	0.94	0.764	0.362

The calibration functions were evaluated for their accuracy and stability in type-independent moisture content determination in peanuts over frequencies ranging from 5 to 15 GHz. Stability is assessed by evaluating the *SEC* and r^2 values of each function at each frequency. Figures 9.11 and 9.12 show graphical illustrations of the evaluation of the accuracy and stability of each calibration function for all peanut lots combined.

When comparing the graphs, better uniformity in the behavior of the three functions is observed for kernels than pods when determining moisture content with insensitivity to type. However, both sets of graphs show that as frequency increases, the standard error of calibration tends to increase and the coefficient of determination tends to decrease. The ideal frequency ranges for type-independent moisture content determination in kernels and pods with ψ_1 , ψ_2 , and ψ_3 , based on these measurements, are 5 to 11 GHz and 6 to 12 GHz, respectively. The best performance of all three functions is observed at approximately 6 GHz and 9 GHz.

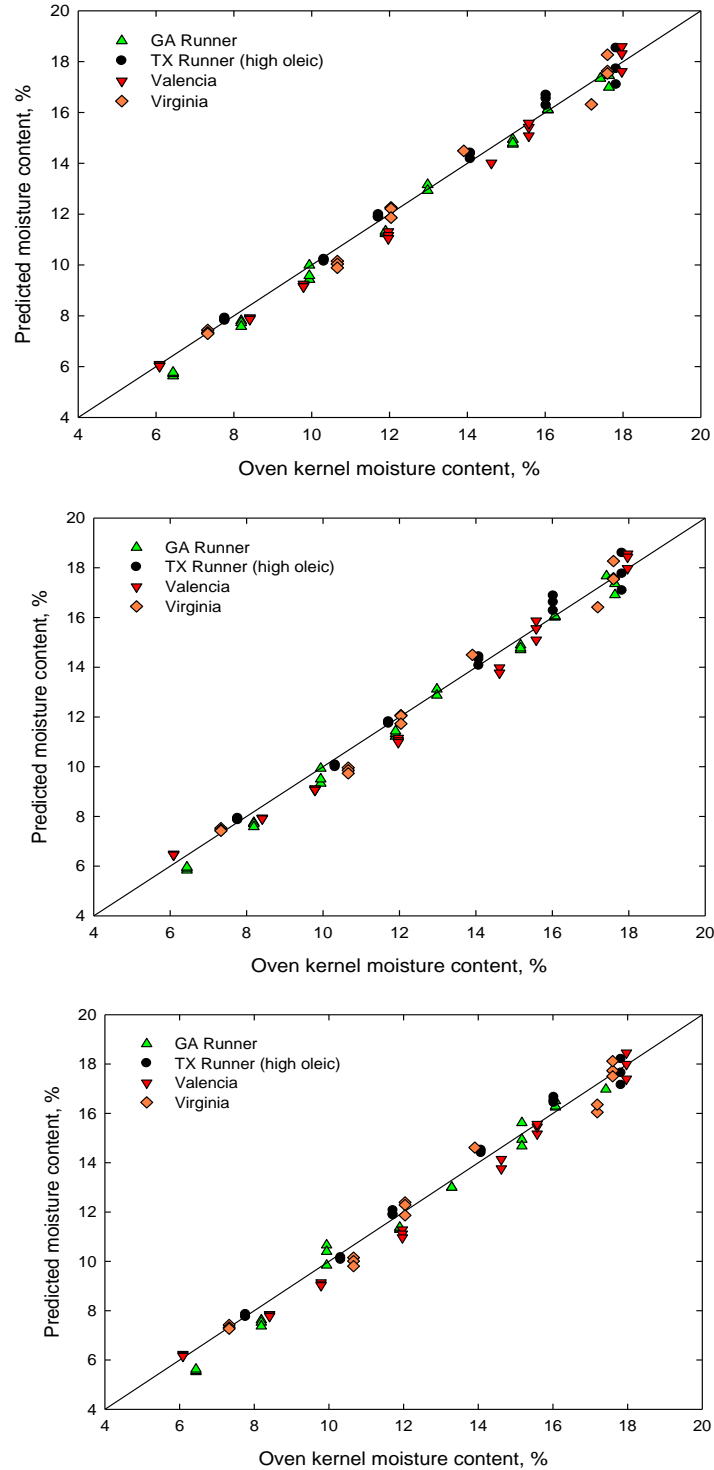


Figure 9.9: Predicted kernel moisture for ψ_1 , ψ_2 , and ψ_3 (top to bottom) versus reference moisture determined by oven drying

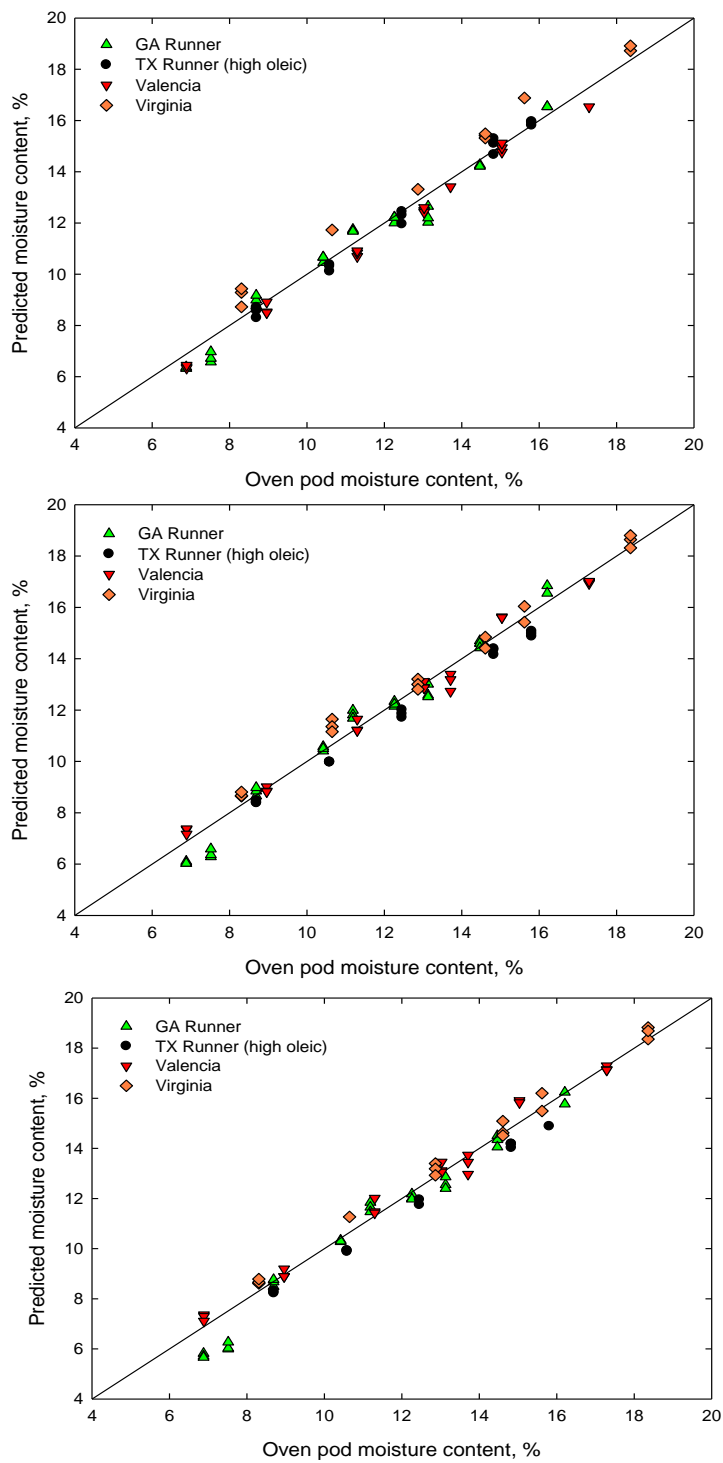


Figure 9.10: Predicted pod peanut moisture for ψ_1 , ψ_2 , and ψ_3 (top to bottom) versus reference moisture determined by oven drying

Table 9.5: Ranges of physical characteristics and measurement data for kernel and pod samples used for validation

Peanut form	Moisture content range, %	Density, g/cm³	Attenuation, dB	Phase Shift, degrees	ϵ'	ϵ''
Kernels	6.1 – 18.0	0.601 – 0.723	5.5 – 15.5	-594.2 – -280.4	2.2 – 4.7	0.10– 1.11
Pods	6.9 – 18.4	0.289 – 0.390	3.6 – 12.6	-374.4 – -252.5	1.5 – 2.1	0.04 – 0.31

In Figures 9.13 and 9.14, *SEP* values from the validation measurements are shown for each calibration function over a broad range of frequencies for kernels and pods, respectively. Better uniformity in the behavior of the three functions is again observed for kernels than pods. However, for kernels and pods, the standard error of performance supports the standard error of calibration. Trends observed in Figures 9.13 and 9.14 (for the validation set) are similar to those observed in Figures 9.11 and 9.12 (for the calibration set).

The reason for the better performance at lower frequencies is due to the fact that as the frequency increases from 5 to 15 GHz, the free-space wavelength decreases from 6 to 2 cm, respectively. Better performance from the three functions was observed for kernels because even though the wavelength is shorter at higher frequencies, the wavelength is still greater than the average kernel length. For pods, the wavelength becomes shorter than the length of the average pod at 11 GHz where the wavelength is 2.7 cm.

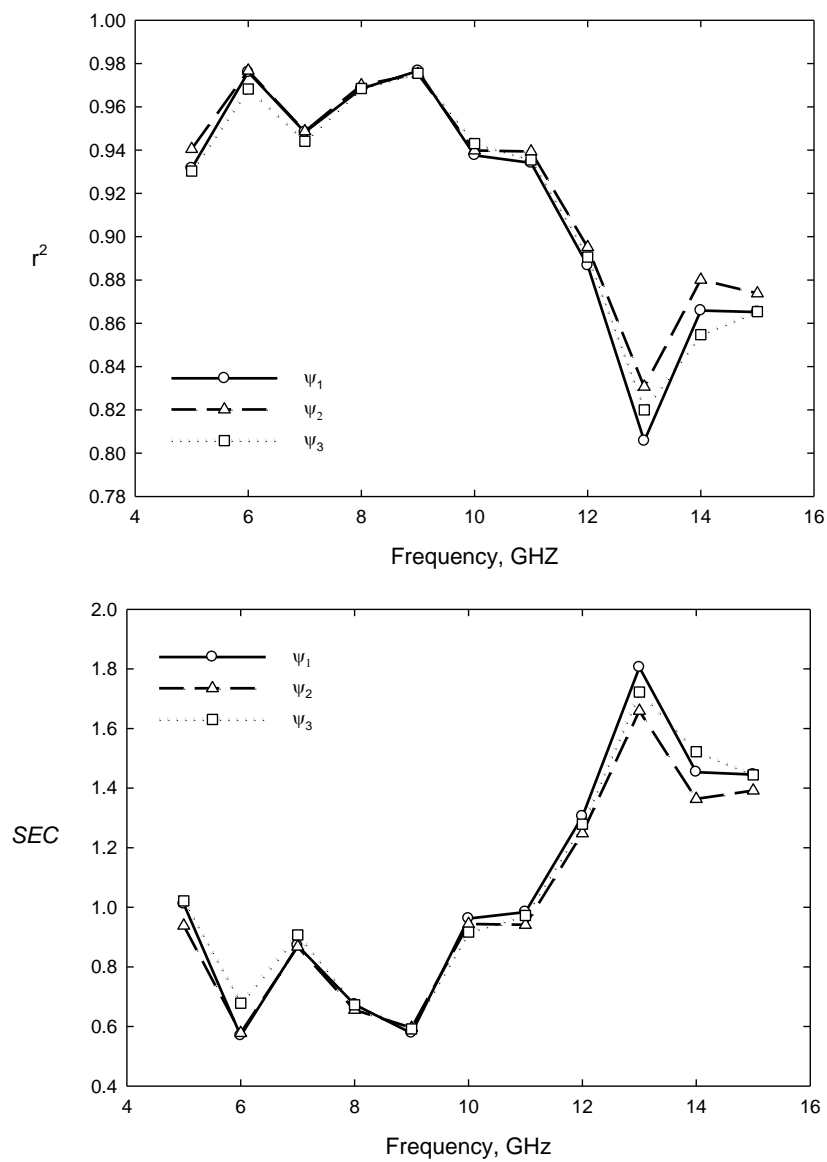


Figure 9.11: Variation of r^2 and SEC for ψ_1 , ψ_2 , and ψ_3 as frequency increases (peanut kernels)

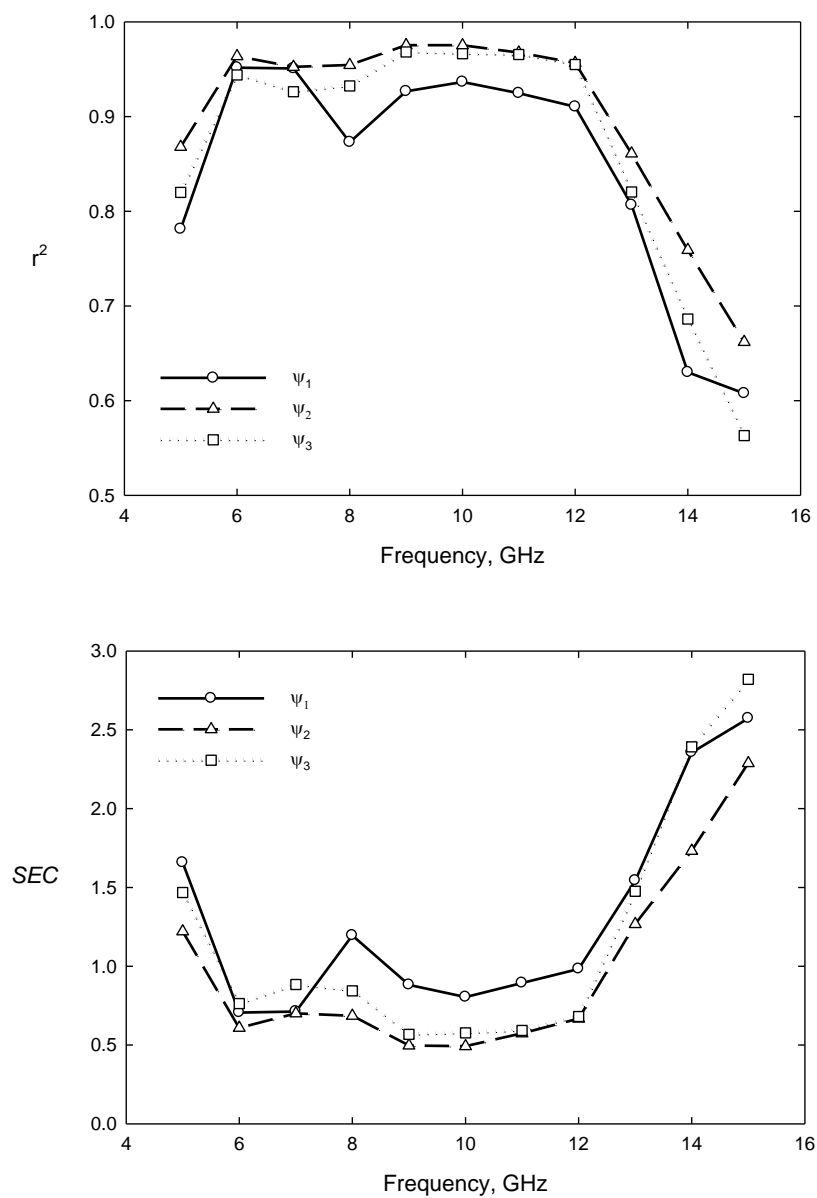


Figure 9.12: Variation of r^2 and SEC for ψ_1 , ψ_2 , and ψ_3 as frequency increases (pod peanuts)

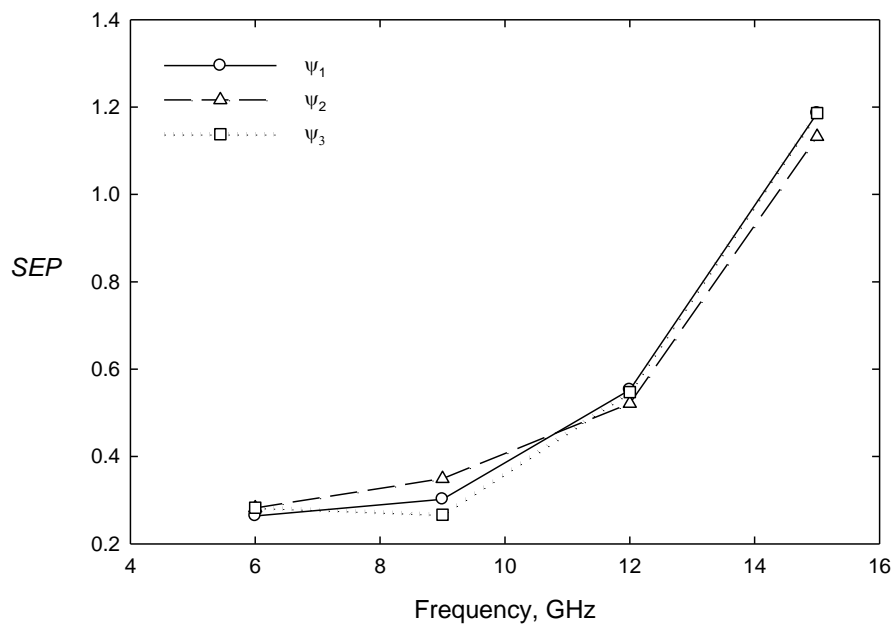


Figure 9.13: Variation of SEP for ψ_1 , ψ_2 , and ψ_3 as frequency increases (peanut kernels)

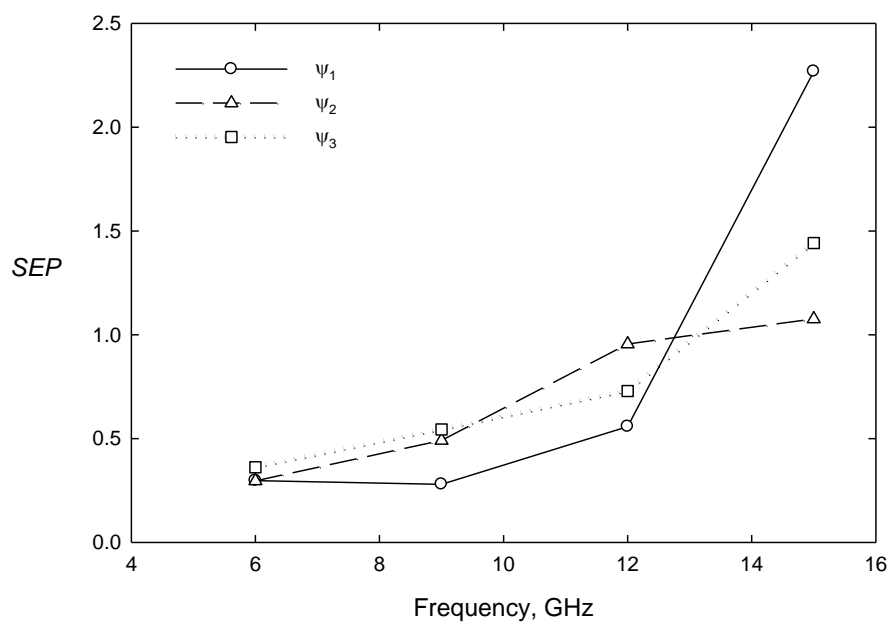


Figure 9.14: Variation of SEP for ψ_1 , ψ_2 , and ψ_3 as frequency increases (pod peanuts)

9.5 Conclusion

This study reaffirmed the feasibility of moisture content determination by microwave measurements in kernels and pod peanuts for various types of peanuts independent of density. It also demonstrated the feasibility of type-independent moisture content determination in both kernels and pod peanuts and confirmed suitable stability of type-independent calibration functions.

It was demonstrated that moisture content determination in peanut kernels and pods with insensitivity to density and type is achievable through free-space-transmission measurements of the complex permittivity. Type independence was demonstrated despite the compositional and structural differences in different peanut types. Stability and accuracy were analyzed and illustrated for microwave frequencies from 5 to 15 GHz with best accuracy shown in the 6 to 11 GHz range. Implementation of these density and type-independent calibration functions will be useful in decreasing the complexity of future microwave moisture sensors and in improving the utility of moisture meters.

Acknowledgements

The authors would like to thank Dr. Stanley Fletcher, Professor in Agricultural and Applied Economics at the University of Georgia and GA-Federal State Inspection Service personnel for supplying shelled and unshelled peanuts. Thanks are also expressed to Sean McKeown, engineering graduate student at the University of Georgia, for help with measurements and data analysis.

References

American Peanut Council. 2007. About the peanut industry. Available at: <http://www.peanutsusa.com/index.cfm?fuseaction=home.page&pid=12>. Accessed 12 March 2007.

- ASAE Standards, 49th ed. 2002. S410.1: Moisture Measurement - Peanuts. St. Joseph, Mich: ASAE.
- Bussey, H. E. 1967. Measurement of the RF properties of materials - a survey. *Proceedings of the IEEE*. 55(6): 1046-1053.
- Chung, S.-Y., S. Maleki, E. T. Champagne, K. L. Buhr, and D. W. Gorbet. 2002. High-oleic peanuts are not different from normal peanuts in allergenic properties. *Journal of Agricultural and Food Chemistry*. 50(4): 878-882.
- Irudayaraj, J., and C. Reh. 2008. *Nondestructive testing of food quality*. Ames, IA: Blackwell Publishing.
- Jacobsen, R., W. Meyer, and B. Schrage. 1980. Density-independent moisture meter at X-band. *Proceedings of 10th European Microwave Conference*. Warsaw, Poland. 216-220.
- Kraszewski, A. W., and S. Kulinski. 1976. An improved microwave method of moisture content measurement and control. *IEEE Transactions on Industrial Electronics and Control Instrumentation*. 23(4): 364-470.
- Lewis, M., S. Trabelsi, S. O. Nelson, and E. W. Tollner. 2009. Type-independent calibration method for microwave moisture sensing in unshelled and shelled peanuts. Paper No. 096136. St. Joseph, Mich.: ASABE.
- Lewis, M., S. Trabelsi, S. O. Nelson, and E. W. Tollner. 2010. Stability and type-independence analysis of density-independent calibration functions for microwave moisture sensing in unshelled and shelled peanuts. Paper No. 1009857. St. Joseph, Mich.: ASABE.
- Meyer, W., and W. Schilz. 1980. A microwave method for density independent determination of the moisture content of solids. *Journal of Physics D: Applied Physics*. 13(10): 1823-1830.
- Nelson, S. O. 1973. Electrical properties of agricultural products - a critical review. *Transactions of the ASAE*. 16(2): 384-400.
- Nelson, S. O. 1982. Factors affecting the dielectric properties of grain. *Transactions of the ASAE*. 25(4): 1045-1049.
- Nelson, S. O., and S. Trabelsi. 2004. Principles for microwave moisture and density measurements in grain and seed. *Journal of Microwave Power and Electromagnetic Energy*. 39(2): 107-118.
- Trabelsi, S., A. W. Kraszewski, and S. O. Nelson. 1998. New density-independent calibration function for microwave sensing of moisture content in particulate materials. *IEEE Transactions on Instrumentation and Measurement*. 47(3): 613-622.
- Trabelsi, S., A. W. Kraszewski, and S. O. Nelson. 1999. Determining physical properties of grain by microwave permittivity measurements. *Transactions of the ASAE*. 42(2): 531-536.

- Trabelsi, S., A. W. Kraszewski, and S. O. Nelson. 2000. Phase-shift ambiguity in microwave dielectric properties measurements. *IEEE Transactions on Instrumentation and Measurement*. 49(1): 56-60.
- Trabelsi, S., A. W. Kraszewski, and S. O. Nelson. 2001. Universal calibration method for microwave moisture sensing in granular materials. *Transactions of the ASAE*. 44(3): 731-736.
- Trabelsi, S., M. A. Lewis, and S. O. Nelson. 2008. Frequency, temperature, density, and moisture dependence of dielectric properties of unshelled and shelled peanuts. Paper No. 084412. St. Joseph, Mich.: ASABE.
- Trabelsi, S., S. Nelson, and M. Lewis. 2009. Microwave nondestructive sensing of moisture content in shelled peanuts independent of bulk density and with temperature compensation. *Sensing and Instrumentation for Food Quality and Safety*. 3(2): 114-121.
- Trabelsi, S., and S. O. Nelson. 1998. Density-independent functions for on-line microwave moisture meters: A general discussion. *Measurement Science and Technology*. 9(4): 570-578.
- Trabelsi, S., and S. O. Nelson. 2003. Free-space measurement of dielectric properties of cereal grain and oilseed at microwave frequencies. *Measurement Science and Technology*. 14(5): 589-600.
- Trabelsi, S., and S. O. Nelson. 2004a. Calibration methods for nondestructive microwave sensing of moisture content and bulk density of granular materials. *Transactions of the ASAE*. 47(6): 1999-2008.
- Trabelsi, S., and S. O. Nelson. 2004b. Microwave dielectric properties of shelled and unshelled peanuts. *Transactions of the ASAE*. 47(4): 1215-1222.
- Trabelsi, S., and S. O. Nelson. 2006. Microwave sensing technique for nondestructive determination of bulk density and moisture content in unshelled and shelled peanuts. *Transactions of the ASAE*. 49(5): 1563-1568.
- University of Georgia. 2003. World geography of the peanut. Available at: <http://lanra.anthro.uga.edu/peanut/>. Accessed 20 February 2007.
- Virginia-Carolina Peanut Promotions. 2007. Everything about peanuts. Available at: <http://www.aboutpeanuts.com>. Accessed 22 March 2007.
- Von Hippel, A. R. 1954. *Dielectric materials and applications*. New York, NY: The Technology Press of MIT. and John Wiley and Sons.

CHAPTER 10
INTEGRATING AN EMBEDDED SYSTEM WITHIN A MICROWAVE MOISTURE
METER¹

¹ Lewis, M.A. and S. Trabelsi. Submitted to *Biological Engineering*, 11/29/11.

Abstract

The conversion of a PC or laptop-controlled microwave moisture meter to a stand-alone meter hosting its own embedded system is discussed. The moisture meter measures the attenuation and phase shift of low power microwaves traversing the sample, from which the dielectric properties are calculated. The power level of the microwaves is similar to that of Wi-Fi. Therefore, the sample is unharmed and no heating occurs. The dielectric properties are then used for rapid and nondestructive determination of the moisture content in the grain or seed sample. The previous system consisted of the moisture meter being controlled via USB interface by an external laptop or PC. Though effective, the system lacked full portability and was susceptible to computer crashes and interruptions in communication between the meter and laptop. To improve the system, a microcontroller was selected in the design of an embedded system for the moisture meter. The microcontroller provides a graphical 144 x 32 pixel LCD and 16-button keypad to facilitate user interaction. The embedded system provides the following functionalities: user interface (input/output), event execution, process control, data acquisition and data storage. Testing shows that the moisture meter with the new embedded system maintains the performance and accuracy observed for the original meter with PC or laptop control. Results are included to show the similarity of measurements taken with the microwave meter (both versions) to measurements taken with a vector network analyzer. The integration of the embedded system with the microwave moisture meter provides a cost-effective, portable, and robust solution for microwave moisture sensing.

10.1 Introduction

As the world's population continues to increase, so does the demand for foods and other goods produced by the agricultural industry. However, as the demand of production increases, so does the strain of quality and safety assurance. Farming, handling, and processing of grain and seed commodities require rapid and accurate testing methods for characterization. One parameter often tested in agricultural goods is moisture content, as it aids decision making for storage, drying and production applications. For example, when the quality of peanuts is assessed, the moisture content accounts for 20% of the final grade. Determination of physical properties such as moisture content with high efficiency and accuracy is imperative in the assessment of quality and safety. Standard reference methods require oven-drying at specified temperatures for predetermined lengths of time (ASAE, 2002). To determine the moisture content of unshelled peanuts (pod peanuts), 100 g of sample must be dried at 130 °C for six hours. Such methods are time consuming and are destructive to the material, making their use impractical in industrial settings. For this reason, secondary methods have been established and are in development for moisture content determination.

Research has shown that dielectric properties can be successfully used to determine physical properties of cereal grain and oilseed (Nelson, 1973; Nelson et al., 1998; Trabelsi et al., 1999a; Trabelsi and Nelson, 1998). Dielectric properties can be determined from accurate and effective microwave measurements of complex permittivity, ϵ . The relative complex permittivity, $\epsilon = \epsilon' - j\epsilon''$, influences the wave-matter interaction and can be considered as the electrical signature of a given material (Trabelsi et al., 1999a). The dielectric constant ϵ' and the dielectric loss factor ϵ'' are indicative of the capability of a material to store electric energy and dissipate electric energy, respectively. For this purpose, a microwave moisture meter was

developed within USDA ARS (Trabelsi et al., 2001a; Trabelsi et al., 2010; Trabelsi and Nelson, 2003b; Trabelsi et al., 2008b; Trabelsi et al., 2008c). The moisture meter is based on the free-space transmission measurement technique (Trabelsi and Nelson, 2003a) and uses low-power microwaves for rapid and nondestructive determination of moisture content in grain or seed samples. Microwave power levels used are ≤ 32 mW, which is comparable to Wi-Fi power levels; therefore, the sample is unharmed and no microwave heating occurs.

The measurement process begins with the measurement of two voltages from electronic circuits while an empty sample holder is placed between two antennas; these voltages are referred to as the reference voltages. After the sample holder has been filled with the material of interest, it is replaced between the antennas, and the two voltages are measured again. Using the two sets of voltages, the attenuation and phase shift caused by the material are determined, and from these values the dielectric properties are calculated. By using the dielectric properties of the material, moisture content is determined with appropriate calibration functions (Trabelsi et al., 1998; Trabelsi and Nelson, 1998; Trabelsi and Nelson, 2004a).

The previous version of the microwave moisture meter developed for peanuts is shown in Figure 10.1. Figure 10.2 shows the power connection and the USB connection to the controlling laptop or PC. Original software was developed in Visual Basic to provide a graphical user interface (GUI) to facilitate the measurement process. The voltages were measured with a Measurement Computing¹ USB-1608FS 16-bit data acquisition module. Its libraries were embedded into original software to control data acquisition.

¹ Mention of company or trade names is for purpose of description only and does not imply endorsement by the U. S. Department of Agriculture or The University of Georgia



Figure 10.1: Previous version of microwave moisture meter (controlled by external laptop)

Throughout extensive testing in the laboratory and during deployment at peanut buying points, the moisture meter has proven to be robust in accuracy and repeatability. However, its major vulnerability lies within the controlling laptop. In the past, laptop crashes or interrupts in communication with the laptop have rendered the moisture meter unusable. Such events, as well as the lack of full portability, made it desirable to develop a portable, stand-alone system, nonsusceptible to breaches in operation due to failure of an external controller. Therefore, an embedded solution was sought to integrate with the microwave moisture meter.

A SensorCore (SC) microcontroller, manufactured by Tern, Inc., was selected and programmed to control the measurement process and data acquisition. This controller was used in the development of an embedded system providing user interface (input/output), event execution, process control, and data acquisition and storage. The methodology for implementing the stand-alone system and the comparative results are discussed.



Figure 10.2: USB connection on rear of moisture meter

10.2 Materials and Methods

Microcontroller Selection

In many of today's electronic devices, microcontrollers are at the helm of operation and functionality. Household appliances such as microwave ovens and washing machines have at least one microcontroller embedded. Such appliances usually have one main function and do it repetitively. Microcontrollers are also used in research and engineering applications to aid in control and data acquisition (Li et al., 2006; Siyami et al., 1987). They usually receive some type of user input and are programmed to perform one task repeatedly and accurately (Heath, 2003). Therefore, the hardware and software involved are usually robust and simplified as much as possible to reduce number of working parts and complexity.

The most critical step in the design of the embedded system was the selection of the appropriate microcontroller. A suitable microcontroller was needed to integrate within the existing microwave moisture meter; one that would provide at least the same performance as the previous system and provide room for future expansion. As several microcontrollers were

evaluated, the following criteria were taken into consideration: analog-to-digital converter (ADC) resolution, static random-access memory (SRAM) size, cost, feasibility of interface with LCD and keypad, availability of ports for added sensors, and provisions for data storage.

The ADC resolution is the most important attribute. Many potential microcontrollers were quickly eliminated because ADC resolution was less than 16-bit. During the selection process, it was also discovered that there were minimal options in which a microcontroller had an ADC that read bipolar voltage ranges. Therefore, a voltage level shifter circuit was considered. After microcontrollers with qualifying ADC resolution were identified, they were screened out by cost and interface possibilities with LCD and keypad. Upon the conclusion of the selection process, the SensorCore (SC) microcontroller was chosen. Its main attributes include reasonable cost, 24-bit Sigma Delta ADC, 512 MB RAM, 512 MB electrically erasable programmable read-only memory (EEPROM), data storage up to 2 GB via CompactFlash interface, compact size (2.0" x 4.5"), and 16-button keypad with graphical LCD. The microcontroller is easy to program, and it provides feasibility for future expansion. Figure 10.3 shows an illustration of the microcontroller with keypad and LCD. The original keypad configuration consisted of alphanumeric buttons, 0-9 and A-F. However, modifications were made to make the following options available: backspace (←), decimal (.) and enter (↵).

Data Acquisition

Although the resulting output is moisture content of the measured sample, the essence of the microwave moisture meter lies within the measurement of attenuation and phase shift, which are used to calculate the dielectric properties. The accuracy with which the voltages representing attenuation and phase shift are measured determines the accuracy of the moisture content prediction.

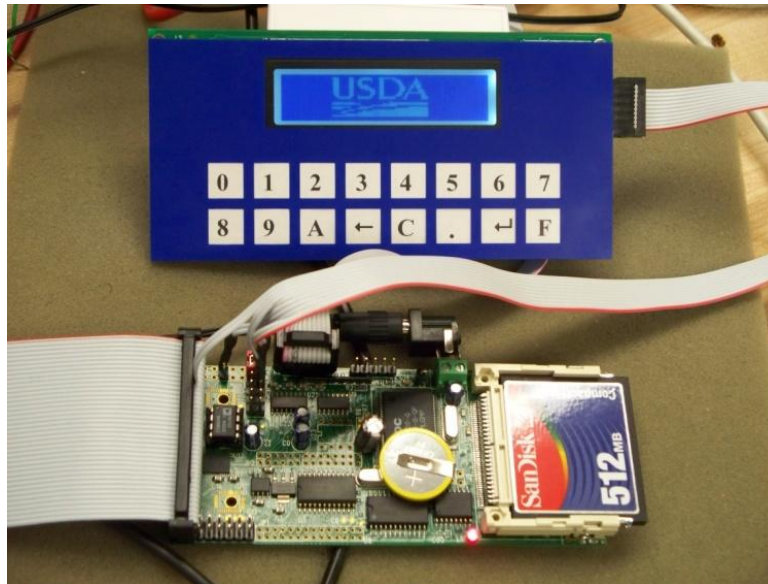


Figure 10.3: SensorCore (Tern, Inc.) microcontroller shown with 16-button keypad and graphical LCD

In the previous system, the data acquisition system provided 16-bit resolution, 100 M Ω input impedance, and capability of reading voltages in a bipolar range. Measurements with that system have shown that, depending on the moisture content and/or temperature of the sample, voltages can be measured as small as 0.1 mV. This is why high-order resolution was needed. Table 10.1 shows the achievable resolution at specified bit configurations. A minimum of 16-bit resolution is needed to provide a voltage resolution that is less than 0.1 mV. It was also observed from measurements with the previous system that the output voltages from the moisture meter were within a range from -1 V to +1 V, which emphasizes the need for distinguishing bipolar voltages.

The SC microcontroller was configured with a Linear Technology® 24-bit sigma delta ADC. The sigma-delta architecture provides the ability to adjust the resolution of the ADC by changing the sampling rate. The reference voltage is configured so that the ADC reads voltages

in a range from 0 to 2.5V. The range of voltages the ADC reads is unipolar; however, the range of voltages that is provided by the moisture meter is bipolar. Level shifter circuitry was implemented to shift the voltages output by the moisture meter from a bipolar range to a unipolar range.

Table 10.1: Resolution for various standard bit configurations over a 0 to 2.5 V range

	Number of digital values	Digital range	Voltage resolution, V (for range 0 – 2.5V)
8-bit	256	0 – 255	0.009766
10-bit	1024	0 – 1023	0.002441
12-bit	4096	0 – 4095	0.0006104
16-bit	65536	0 – 65535	0.00003815
24-bit (variable sample rate)	8388608	0 - 8388607	0.0000002980

The output voltages from the moisture meter serve as input to the ADC of the microcontroller. From previous measurements, an input range of ± 1 V was defined. Therefore, a level shifter circuit was implemented to add 1 V to the voltages output by the moisture meter and account for this shift later within the software. This changed the ± 1 V bipolar input range to a unipolar range of 0 to 2 V. The level shifter was implemented by designing a summing amplifier that would add 1 V to the incoming signal. The equation for the summing amplifier is:

$$V_{out} = -R_F \left(\frac{V_1}{R_1} + \frac{V_2}{R_2} \right) \quad (10.1)$$

where V_1 is the voltage output from the moisture meter, V_2 is the added voltage of 1 V, R_1 and R_2 are the resistors to which the corresponding voltages were applied, R_F is the feedback resistor for the signal feedback to the negative input of the operational amplifier (op-amp) and V_{out} is the voltage measured from the output of the summing amplifier. In this application, the initial

voltage range is only being shifted up by +1 V. Therefore, the gain value is equal to one, and all the resistor values are equal. Thus, Equation 10.1 reduces to:

$$V_{out} = -(V1 + V2) \quad (10.2)$$

In the implementation of the circuit, 100 kΩ resistors were used to provide valid input impedance. Through simulation and testing, an OP07 ultralow offset voltage op-amp was used in the circuit because of its provision of minimal offset. In the completion of the circuit, an inverting amplifier was added to the output of the summing amplifier to invert the voltages to the proper signs for correspondence. Table 10.2 shows the values as measured at the output of both amplifiers within the circuit. The voltages in the table show that it is only at the output of the inverting amplifier that the proper voltage shift is achieved.

Table 10.2: Voltage values measured throughout the level shifter

After Summing Amp			After Inverting Amp		
V ₁	V ₂	V _{out}	V ₁	V ₂	V _{out}
-1	1	0	-1	1	0
0	1	-1	0	1	1
1	1	-2	1	1	2

Figures 10.4 and 10.5 show a schematic diagram of the simulated circuit and an illustration of the implemented circuit, respectively. In Figure 10.4, V1 represents one of the output voltages from the moisture meter, and V2 represents the added 1 V. The summing amplifier is represented as U1, and voltages V1 and V2 serve as input to U1. The output of the summing amplifier (U1) is used as input to the inverting amplifier, U2. The output from U2 is the voltage that is read by the ADC.

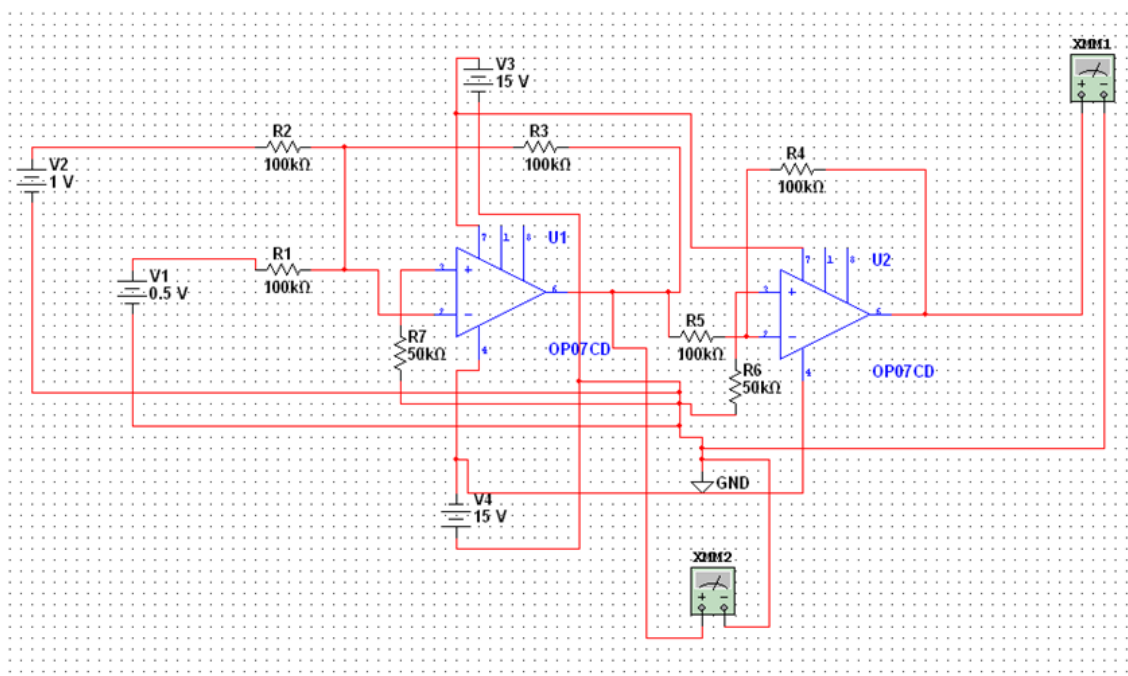


Figure 10.4: Schematic diagram of level shifter circuit simulated in Multisim

The level shifter circuit was tested in the laboratory with an Agilent E3631A triple output DC power supply. It was used to supply the added 1 V that provides the shift, and it was used to provide the 15 V and -15V supply voltages to the op-amps. The power supply in the microwave moisture meter is an HK15A-15/A single output 115VAC input industrial power supply manufactured by TDK-Lambda. It has an output of 15 V and was chosen because of its stability, compact size and low price to power the microwave circuits in the moisture meter. Integrating the level shifter circuit with a single output power supply required a few hardware innovations to account for the 1 V needed and the negative supply voltage. The original 15 V output of the power supply was used to provide the positive supply voltage to the op-amps.

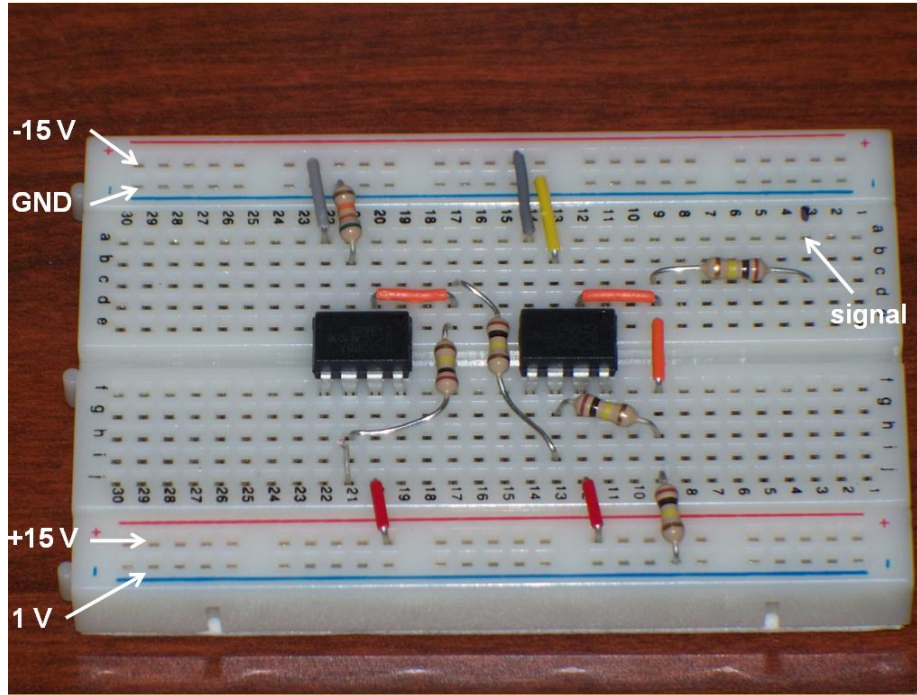


Figure 10.5: Implementation of level shifter circuit

Utilizing the stability of the power supply, a voltage divider was used to generate 1 V from the 15 V output. Voltage dividers are simple circuits used to produce an output voltage, V_{out} , which is a fraction of its input voltage, V_{in} . The equation for the voltage divider is expressed as:

$$V_{out} = \frac{R_2}{R_1 + R_2} \times V_{in} \quad (10.3)$$

where V_{in} is the voltage supplied to the divider, R_1 and R_2 are resistor values, and V_{out} is the resulting voltage. In this instance, R_1 was equal to 17.2 k Ω which consisted of a 15 k Ω resistor and 2.2 k Ω resistor connected in series; R_2 was 1239.2 Ω which consisted of resistors of 1.5, 2.2, 22 Ω and 1.2 k Ω values connected in series. Theoretically, these values, with a V_{in} of 15 V, would yield a V_{out} value of 1.008 V. However, since actual resistance values for the resistors were not exactly as specified, the measured V_{out} value was 0.994 V. Figure 10.6 shows the

implementation of the voltage divider. The 1 V output from the voltage divider was applied to a strip on the breadboard that supplies the appropriate pins of the op-amps used in the level shifter. A capacitor was connected between R_2 and ground.

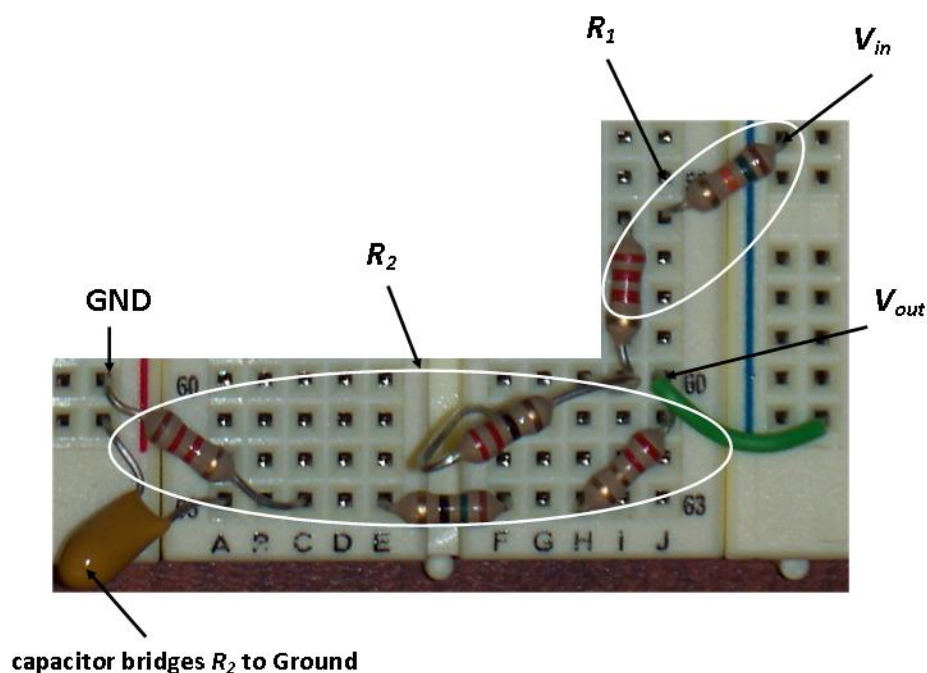


Figure 10.6: Voltage divider implemented for level shifter circuit

Next, a hardware solution was sought to account for the negative supply voltage needed for each op-amp. In ideal cases, the positive and negative supply voltages are symmetric. However, unless the full negative voltage swing is needed, stability can be maintained with a higher negative supply voltage, > -15 V for this application. In order to test for the maximum negative supply voltage needed to maintain stability, -15 V was applied to the op-amp and was increased until the output of the op-amp was observed to deteriorate. Voltages were measured with an Agilent 34401A 6 $\frac{1}{2}$ digit multimeter. Results showed that a maximum of -3.9 V was needed at the negative supply to maintain stability. A MAX1044 switched-capacitor voltage

converter was used to generate the negative supply voltage required by the op-amps. It required a 10 V input; therefore, an LM7810 3-terminal positive voltage regulator was used to supply the 10 V. The LM7810 was able to use the 15 V already available as input. Figure 10.7 shows the MAX1044 and LM7810 as implemented on the breadboard. The measured output from the MAX1044 was -8.03 V. Figure 10.8 shows the entire circuit responsible for conditioning the signals output from the microwave moisture meter (level shifter, voltage divider, and components for negative supply voltage). Capacitors throughout the circuit were added for decoupling, buffering and filtering purposes. The microwave moisture meter, complete with installed microcontroller, LCD display, and keypad, is shown in Figure 10.9.

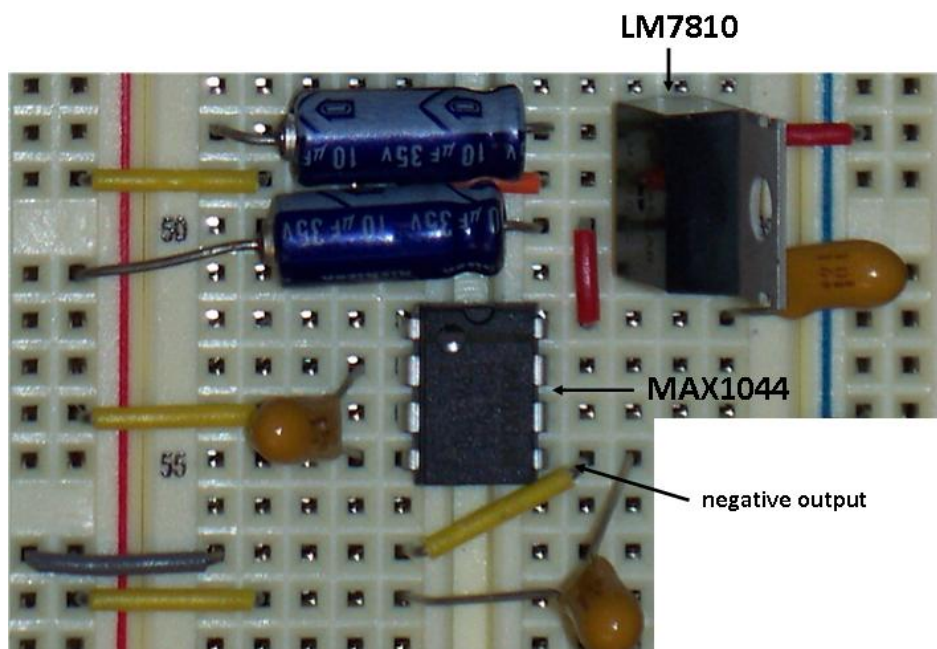


Figure 10.7: Circuitry solution for negative supply voltage

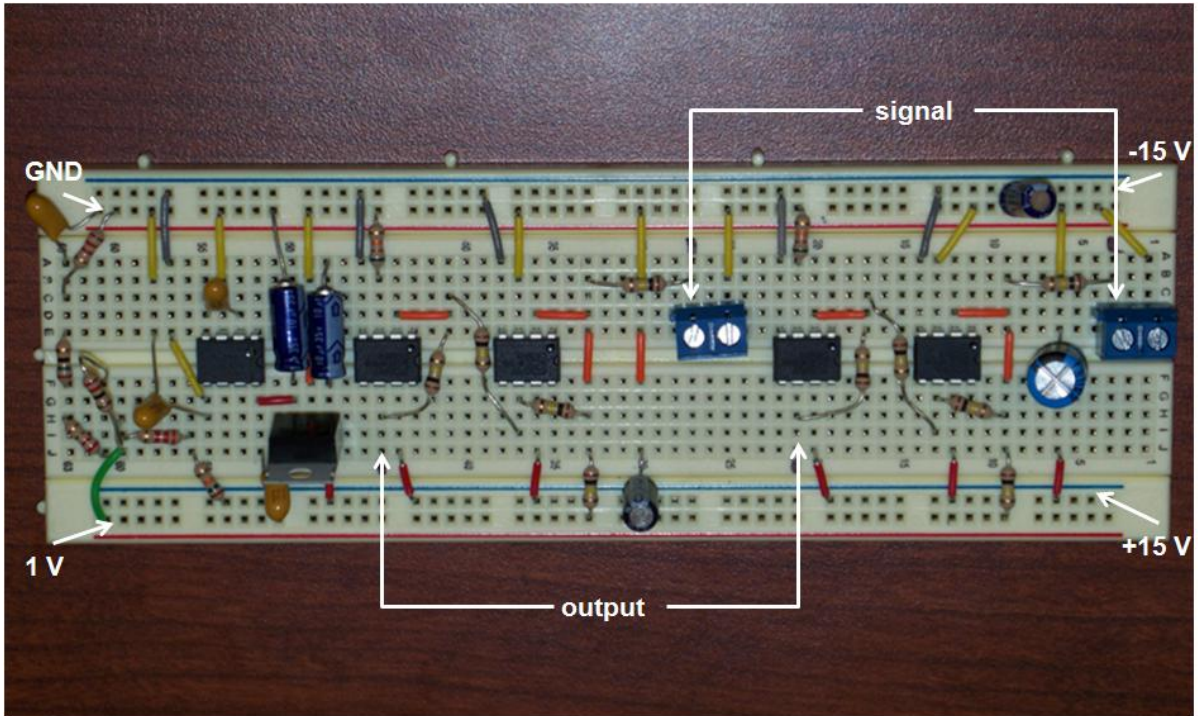


Figure 10.8: Complete circuit for signal conditioning



Figure 10.9: Microwave moisture meter shown with LCD and keypad (embedded system)

Software Generation

Software for the previous version of the microwave meter was written in Visual Basic. The user was able to proceed with the measurement process through interaction with the GUI. The software to control the embedded system and guide the measurement process was written in C programming language and was created in the Paradigm Integrated Development Environment which was provided with the microcontroller. User interaction is now established via LCD and keypad. The software was created to be event-driven and user friendly. The code was developed in a modular format and was divided into four classes: `bitmap`, `port_sens`, `data_acquisition`, and `calculations`. The classes are listed in order of execution.

The `bitmap` class controls the scrolling bitmap images that display when the moisture meter is turned on initially or reset. The `port_sens` class governs the measurement process and serves as the main class for the software. Upon its execution, steps are given plainly such that the measurement process can be followed by non-skilled workers. It is also during this time that information regarding the sample is entered, and the sample is inserted into the meter. The `data_acquisition` class handles the reading of the voltages and conversion from analog to digital to float values that can be manipulated later in calculations. The `calculations` class uses the voltages to calculate the dielectric properties of the sample. Coded algorithms are then used to determine the moisture content from the dielectric properties (Trabelsi and Nelson, 1998). Once the calculation of the moisture content of the material is completed, the moisture content is displayed on the LCD. A flowchart supporting this is shown in Figure 10.10.

Each step in the measurement procedure for the moisture meter is shown on the LCD, and user interaction is required before it advances to the next step. Instructions and help documentation are also available to aid users.

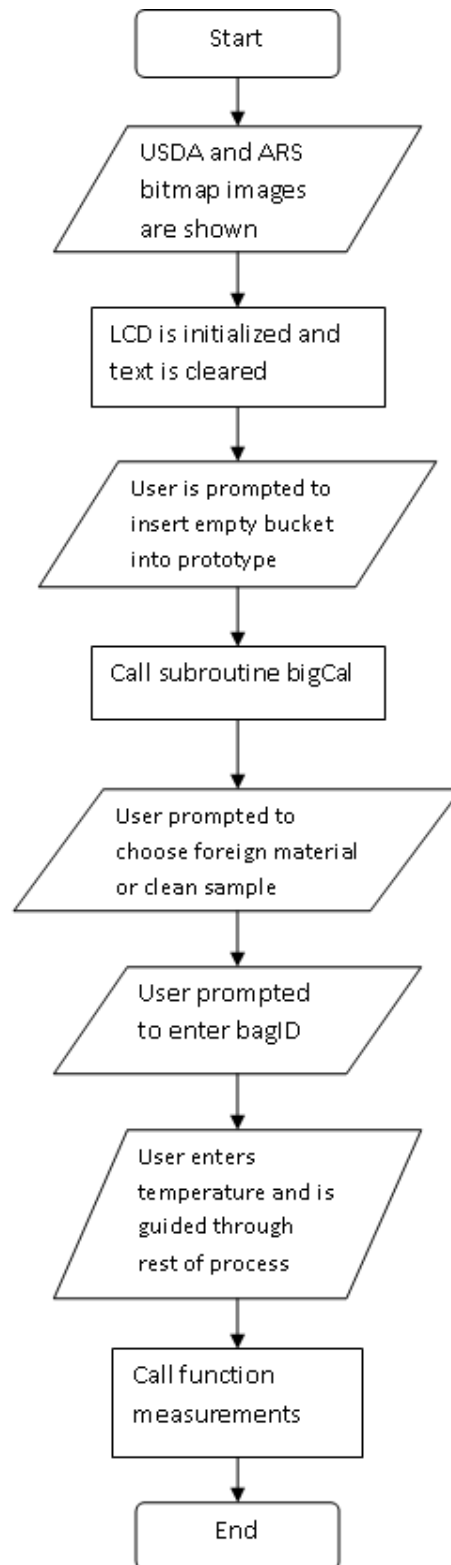


Figure 10.10: Flowchart for main program execution

During the development of the software, it was tested by users of various skill sets to aid in the creation of a user-friendly measurement experience. The end result was an executable program with installation and operation and instructions to guide the user.

10.3 Results and Discussion

The underlying goal throughout the implementation of the embedded system was to at the very least maintain the performance observed in the previous system in which the microwave moisture meter was controlled by an external laptop. Low-cost and practical components were chosen to make this goal theoretically achievable. Five percent tolerance resistors were used because of their availability and the provision of a foundation with which to assess performance. System behavior was stable with these resistors. The OP07 op-amps were used instead of the common LM741 op-amps because of their minimal offset.

Once the embedded system was completed, measurements were conducted with unshelled Georgia Runner type peanuts to compare the performance of the embedded system with that of the laptop-controlled system. Table 10.3 shows the results from 10 replications taken on both systems within a 17-minute period. For each replication, the same sample was measured with each system with no changes in the presentation of the sample. An identical separate sample holder was used for the reference measurement requiring an empty sample holder. This experiment was performed to assess the stability of measurements with the embedded system.

The data in the table for the embedded system compare well with those of the laptop-controlled system. As mentioned earlier, the accuracy of moisture content determination depends on the accuracy with which the dielectric properties are determined. Therefore, in Table 10.3 the raw data are shown from measurements.

Table 10.3: Results from measurements taken on unshelled Georgia Runner type peanuts comparing the embedded system to the laptop-controlled system

Laptop-Controlled System				Embedded System			
Attn, dB	Phase, degrees	ϵ'	ϵ''	Attn, dB	Phase, degrees	ϵ'	ϵ''
2.47	131.799	1.615	0.049	2.60	132.261	1.614	0.052
2.48	131.790	1.615	0.049	2.60	131.786	1.615	0.052
2.44	131.210	1.617	0.049	2.61	131.880	1.615	0.052
2.43	130.976	1.617	0.048	2.60	131.506	1.616	0.052
2.46	130.978	1.617	0.049	2.63	131.512	1.616	0.052
2.43	130.527	1.619	0.048	2.60	131.007	1.617	0.052
2.45	133.647	1.609	0.049	2.60	130.940	1.618	0.052
2.44	132.983	1.611	0.049	2.62	130.906	1.618	0.052
2.45	132.623	1.613	0.049	2.59	130.505	1.619	0.052
2.48	132.233	1.614	0.049	2.60	130.569	1.619	0.052

The standard deviations observed in the attenuation and phase shift from measurements taken with the laptop-controlled system were 0.018886 and 0.996685, respectively. The standard deviations observed in the attenuation and phase shift from measurements taken with the embedded system were 0.011785 and 0.588683, respectively. Therefore, these results confirm that the performance of the microwave moisture meter was maintained in the conversion to the embedded system.

To further evaluate the performance of the embedded system, more measurements were taken with it, and they were compared to measurements taken in free space with a Hewlett-Packard 8510C vector network analyzer (VNA) and a pair of horn-lens antennas (Trabelsi and Nelson, 2003a). Previous research has shown how the response and performance of the microwave moisture meter compares well to that of the VNA (Trabelsi and Nelson, 2007; Trabelsi et al., 2008b). Figures 10.11 and 10.12 show variation of the dielectric properties, each

divided by density, with moisture content as determined by the oven drying method. Figure 10.11 shows a comparison between the laptop-controlled system and the VNA from measurements on Georgia Runner type unshelled peanuts from the 2007 harvest season. Figure 10.12 shows a comparison between the embedded system and the VNA from measurements on Runner type unshelled peanuts from the 2010 harvest season.

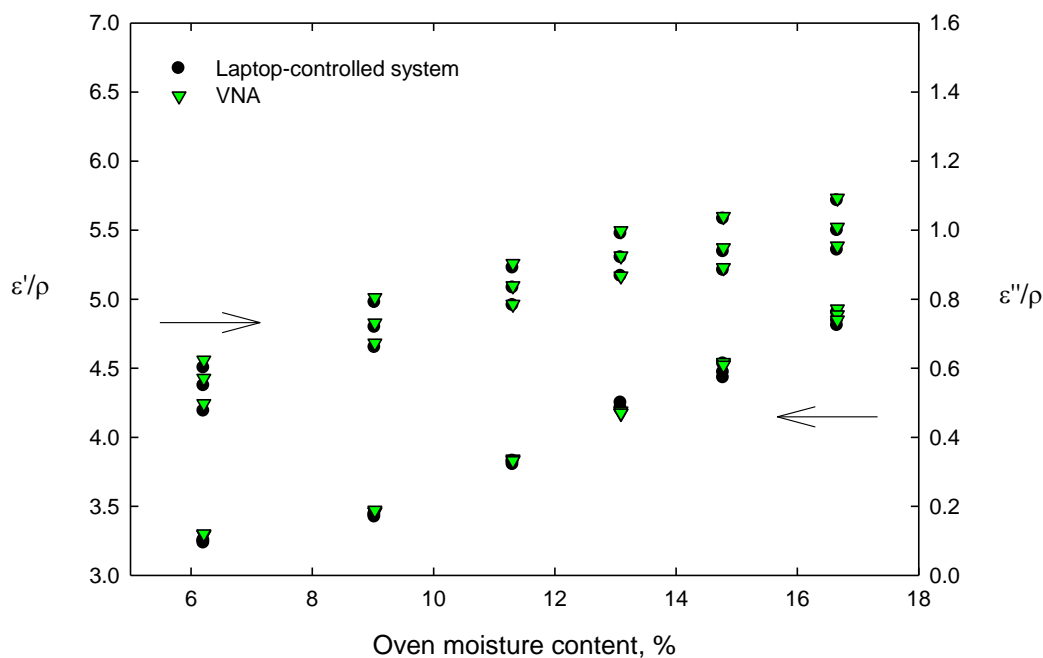


Figure 10.11: Variation of dielectric properties with moisture content shown on laptop-controlled system and VNA

One-way, analyses of variance (ANOVA) were performed to analyze the data for any significant differences between measurements taken with the microwave moisture sensor (laptop controlled or embedded system) and the VNA. In each case, the two measurement systems being compared were considered as two treatments. As shown in Figure 10.11, three replicates of measurements for dielectric properties with both systems were taken when the microwave sensor

was laptop controlled. As shown in Figure 10.12, two replicates of measurements were taken when the microwave sensor was controlled by the embedded system. The null hypothesis assumes there is no significant difference between the two treatments in each case. Observing the ANOVA results in Table 10.4, we accept the null hypothesis at the 1 % level and the 5 % level because all p-values in the table are much greater than 0.01 and 0.05. We can conclude that measurable differences between the measurement systems are minimal because the p-values are so high.

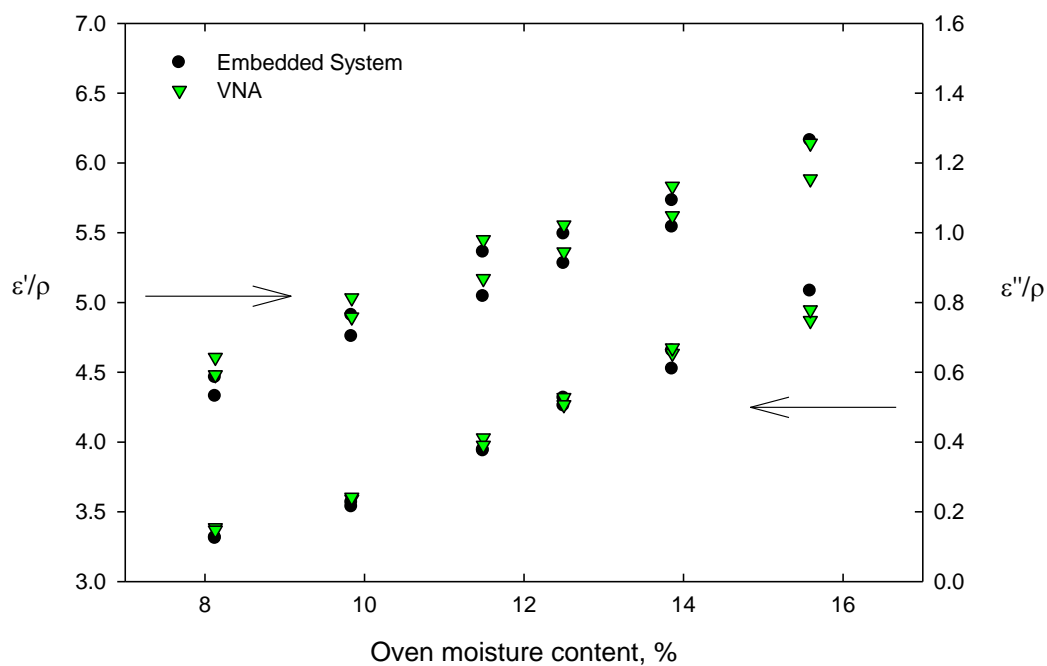


Figure 10.12: Variation of dielectric properties with moisture content shown on embedded system and VNA

Table 10.4: One-way analysis of variance results for system comparison

Parameter	P-values	
	VNA vs. Embedded System	VNA vs. Laptop-controlled System
Dielectric Constant	0.8891	0.8434
Dielectric Loss Factor	0.9232	0.8926

The data from the graphs show that in both cases, even with data taken from measurements three years apart, the microwave moisture meter's performance is comparable to that of the VNA. Data values obtained from measurements with the moisture meter, whether laptop-controlled or stand-alone, are virtually superimposed on those obtained from measurements with the VNA. The statistical analysis shows no significant differences between the measurement systems. These results confirm that integration of the embedded system caused no deterioration in performance of the microwave moisture meter.

10.4 Conclusion

A microcontroller was used in the implementation of an embedded system, resulting in the development of a stand-alone version of the previous laptop-controlled microwave moisture meter. All phases of development were approached systematically, and all desired levels of functionality in the system were achieved. Software was tested to ensure that the measurement process was user friendly. Standard deviation values for attenuation and phase shift from measurements taken with embedded system (0.011785 and 0.588683) were less than those observed from measurements with the laptop controlled system (0.018885 and 0.996685). ANOVA results show no significant differences between the microwave moisture sensor and the VNA at the 1 % and 5 % level. Resulting p-values are high, confirming minimal difference between systems. Performance compared well with that of VNA. Therefore, the performance and stability of the system were maintained.

The implementation of the embedded system enhances the reliability of the moisture meter and eliminates the need for external control from a peripheral instrument, increasing the portability. Implementing the embedded system also reduces the cost of the moisture meter, making it more attractive for widespread use.

Acknowledgements

The authors would like to thank Professor Takoi Hamrita, Department of Biological and Agricultural Engineering, The University of Georgia, Athens, GA, for guidance in microcontroller selection and insight towards a systematic and methodical approach to design, development and integration of the embedded solution. The authors would also like to thank Professor Mark Haidekker, Department of Biological and Agricultural Engineering, The University of Georgia, for guidance in signal conditioning and circuit completion.

References

- ASAE Standards*, 49th ed. 2002. S410.1: Moisture Measurement - Peanuts. St. Joseph, Mich: ASAE.
- Heath, S. 2003. *Embedded systems design*. United Kingdom: Newnes.
- Li, Z., N. Wang, G. S. V. Raghavan, and W. Cheng. 2006. A microcontroller-based, feedback power control system for microwave drying processes. *Applied Engineering in Agriculture*. 22(2): 309-314.
- Nelson, S. O. 1973. Electrical properties of agricultural products - a critical review. *Transactions of the ASAE*. 16(2): 384-400.
- Nelson, S. O., S. Trabelsi, and A. W. Kraszewski. 1998. Advances in sensing grain moisture content by microwave measurements. *Transactions of the ASAE*. 41(2): 483-487.
- Siyami, S., B. R. Tennes, H. R. Zapp, G. K. Brown, B. A. Klug, and J. R. Clemens. 1987. Microcontroller-based data acquisition system for impact measurement. *Transactions of the ASAE*. 30(6): 1822-1826.
- Trabelsi, S., A. W. Kraszewski, and S. O. Nelson. 1998. New density-independent calibration function for microwave sensing of moisture content in particulate materials. *IEEE Transactions on Instrumentation and Measurement*. 47(3): 613-622.

- Trabelsi, S., A. W. Kraszewski, and S. O. Nelson. 1999. Determining physical properties of grain by microwave permittivity measurements. *Transactions of the ASAE*. 42(2): 531-536.
- Trabelsi, S., A. W. Kraszewski, and S. O. Nelson. 2001. New calibration technique for microwave moisture sensors. *IEEE Transactions on Instrumentation and Measurement*. 50: 877-881.
- Trabelsi, S., M. A. Lewis, and S. O. Nelson. 2010. Microwave moisture meter for rapid and nondestructive grading of peanuts. Paper No. 1009183. St. Joseph, Mich.: ASABE.
- Trabelsi, S., and S. O. Nelson. 1998. Density-independent functions for on-line microwave moisture meters: A general discussion. *Measurement Science and Technology*. 9(4): 570-578.
- Trabelsi, S., and S. O. Nelson. 2003a. Free-space measurement of dielectric properties of cereal grain and oilseed at microwave frequencies. *Measurement Science and Technology*. 14(5): 589-600.
- Trabelsi, S., and S. O. Nelson. 2003b. Nondestructive multiparameter microwave sensor. Paper No. 036129. St. Joseph, Mich.: ASAE.
- Trabelsi, S., and S. O. Nelson. 2004. Calibration methods for nondestructive microwave sensing of moisture content and bulk density of granular materials. *Transactions of the ASAE*. 47(6): 1999-2008.
- Trabelsi, S., and S. O. Nelson. 2007. A low-cost microwave sensor for simultaneous and independent determination of bulk density and moisture content in grain and seed. Paper No. 076240. St. Joseph, Mich.: ASAE.
- Trabelsi, S., S. O. Nelson, and M. Lewis. 2008a. Microwave moisture sensor for grain and seed. *Biological Engineering*. 1(2): 195-202.
- Trabelsi, S., S. O. Nelson, and M. Lewis. 2008b. Practical microwave meter for sensing moisture and density of granular materials. *Instrumentation and Measurement Technology Conference Proceedings, 2008. IMTC 2008. IEEE*. 1021-1025.

CHAPTER 11

**AN AUTOMATED APPROACH TO PEANUT DRYING WITH REAL-TIME
MONITORING OF IN-SHELL MOISTURE CONTENT WITH A MICROWAVE
SENSOR¹**

¹ Lewis, M.A., S. Trabelsi, S.O. Nelson, E.W. Tollner, and M.A. Haidekker. To be submitted to Transactions of the ASABE

Abstract

Peanut drying is an essential task preceding the grading process. Kernel moisture is one of five parameters used to establish the grade for a specific lot of peanuts, and it is imperative that peanuts be dried to a kernel moisture content $< 10.5\%$ wet basis for grading and storage purposes. Today's peanut drying processes utilize decision support software based on modeling and require substantial human interaction for moisture sampling. These conditions increase the likelihood of peanuts being overdried or underdried. This research addresses the need for an automated controller with real-time, in-shell kernel moisture content determination capabilities. By using a microwave moisture meter, developed within USDA ARS, the moisture content of the peanut kernel can be determined without having to shell the peanut pod. The kernel moisture content and atmospheric conditions serve as inputs to the controller, and thus, air temperature and drying time are controlled automatically. Such implementation reduces overdrying and underdrying, preserves quality of peanuts, and minimizes energy consumption through efficient control of the heater. In this paper, a quarter-scale drying system with automated control is discussed. Results show promise for large-scale implementation and testing.

11.1 Introduction

After being harvested, peanuts are inspected and graded to determine the overall quality and on-farm value for commercial sales. The grading process is facilitated by inspectors of the Agricultural Marketing Service (AMS) and the Federal-State Inspection service (FSIS) at buying points or shelling plants near the peanut fields (American Peanut Council, 2007; Butts et al., 2008). During this process, a representative sample of uncleaned and unshelled peanuts, weighing about 3 kg, is taken from each drying trailer and is analyzed to determine meat content, size of pods (unshelled peanuts), amount of damaged kernels (shelled peanuts), amount of foreign material, and kernel moisture content. These five parameters are used to establish the grade. However, when peanuts initially arrive at buying points and shelling plants, they are considerably high in moisture content, despite having been left in windrows to dry naturally before being collected with combines (Virginia-Carolina Peanut Promotions, 2007). Therefore, drying is an essential task preceding the grading process. It is imperative for peanuts to be dried below 10.5% w.b. kernel moisture content for grading and storage purposes.

To facilitate the drying process, peanuts are loaded into drying wagons. These wagons are 6.4 m long, 2.4 m wide, and 1.27 m deep above a perforate floor, which is at the top of a 23 cm high air plenum (Butts and Williams, 2004). Then dryers (propane or natural gas) are connected to the wagons through canvas ducts, and heated air is blown into the airspace below the bed of peanuts. The airspace pressurizes, forming an air plenum, and air is forced up through the peanuts to decrease the moisture content of the bed (Butts, 1995; Butts et al., 2004; Butts and Williams, 2004). Peanuts are dried in this fashion until the target moisture is reached. Then, a representative sample of peanuts is extracted from the wagon and taken to be graded. While being graded, if the kernel moisture content is determined to be $\geq 10.50\%$, the sample is marked

with a label, “NO SALE”, and the corresponding lot of peanuts has to be taken back to the drying shed and further dried.

When peanuts arrive at buying points and shelling stations, they are in peanut pod form and are mixed with foreign material. Foreign material includes rocks, dirt, sticks, and other field debris collected by the combine during harvesting. Current official moisture meters used in the peanut grading industry require sample preparation for kernel moisture content determination. To sample kernel moisture content, a sample of a few hundred grams of peanuts is taken from the trailer. At this point, the sample still contains foreign material; therefore, the sample has to be cleaned using machinery that separates the peanut pods from foreign material found in the sample. After the sample is cleaned, it is shelled to separate the peanut kernels from the shells. Then the kernels are analyzed for kernel moisture content. This process is performed when the peanuts first arrive to determine the initial kernel moisture content and is repeated every time the kernel moisture content of the drying bed of peanuts is analyzed.

There are decision support systems and other control systems that are presently used commercially to estimate the drying time based on initial atmospheric conditions and the initial kernel moisture content of the bed of peanuts (Butts et al., 2003; Butts et al., 2004; Butts and Hall, 1994; Microtherm Inc, 2000). Such systems are based on peanut drying models and either assume certain atmospheric conditions or require frequent updates of any changes in the atmospheric conditions. However, because of the present methodology for kernel moisture content determination, these systems demand heavy user interaction such as sampling for kernel moisture content and updating current atmospheric conditions. Atmospheric conditions affect drying dynamics greatly (Beasley and Dickens, 1963; Troeger, 1989). If these parameters are not updated appropriately, the peanuts are likely to be overdried or underdried. In many instances,

peanut buying points are under-staffed; therefore, an operator may or may not be able to manage the drying process with the frequency needed. Systems that are able to monitor the atmospheric conditions in real-time still lack such capabilities for kernel moisture content.

There is ongoing research to address problems observed in the peanut grading process, which has remained unchanged for approximately 50 years. Several projects have targeted the need for innovation in the determination of kernel moisture content (Allgood et al., 1995; Allgood et al., 1993; Blankenship and Davidson, 1980; Blankenship and Davidson, 1984; Paine, 1969). However, many of these works discuss monitoring weight loss of the entire wagon of drying peanuts to indirectly observe the change in moisture content. Such methods have not been adopted for many reasons. Weighing platforms are costly to add to every stall of a drying bay. Weight loss unrelated to moisture content can result in false predictions, resulting in underdrying. These methods do not provide information on uniformity of the moisture content throughout the entire drying wagon.

The kernel moisture content is the main parameter of interest in the drying process, and it is the only parameter, besides temperature, that the drying system is working to control. However, since it is difficult to obtain, control for it is often indirect and misguided. Therefore, providing a simple, in-process, accurate method for determination of kernel moisture content while drying would significantly reduce troubles faced presently with drying. For this reason, this paper discusses a feedback controlled system that monitors kernel moisture content in real-time, without need to shell the peanut pods. Kernel moisture content is determined in-shell with a microwave moisture meter that uses dielectric properties to determine moisture content (Nelson, 1973; Nelson et al., 1998; Trabelsi et al., 1999a). Atmospheric conditions are monitored in real-time to facilitate automated control of drying parameters. Such a system shows promise in

eliminating underdrying and overdrying, reapportioning labor, and minimizing energy consumption while providing efficient, automated drying control.

11.2 Materials and Methods

System Design

A system design was devised to define the scope of the system and illustrate the functions of each component. The system consists of four major components: the sensor network, data acquisition unit, microcontroller unit, and display. Figure 11.1 shows how the four components interact within the system as data flow between them. As data are retrieved from the sensor network, they enter the data acquisition unit as analog data.

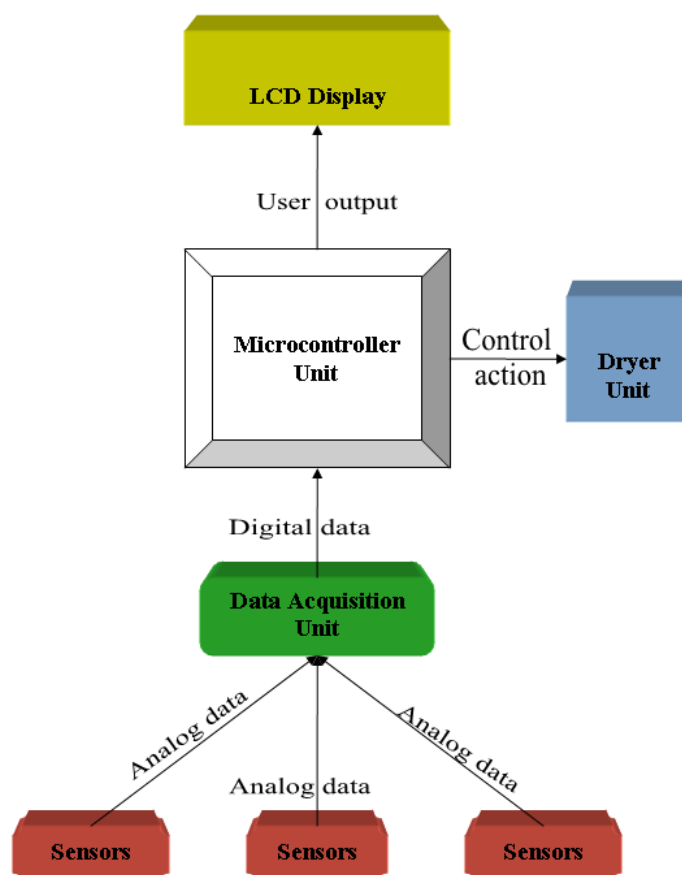


Figure 11.1: Complete system diagram and data flow

They exit as digital data and enter the microcontroller unit where they are converted to float values representing the appropriate measured parameter. The data are then assessed and compared against stored conditions and criteria within the microcontroller unit. From those comparisons, decisions are made, and the appropriate control action is relayed to the dryer unit. The microcontroller unit, and display, discussed here is the embedded solution that controls the microwave moisture meter (Lewis and Trabelsi, 2011a; Lewis and Trabelsi, 2011b). The original software of the microcontroller was modified and sensors were added to adapt to the drying process.

The components of the control system work together to govern the drying process without human interaction. The decision-making capabilities of the control system are essential for optimizing the drying process in its entirety. Such a system eliminates the need for drying time estimation. However, drying is terminated when peanuts are known to be at desired kernel moisture content. The following conditions are enforced by the system:

- aeration is terminated when current kernel moisture content is equal to the desired kernel moisture content
- aeration is suspended while relative humidity of ambient air is $> 85\%$
- temperature of air blown into peanuts must be no greater than $15\text{ }^{\circ}\text{F}$ above the ambient temperature to ensure optimal drying rate (Beasley and Dickens, 1963; Blankenship and Davidson, 1984; Butts et al., 2008)
- air blown into peanuts must never exceed $95\text{ }^{\circ}\text{F}$ to prevent off-flavor development and degradation in milling quality (Beasley and Dickens, 1963; Butts et al., 2008).

The last three conditions are normally monitored and enforced manually by an operator in the present drying process. However, the components of this system provide an automated solution.

Together, the four components provide feedback control, data acquisition and real-time monitoring.

Sensor Network

The sensor network is comprised of five sensors. These include three temperature sensors (LM35DH in TO-46 metal can package), a relative humidity sensor (HIH-4000-001), and a microwave moisture meter for peanut kernel moisture content determination. Two of the temperature sensors are used in conjunction with the feedback controller. One temperature sensor is used to measure the temperature of the inlet air to the drying trailer, and the other is used to measure the ambient air temperature. Using one of the conditions stated above, the feedback controller assesses the difference between the temperature of air at the trailer inlet and the temperature of the ambient air plus 15 °F. The difference between these two temperatures is used to determine the control action that is sent to the dryer. Hence, the temperature of the inlet air is “fed back” to control the temperature of the inlet air. The relative humidity sensor is used to monitor the RH of the ambient air. The other temperature sensor is used to measure the temperature of the peanuts at the location of the microwave meter for temperature compensation. Figure 11.2 shows the circuitry for these sensors. The temperature sensors output 10 mV/°C, and voltage increases linearly with increasing temperature. Therefore, an accurate measurement of the voltage yields a temperature reading. The relative humidity sensor provides a linear increase in voltage with increasing relative humidity. With an accurate voltage measurement from the sensor, relative humidity is defined as:

$$RH\% = (V_{out} - 0.79283) / 0.031393 \quad (11.1)$$

Using the 15-V single output power supply that is available within the microwave moisture meter (Lewis and Trabelsi, 2011a; Lewis and Trabelsi, 2011b), an LM7805 voltage regulator is

interest, it is replaced between the antennas, and the two voltages are measured again. From the two sets of voltages, the attenuation and phase shift caused by the material are determined, and the dielectric properties are calculated. By using the dielectric properties of the material, moisture content is determined with appropriate calibration functions (Trabelsi et al., 1998; Trabelsi and Nelson, 1998; Trabelsi and Nelson, 2004a). The microwave meter uses a trend observed empirically to determine the moisture content of the peanut kernels from dielectric measurements of the peanut pods (Trabelsi et al., 2009b; Trabelsi et al., 2010; Trabelsi et al., 2009c; Trabelsi and Nelson, 2006a).

Quarter-scale Drying Trailer

To preserve the integrity of experiments performed with the control system, the appropriate dimensions for a small-scale drying trailer were sought. Table 11.1 shows the original dimensions along with the following four options considered:

Table 11.1: Possible dimensions for small-scale peanut drying trailer

Option	Length, m	Width, m	Depth, m	Volume, m³	Plenum Depth, m
Original Wagon	6.4	2.4	1.27	19.51	0.23
Option 1	0.4	0.15	0.079	0.0047	0.014
Option 2	0.8	0.3	0.158	0.0379	0.029
Option 3	1	0.375	0.198	0.0743	0.036
Option 4	1.5	0.563	0.297	0.251	0.054

For all options, the aspect ratio observed in the original drying wagon was preserved. After deliberation, option 4 was chosen because of its size and realistic representation as a quarter-

scale model. A small-scale peanut drying trailer was constructed with the dimensions listed in option 4. The inlet to the air plenum was also designed to scale based on dimensions provided for the plenum inlet on the actual drying wagon (Butts and Williams, 2004). Perforated sheet metal with the same specifications as the original wagon was installed as the upper surface of the air plenum in the small-scale trailer. The sheet metal had 3.17 mm diameter holes on 4.76 mm staggered centers yielding 40% open area. The sides were made of polystyrene sheathing 0.75 in. (1.905 cm) thick to allow versatility in application of the microwave moisture meter. Figure 11.3 shows the small-scale peanut drying trailer. With historical data available from peanut samples used in the lab, it was determined that the small-scale trailer would hold approximately 180 lbs (81.6 kg) of peanuts.



Figure 11.3: Quarter-scale peanut drying trailer

Dryer Modification and Implementation

When searching for a dryer to use within the small-scale drying system, the main search criterion was for heat control capabilities. Many small-scale dryers found initially were not equipped with heating elements. They merely circulated ambient air. The dryer used in this study was the ChallengAir 560 advanced cage dryer manufactured by Double K Industries¹. A picture of the unmodified dryer is shown in Figure 11.4. The dryer provides two fan speeds, three heat settings, and a 60-minute timer.

The dryer was disassembled to observe the internal controls. The block diagram for the electrical circuits of the dryer was used to make modifications to the dryer so that it could be externally controlled by the microcontroller. First, the rotary-switch timer was bypassed so that the dryer would stay on. The two rocker switches used for heat settings were observed to control two internal heating elements. By measuring the coil resistance of each and using $P=V^2/R$, power was determined for all settings. The bottom element has a coil resistance of 18.8 Ω and uses 765 W. The top element has a coil resistance of 12.7 Ω and uses 1135 W. Together, connected in parallel, the two elements have a coil resistance of 7.7 Ω and use 1850 W. The rocker switches were disconnected, and each heating element was wired to a Crydom CSW2410-10 solid-state relay. The microcontroller was programmed to provide the control voltages needed for switching by the solid-state relays. Control of the heating elements by way of switching the solid-state relays was set up to resemble 2-bit digital control. The control configuration is shown in Table 11.2. On is represented by 1, and off is represented by 0. Lastly, to complete modification of the dryer, a frame was added to its outlet to allow for connection with the duct that would connect the dryer and trailer. The modified dryer is shown in Figure 11.5.

¹ Mention of company or trade names is for purpose of description only and does not imply endorsement by the U. S. Department of Agriculture or The University of Georgia



Figure 11.4: Unmodified ChallengAir 560 dryer

Table 11.2: 2-bit control for heating elements

Low-power element	High-power element	Power, W	Percent of total power
0	0	0	0
0	1	765	41
1	0	1135	61
1	1	1850	100



Figure 11.5: Modified ChallengeAir 560 dryer

The dryer was tested to evaluate heating response at the three heat settings. With the dryer connected to the trailer, a thermocouple was inserted into the plenum inlet and was monitored with readings every second by an Agilent 34970A data acquisition/switch unit. The data were plotted to observe the time coefficient and the equilibrium temperature for each heat setting. The equilibrium temperature occurred at the temperature where the power going into the heating element was equal to the power loss into the environment; resulting in no increase or decrease in temperature. The dryer response at the three heat settings is shown in Figure 11.6.

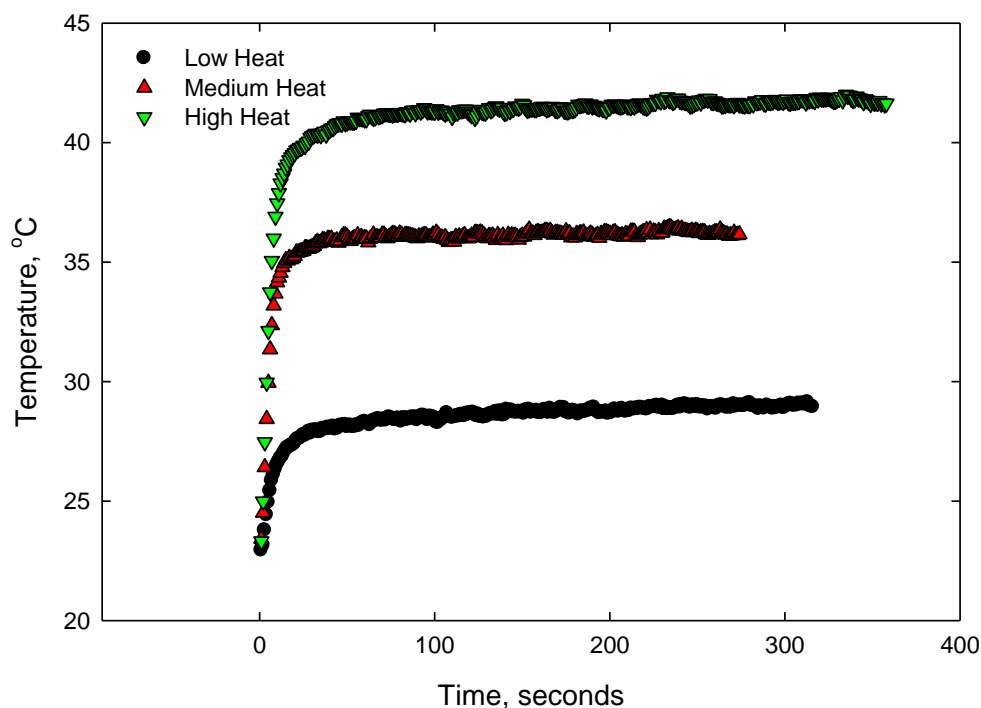


Figure 11.6: Dryer response at different heat settings

The equilibrium temperatures recorded at the low, medium and high heat settings were 28.9 °C, 36.1 °C and 41.7 °C, respectively. These temperatures, along with the time coefficient, were used to develop the algorithm for temperature control during the drying process.

Software Generation

The software to facilitate the automated control of peanut drying was written in C programming language and was created in Paradigm Integrated Development Environment, which was provided with the SensorCore microcontroller manufactured by Tern, Inc. This microcontroller was originally used to control the measurement process and data acquisition of the microwave moisture meter (Lewis and Trabelsi, 2011a; Lewis and Trabelsi, 2011b). Its features and room for expansion made it a suitable selection for the peanut drying controller.

The code was written to create a monitoring-type software. The user is asked initially to enter the target kernel moisture content. Then, no further input from the user is required. The target kernel moisture content can also be embedded in the code as a constant so that no user input is required. Once drying has started, the software monitors the temperature of the air at the inlet to the air plenum, the temperature of the peanuts at the location of the microwave moisture meter, the ambient air temperature and relative humidity, and the peanut kernel and peanut pod moisture content. Assessment of these parameters is performed to determine the appropriate control action for the dryer. The microcontroller has a digital-to-analog converter (DAC) which can output voltages up to 4.09 V. The two channels of the DAC are used to switch the solid-state relays, providing power to the heating elements individually or simultaneously. The software uses a pulse-width-modulation (PWM) algorithm to vary the power, based on air temperature required at the inlet to the plenum. A flowchart of event execution is shown in Figure 11.7.

The software was developed in modular format and was divided into five classes: `bitmap`, `dry_mon`, `data_acquisition`, `calculations`, and `data_out`. The classes are listed in order of execution. The `bitmap` class is only executed upon initialization; however, the other classes loop for the duration of the drying process.

The `bitmap` class controls the scrolling bitmap images that display when the moisture meter is turned on initially or reset. The `dry_mon` class controls the constant and real-time monitoring of the various sensors. It also schedules the display of measured parameters on the graphical LCD periodically. The `data_acquisition` class handles the reading of the voltages and conversion from analog to digital to float values that can be manipulated later in calculations. The `calculations` class uses the voltages acquired from the microwave meter to calculate the dielectric properties of the sample. Coded algorithms are then used to determine the moisture

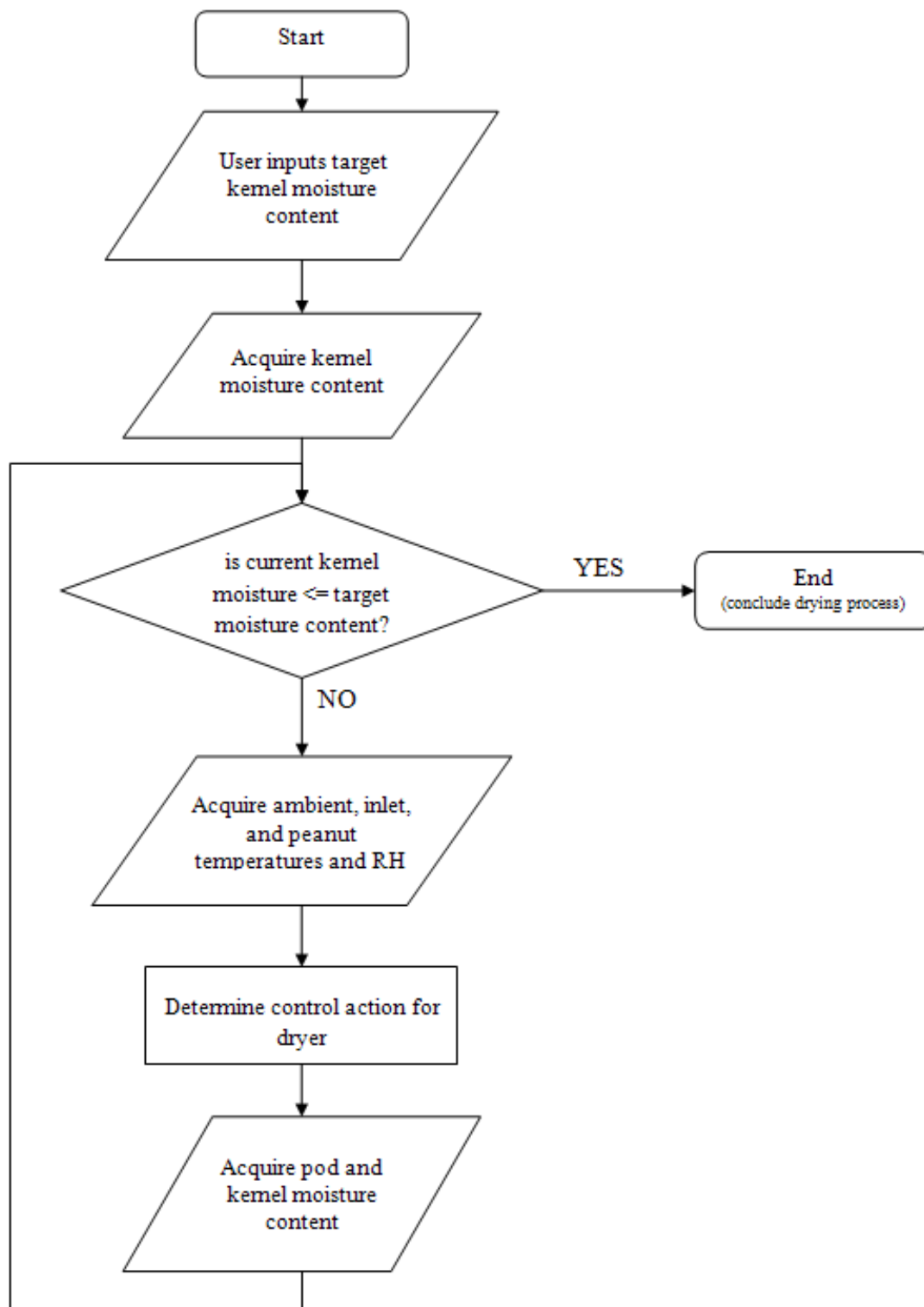


Figure 11.7: Flowchart for main program execution

content from the dielectric properties (Trabelsi and Nelson, 1998). The voltages acquired from the temperature sensors are used to calculate the temperature in degrees Celsius using the relationship of 10 mV/°C. The voltage acquired from the relative humidity sensor is used to determine RH by Equation 11.1. The data_out class controls the high and low output to the heating elements to control the temperature of the drying air.

The five classes work together to provide automated control of the drying process. Atmospheric conditions are monitored in real-time, and thus, drying parameters are controlled in real-time. Real-time monitoring of kernel moisture content allows the user to know the kernel moisture content of the bed at all times.

Aeration Evaluation

The dryer was connected to the small-scale drying trailer through a vinyl duct with a 174.7 cm² average cross-sectional area, measuring 48 cm in length. The trailer was filled with peanut pods to 4 cm from the top, resulting in a bed depth of 26 cm. As air was forced through the peanuts, airflow and temperature distribution were evaluated to determine the uniformity of the aeration through the peanuts. Figure 11.8 shows the trailer filled with peanut pods with the dryer connected.

The trailer was divided into sections to evaluate airflow and temperature distribution. Observing the trailer length-wise, the center line was treated as zero, being located 23 cm from either sidewall (56.3 cm width). The left line was 14 cm to the left of the center line, and the right line was 14 cm to the right of the center line. Starting from the end of the trailer that is opposite the plenum inlet, thermocouples were placed in the peanuts along the left, center and right line at 15, 45, 75, 105, and 135 cm from the end wall as shown in Figure 11.9. Thermocouples were placed 5, 10, 15 and 20 cm deep within the peanuts.



Figure 11.8: Drying trailer with dryer connected

The thermocouples were connected to the Agilent 34970A unit via a 20-channel multiplexer as shown in Figure 11.10. The temperature at these locations and the plenum inlet were monitored with readings every second. Airflow was also measured at each of the described locations with an Omega HHH11A anemometer.

The air velocity measured at the plenum inlet was 456 m/min (1496.1 ft/min). The measured air velocity was acceptable by industry standards (Beasley and Dickens, 1963; Butts and Williams, 2004). An air velocity greater than 609.6 m/min (2000 ft/min) creates a risk of eddies forming in the plenum. The airflow exhausted from the peanuts ranged from 5.2 to 10.4 m³/min per cubic meter. The recommended range for average airflow is from 8 to 10 m³/min per cubic meter (Butts et al., 2008; Butts and Williams, 2004). Deviations in aeration uniformity were comparable to those observed in the peanut industry.

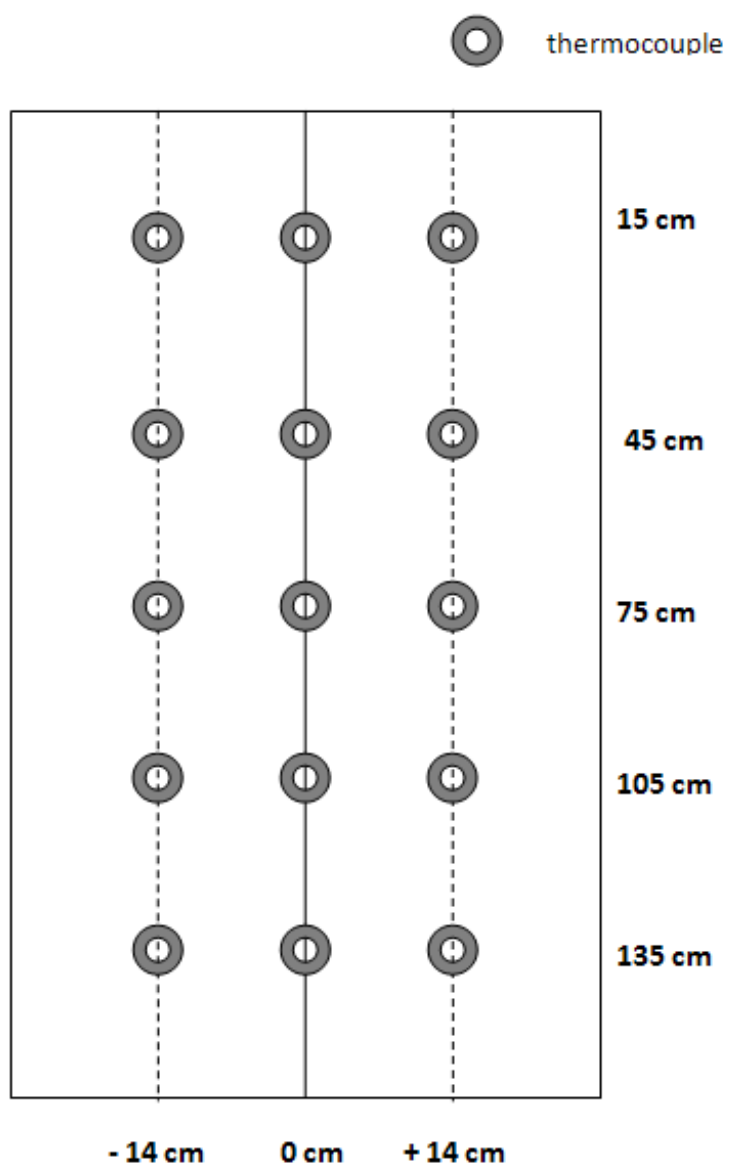


Figure 11.9: Schematic diagram for thermocouple distribution



Figure 11.10: Drying trailer shown with thermocouples placed throughout

Evaluation of temperature distribution showed that the temperature throughout the peanuts varied by 4 °C. Minor temperature differences were observed in relation to depth of the thermocouples. However, as one would expect, regions with lower airflow had lower temperatures than those with higher airflow. Unloading of the peanuts showed that soil on the perforated floor could have been a likely factor affecting the airflow, and thus the temperature in certain regions of the peanuts within the trailer. With the conclusion of the evaluation of airflow and temperature distribution throughout the trailer of peanuts, results were considered sufficient to yield a credible drying simulation.

Experiment Setup

For this study, Runner type peanut pods grown in Georgia, Alabama, Mississippi and Texas were used. These peanuts were collected from the 2010 peanut harvest season during a

study which compared the microwave moisture meter against the official moisture meters used in the peanut grading industry. A total of 165.9 lbs (75.4 kg) of peanut pods were used. Initial moisture content for the pods and kernels was tested using the reference oven drying method (ASAE, 2002). Initial peanut pod moisture was between 5.3% and 5.57% w.b. The peanut pods were divided into six bags and were conditioned to higher moisture content. Moisture content was increased by spraying the peanuts with a fine mist of distilled water, with an Ortho Heavy Duty sprayer. The bags of peanuts were then stirred and mixed for approximately five minutes to ensure that the water was evenly distributed. The quantity of water (grams) added, m_{wa} , to each bag was proportional to the difference in its initial moisture content M_i and the desired moisture content M_d and was calculated as

$$m_{wa} = m_s \left(\frac{M_d - M_i}{100 - M_d} \right) \quad (11.2)$$

where m_s is the mass of the sample in grams. Each bag was moistened to raise the peanut pod moisture content to 18% w.b. Table 11.3 shows the breakdown of how more than 11 kg of water was added to the peanuts, collectively. After the water was added to all bags and all were stirred, the bags were sealed and stored for a week at 4 °C for equilibration.

Table 11.3: Breakdown of water added to peanuts

Weight, kg	Initial Moisture Content, %	Desired Moisture Content, %	Water Added, g
13.2	5.30	18	2001
11.8	5.32	18	1789
13.6	5.57	18	2062
12.4	5.50	18	1880
12.3	5.30	18	1864
12.1	5.50	18	1834
Total = 75.4			Total = 11,430

To begin the experiment, the antennas for the microwave moisture meter were placed inside the peanut trailer, Figure 11.11. The peanuts were removed from cold storage and allowed to warm while remaining sealed in plastic bags. By the start of the experiment, the peanuts had warmed to an average temperature of 18.5 °C. The trailer was slowly filled with peanuts, being careful to ensure that peanuts from the six bags were thoroughly mixed. Once the trailer was filled with all conditioned peanuts, the drying process was begun. Samples were extracted periodically to compare the kernel moisture content as determined by the microwave meter to that as determined by the oven method. The extracted peanut pod samples were manually shelled for kernel moisture content determination with the oven method. For testing, 15 g samples for kernels and 100 g samples for pods were oven-dried for 6 hours at 130 °C. Upon completion, moisture content (%) was calculated on the wet basis as follows:

$$M(\%) = \frac{m_w}{m_w + m_d} \times 100 \quad (11.3)$$

where m_w is the mass of the water and m_d is the dry mass of the material. The experiment was allowed to run, governed by the feedback-controlled system, free of any human interaction. Drying was terminated once the desired kernel moisture content was reached.



Figure 11.11: Antennas mounted within drying trailer

11.3 Results and Discussion

Initial peanut kernel moisture content at the beginning of the experiment was 16.66%, and initial peanut pod moisture was 18.15%. The goal was to dry the peanuts down to a desired kernel moisture content entered by the user. For this instance, the peanuts were dried down to 10.51% kernel moisture content. The total drying time was six hours and forty minutes. During the drying process, samples were extracted at a location near the antennas, being careful not to disturb the peanuts between the antennas. Peanut pod samples were shelled to prepare kernel samples for moisture content determination with the oven method.

The atmospheric conditions were monitored successfully by the system. Throughout the duration of the drying process, the ambient air temperature ranged from 21.9 °C to 23.26 °C, and the ambient relative humidity ranged from 50.03% to 57.34%. Figures 11.12 and 11.13 show the

measured atmospheric conditions over time. The inlet air temperature and the temperature of the peanuts near the antennas, also shown in Figure 11.13, were also monitored successfully by the drying system. The temperature distribution throughout the bed was monitored using the Agilent 34970A data acquisition/switch unit. Its recorded data is shown in Figures 11.14 and 11.15.

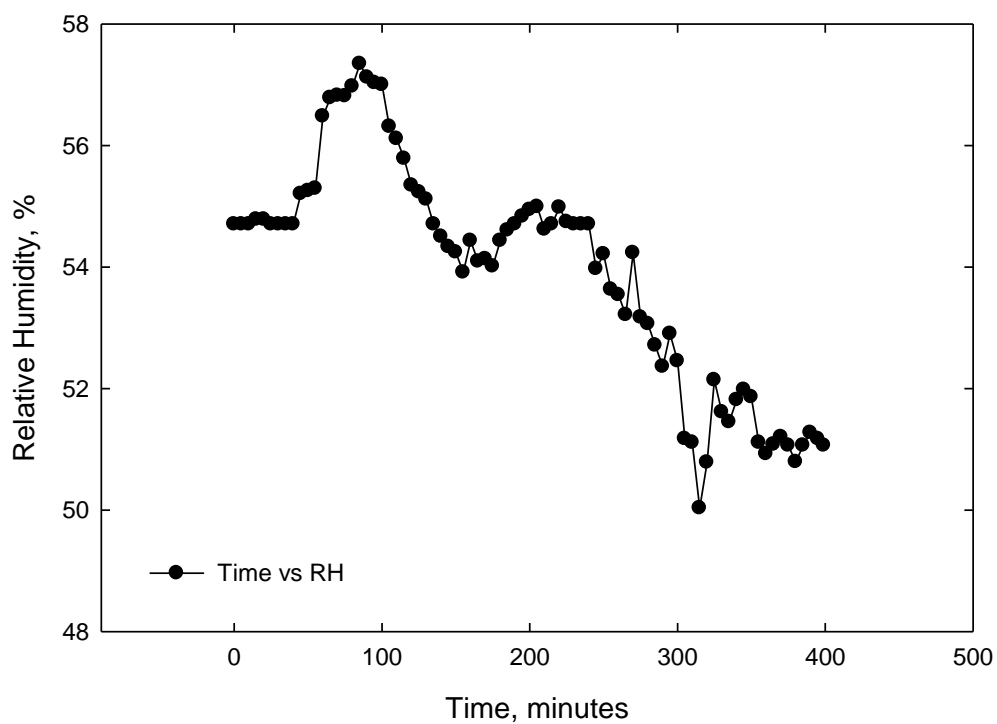


Figure 11.12: Relative humidity versus time during drying process

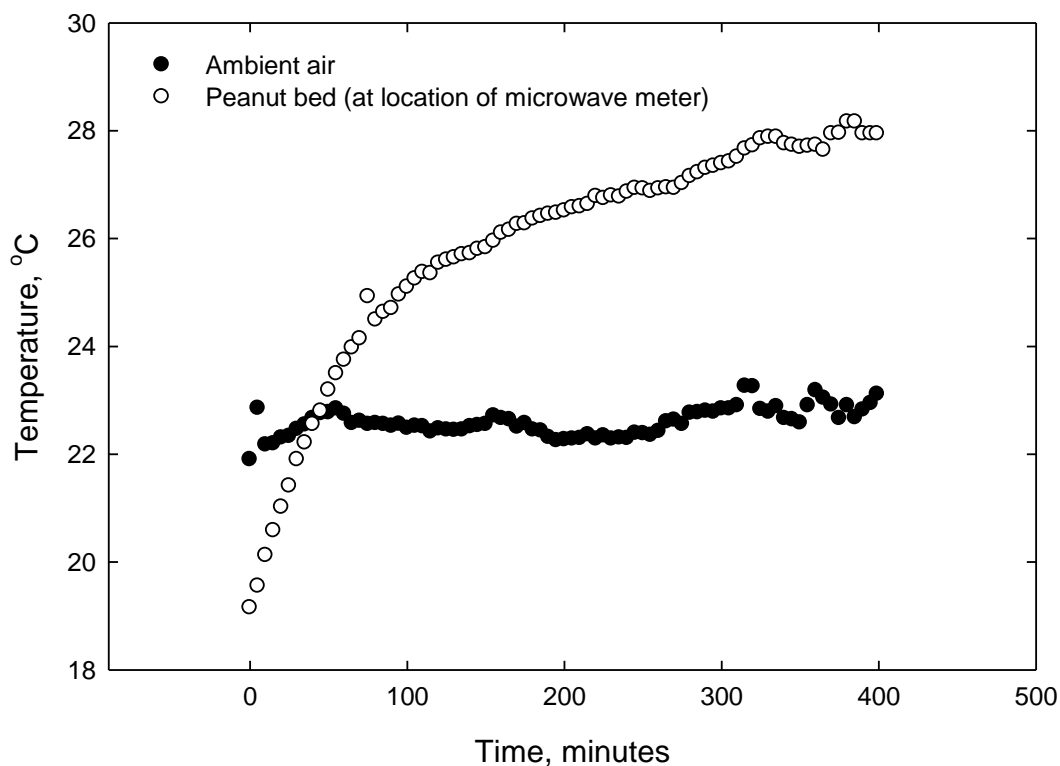


Figure 11.13: Temperature of ambient air and peanuts versus time during drying process

Figure 11.14 shows the inlet air temperature and temperature distribution throughout the peanut bed for the first ten minutes of the drying process. The pulsation observed in the plot for the inlet air follows the pulse width modulation established in the feedback control to govern the temperature of the air blown into the peanuts. The other lines, varying in color, represent temperatures at locations throughout the peanut bed. At the beginning of the drying process, the temperature variation throughout the peanut bed was 1.7 °C.

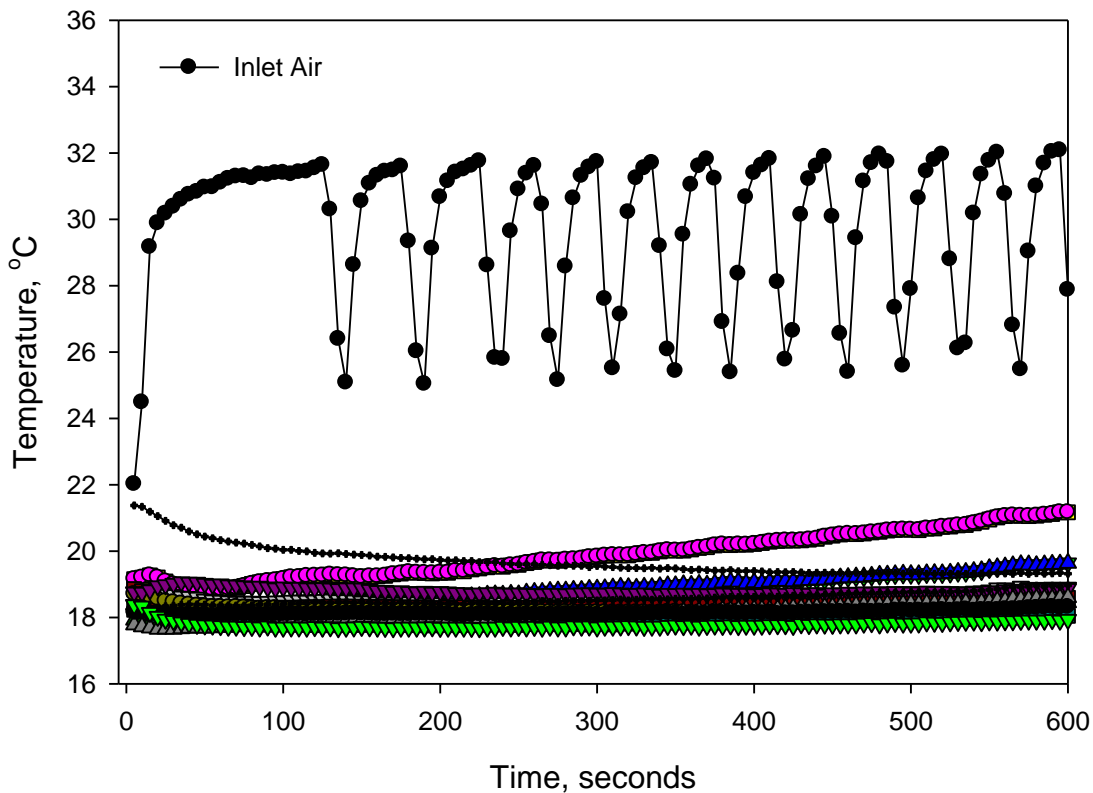


Figure 11.14: Inlet air temperature and temperature distribution of peanut bed versus time shown for first 10 minutes

Figure 11.15 shows the same parameters as Figure 11.14. However, for this instance, data are shown for the last ten minutes of the drying process; thus, six hours and thirty minutes later than the data shown in Figure 11.14. Ambient air temperature, shown in Figure 11.13, was higher in this instance, resulting in a higher peak in inlet air temperature. Also, the temperature variation throughout most of the peanut bed was 4.1 °C. This is excluding the bottom plot which represents the temperature recorded at 135 cm (vertical) and -14 cm (horizontal), referring to Figure 11.9. Low air velocity was also observed in this region, < 0.3 m/s.

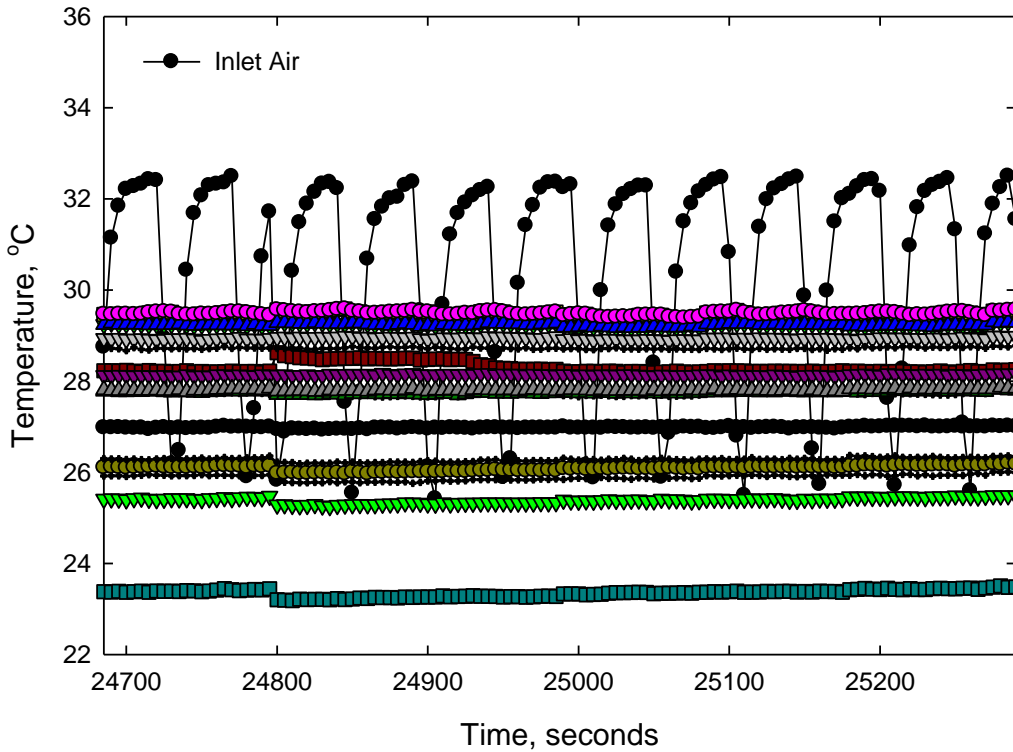


Figure 11.15: Inlet air temperature and temperature distribution of peanut bed versus time shown for last 10 minutes

Pod and kernel moisture contents, as determined with the microwave moisture meter, were compared to those determined with the oven method. Figure 11.16 shows that the two agree well. Values for both instances are shown in Table 11.4. Performance of the microwave meter within the drying system in moisture content determination was evaluated by calculating the standard error of performance (*SEP*) which is defined as:

$$SEP = \sqrt{\frac{1}{N-1} \sum_{i=1}^N (\Delta M_i - M)^2} \quad (11.4)$$

$$M = \left(\frac{1}{N}\right) \sum_{i=1}^N \Delta M_i \quad (11.5)$$

where N is the number of samples and ΔM_i is the difference between the predicted moisture content and the moisture content determined by the standard method for the i^{th} sample. One-way analyses of variance (ANOVA) were performed to analyze the data for any significant differences between moisture content (pods and kernels) determined with the microwave meter and the oven method. The microwave meter and the oven method were considered as two treatments. Values for SEP and the ANOVA results are shown in Table 11.5.

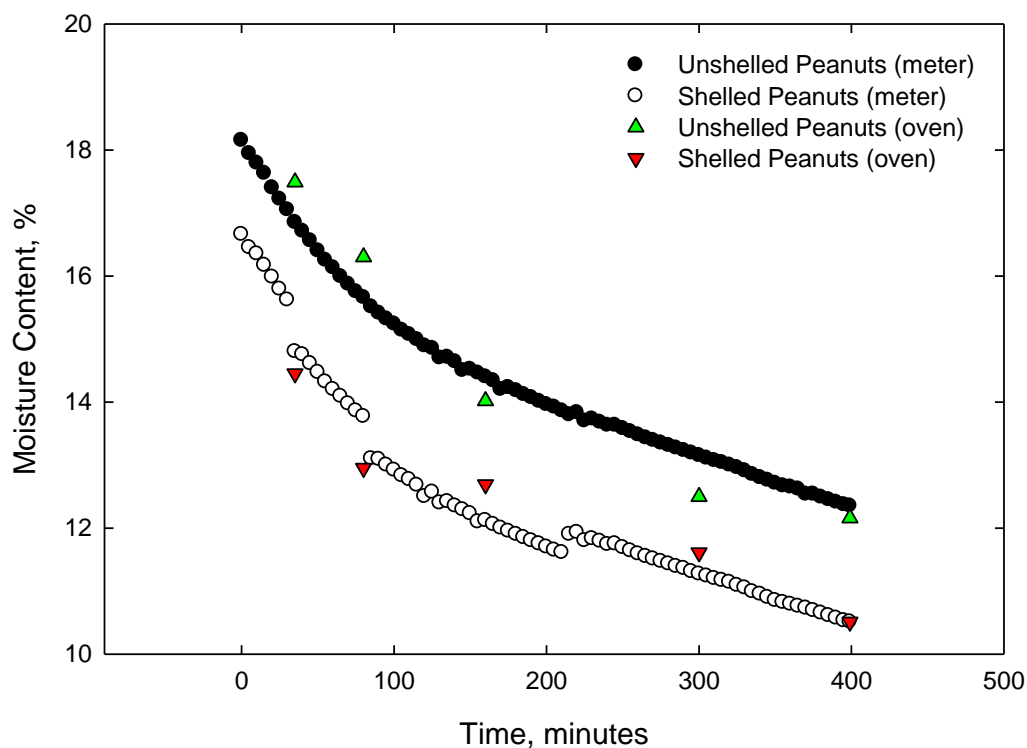


Figure 11.16: Moisture content determination (pods and kernels) compared between microwave meter and oven method

Observing the ANOVA results in Table 11.5, the p-values are quite high. The null hypothesis assumes there is no significant difference between the two treatments. Therefore, for

pod and kernel moisture content determination, we accept the null hypothesis at the 1% level because the p-values are much greater than 0.01. The *SEP* values shown are also well within reported errors observed with the microwave moisture meter. Therefore, we can conclude that differences between moisture content determination with the microwave meter and oven method are minimal.

Table 11.4: Data for comparison between moisture content determination with oven method and microwave moisture meter

Extraction Time, minutes	Peanut Pods		Peanut Kernels	
	Oven Method	Microwave Meter	Oven Method	Microwave Meter
35	17.49	16.85	14.45	14.8
80	16.30	15.66	12.95	13.77
160	14.02	14.4	12.69	12.12
300	12.50	13.15	11.61	11.27
399	12.16	12.35	10.51	10.51

Table 11.5: *SEP* and ANOVA results for moisture content determination

Error Evaluation	Peanut Pods	Peanut Kernels
<i>SEP</i> , %	0.208	0.304
ANOVA, p-values	0.993	0.961

11.4 Conclusion

A microwave moisture meter controlled by an embedded solution was used in the development of a feedback controlled system to automate peanut drying. The controller was used to maintain established drying parameters. Atmospheric conditions, including ambient temperature and relative humidity, were measured in real-time to facilitate automated decision-

making. Kernel moisture content was determined in-shell throughout the drying process with an SEP of 0.304, which is within the *SEP* ranges reported for the microwave meter when applied to static systems. Results from the ANOVA yielded a p-value of 0.961, confirming that there are no significant differences between the kernel moisture content determined within the drying system and the kernel moisture content determined by the oven method. Results from this research show promise for testing and implementation at a larger scale.

Implementation of such a system will minimize energy consumption and the human interaction required to dry peanuts. Most importantly, the occurrences of overdrying or underdrying peanuts will be eliminated because kernel moisture content is available at any time during the drying process. Elimination of such occurrences conserves energy, reduces bottlenecks at the buying point and preserves the flavor and milling qualities of the peanuts.

Acknowledgements

The authors would like to acknowledge Mr. Lewis Fortner and the staff at The University of Georgia Instrument Shop for construction of the quarter-scale drying trailer. They would like to thank Dr. Jochem Roelvink, Research Electronics Engineer at USDA ARS in Athens, GA, for insightful suggestions and assistance with circuit design and troubleshooting. The authors would like to thank Mr. Ron Dozier, buying point manager at Peanut Producers, LLC in Bartow, GA for discussions and assistance with regard to drying and the peanut grading process. Thanks are also due to Dr. Chris Butts, Agricultural Engineer at USDA ARS National Peanut Research Laboratory in Dawson, GA for assistance with design verification and insightful comments.

References

Allgood, M. E., J. M. Allison, and G. Vellidis. 1995. Automated peanut dryer control. *Applied Engineering in Agriculture*. 11(3): 465-467.

- Allgood, M. E., G. Vellidis, J. M. Allison, C. D. Perry, and C. S. Kvien. 1993. Continuous in-process determination of moisture loss from curing peanuts. *Transactions of the ASAE*. 36(3): 935-942.
- American Peanut Council. 2007. About the peanut industry. Available at: <http://www.peanutsusa.com/index.cfm?fuseaction=home.page&pid=12>. Accessed 12 March 2007.
- ASAE Standards, 49th ed. 2002. S410.1: Moisture Measurement - Peanuts. St. Joseph, Mich: ASAE.
- Beasley, E. O., and J. W. Dickens. 1963. Engineering research in peanut curing. *North Carolina Agricultural Experiment Station Tech. Bull. No. 155*: North Carolina State University, Raleigh, NC.
- Blankenship, P. D., and J. I. Davidson. 1980. A method for automatic cutoff of laboratory peanut dryers. *Transactions of the ASAE*. 23(6): 1530-1537.
- Blankenship, P. D., and J. I. Davidson. 1984. Automatic monitoring and cutoff of peanut dryers. *Peanut Science*. 11(2): 58-60.
- Butts, C. L. 1995. Incremental cost of overdrying farmers' stock peanuts. *Applied Engineering in Agriculture*. 11(5): 671-675.
- Butts, C. L., J. I. Davidson, M. C. Lamb, C. V. Kandala, and J. M. Troeger. 2003. A decision support system for curing farmers' stock peanuts. ASAE Paper No. 03-6047. St. Joseph, Mich.: ASAE.
- Butts, C. L., J. I. Davidson, M. C. Lamb, C. V. Kandala, and J. M. Troeger. 2004. Estimating drying time for a stock peanut curing decision support system. *Transactions of the ASAE*. 47(3): 925-932.
- Butts, C. L., and J. Hall III. 1994. Development of a graphical decision support system for a peanut curing operation. ASAE Paper No. 94-6515. St. Joseph, MI: ASAE.
- Butts, C. L., J. Tuggle, and E. J. Williams. 2008. Good agricultural practices for buying point operations. Available at: http://admin.peanutsusa.com/documents/Document_Library/2008%20Final%20Chapter%202%20%20Buying%20Point%20Operations.pdf. Accessed 13 November 2011.
- Butts, C. L., and E. J. Williams. 2004. Measuring airflow distribution in peanut drying trailers. *Applied Engineering in Agriculture*. 20(3): 335-339.
- Lewis, M., and S. Trabelsi. 2011a. Embedded solution for a microwave moisture meter. *Proceedings of 2011 IEEE Southeastcon*. Nashville, TN. pp. 101-104.
- Lewis, M., and S. Trabelsi. 2011b. Integrating an embedded system within a microwave moisture meter. ASABE Paper No. 1110943. St. Joseph, Mich.: ASABE.

- Microtherm Inc. 2000. Opticure2000 dryer control system. Available at: <http://www.microtherm.com/dryctrl.htm>. Accessed 13 January 2010.
- Nelson, S. O. 1973. Electrical properties of agricultural products - a critical review. *Transactions of the ASAE*. 16(2): 384-400.
- Nelson, S. O., S. Trabelsi, and A. W. Kraszewski. 1998. Advances in sensing grain moisture content by microwave measurements. *Transactions of the ASAE*. 41(2): 483-487.
- Paine, M. D. 1969. Constant wet-dry bulb differential controller used for peanut drier control. *Transactions of the ASAE*. 12(6): 741-744.
- Trabelsi, S., A. W. Kraszewski, and S. O. Nelson. 1998. New density-independent calibration function for microwave sensing of moisture content in particulate materials. *IEEE Transactions on Instrumentation and Measurement*. 47(3): 613-622.
- Trabelsi, S., A. W. Kraszewski, and S. O. Nelson. 1999. Determining physical properties of grain by microwave permittivity measurements. *Transactions of the ASAE*. 42(2): 531-536.
- Trabelsi, S., M. A. Lewis, and S. O. Nelson. 2009a. Rapid and nondestructive determination of moisture content in peanut kernels from microwave measurement of dielectric properties of pods. ASABE Paper No. 097043. St. Joseph, Mich.: ASABE.
- Trabelsi, S., M. A. Lewis, and S. O. Nelson. 2010. Microwave moisture meter for rapid and nondestructive grading of peanuts. ASABE Paper No. 1009183. St. Joseph, Mich.: ASABE.
- Trabelsi, S., S. Nelson, and M. Lewis. 2009b. Microwave nondestructive sensing of moisture content in shelled peanuts independent of bulk density and with temperature compensation. *Sensing and Instrumentation for Food Quality and Safety*. 3(2): 114-121.
- Trabelsi, S., and S. O. Nelson. 1998. Density-independent functions for on-line microwave moisture meters: A general discussion. *Measurement Science and Technology*. 9(4): 570-578.
- Trabelsi, S., and S. O. Nelson. 2003a. Free-space measurement of dielectric properties of cereal grain and oilseed at microwave frequencies. *Measurement Science and Technology*. 14(5): 589-600.
- Trabelsi, S., and S. O. Nelson. 2003b. Nondestructive multiparameter microwave sensor. ASAE Paper No. 036129. St. Joseph, Mich.: ASAE.
- Trabelsi, S., and S. O. Nelson. 2004. Calibration methods for nondestructive microwave sensing of moisture content and bulk density of granular materials. *Transactions of the ASAE*. 47(6): 1999-2008.

- Trabelsi, S., and S. O. Nelson. 2006. Microwave sensing technique for nondestructive determination of bulk density and moisture content in unshelled and shelled peanuts. *Transactions of the ASABE*. 49(5): 1563-1568.
- Trabelsi, S., and S. O. Nelson. 2007. A low-cost microwave sensor for simultaneous and independent determination of bulk density and moisture content in grain and seed. ASAE Paper No. 076240. St. Joseph, Mich.: ASAE.
- Trabelsi, S., S. O. Nelson, and M. Lewis. 2008a. Microwave moisture sensor for grain and seed. *Biological Engineering*. 1(2): 195-202.
- Trabelsi, S., S. O. Nelson, and M. Lewis. 2008b. Practical microwave meter for sensing moisture and density of granular materials. *Instrumentation and Measurement Technology Conference Proceedings, 2008. IMTC 2008. IEEE*. 1021-1025.
- Troeger, J. M. 1989. Modeling quality in bulk peanut curing. *Peanut Science*. 16(2): 105-108.
- Virginia-Carolina Peanut Promotions. 2007. Everything about peanuts. Available at: <http://www.aboutpeanuts.com>. Accessed 22 March 2007.

CHAPTER 12

CONCLUSION AND FUTURE WORK

In chapter three, section one, the goals for this dissertation were presented. The goals were successfully accomplished through the research presented in this dissertation. The research is divided into three journal articles, the sum of which show a logical progression toward the development of a feedback controlled peanut drying system.

The first journal article, chapter nine, demonstrated that three density-independent calibration functions used to predict moisture content in peanut pods and peanut kernels were independent of peanut type. Peanut types included in the research were GA Runner, TX Runner (high oleic), Virginia and Valencia. All types have structural and compositional differences. For moisture meters operating at lower frequencies (1 to 20 MHz), separate calibrations have to be included for each type. This is true for commercial moisture meters used in the peanut industry for kernel moisture content determination. However, with microwave moisture sensing technology, calibration equations can be used to accurately predict moisture content in peanuts with insensitivity to type. Such capabilities will decrease complexity of future microwave moisture meters and improve the overall utility of moisture meters. Having one calibration for different types of peanuts will eliminate erroneous type selections at peanut buying points during the grading process.

Standard errors of calibration and performance (*SEC* and *SEP*) were analyzed to compare the calibration functions for the various types with the type-independent calibration functions. *SEC* values for the type-independent functions did not vary much from those observed for the

calibration functions for each individual peanut type. *SEP* values ranged from 0.264 to 0.362 percent moisture content. The best accuracy was achieved in the 6 to 11 GHz range.

The second journal article, chapter ten, discussed the conversion of the microwave moisture meter from a laptop-controlled meter to a stand-alone meter hosting its own embedded system. This improvement was highly anticipated, because the laptop was the most vulnerable component of the microwave moisture meter. Field measurements were often suspended because of laptop crashes and interruptions in communication between the meter and laptop. For this reason, an embedded system was implemented with the microwave meter, in the creation of a cost-effective, portable, and robust solution for microwave moisture sensing. Upon completion of conversion, the performance of the stand-alone meter was compared to that of the vector network analyzer (VNA) and the previous, laptop-controlled meter. An ANOVA yielded high *p*-values, showing that the differences in performance between the three systems were minimal.

Electronic circuits used in signal conditioning for the stand-alone meter were developed such that the original components of the microwave meter required no modification. The microcontroller was chosen to allow room for expansion in future applications.

The third journal article, chapter 11, provided a culmination of years of research and acquired skills in the development of a feedback-controlled drying system. This article discussed the use of a sensor network to monitor parameters of a system and then control those measured parameters. A successful combination of microwave moisture sensing, real-time monitoring, feedback control, data acquisition, decision making and automated control were used in the research and development of an impactful solution to a notable shortcoming in the peanut drying process. Results showed that the microwave moisture meter provided in-shell kernel moisture content determination while statically placed in a dynamic system. The observed *SEP* value was

0.304 percent moisture content, which is well within the range for reported error from laboratory and field measurements in which the system is static.

The microcontroller embedded within the microwave moisture meter was modified to also control the drying system. These modifications included monitoring additional sensors, using sensor input to decide upon appropriate control action for the dryer.

Together, these articles provide a systematic approach to a proof of principle. The type-independent functions were evaluated with the VNA; this was the fundamental research. Likewise, the calibration functions for moisture content determination have been demonstrated fundamentally. The applied research begins with the microwave moisture meter. It uses the same concept as the VNA; however, it provides a more practical and affordable solution. It was continuously modified until a portable, stand-alone version was available. The application of the meter to an impactful problem brought this dissertation research to a successful conclusion. The initial idea was conceptualized, and initial tests were performed to show the feasibility. The next step was design of a small-scale simulation to provide proof of principle. The feedback-controlled drying system performed in a manner that warrants implementation on a larger scale with likely eventual adoption for commercial peanut drying.

Future work topics include integrating the electronic circuitry of the system on printed circuit boards and conversion to surface-mount components. This would improve the appearance of the electronic circuits and provide a robust solution with less likelihood circuit problems.

The present software is written so that input and output are scheduled nonsimultaneously because of functionality of the microcontroller. However, threaded software would be advantageous for queries from the user. At present, the system display scrolls through the values

for the measured parameters every 10 seconds. However, with threaded software, the user could choose the parameter(s) of interest for display as desired.

As noted in the peanut industry and observed in this research, airflow is not uniform throughout the peanut drying trailer. There are requirements put in place that prevent eddies from forming in the air plenum; however, the velocity of the air forced through the peanuts has notable differences throughout the bed, even for a cleaned sample. Research is needed to address the lack of uniformity observed in aeration, since this also affects the lack of uniformity in kernel moisture content throughout the bed of peanuts.

While on the topic of airflow and aeration, the effect of dryers with variable flow rate on the drying process is worth investigating. At present, the heat setting on the dryers is varied while the airflow rate remains constant. A constant airflow rate was also used in this research. However, questions arise as to whether the drying process could be further improved with the addition of variable airflow rate capabilities.

I realize that the research presented in this dissertation is a promising initiative toward solving real-life problems in the agricultural industry. However, future work and testing is required to implement this approach. It is my intent to continue this research toward final acceptance and adoption of the technology for quality assessment and quality assurance with labor and energy cost reductions and labor reapportionment in peanut drying.

REFERENCES

- Allgood, M. E., J. M. Allison, and G. Vellidis. 1995. Automated peanut dryer control. *Applied Engineering in Agriculture*. 11(3): 465-467.
- Allgood, M. E., G. Vellidis, J. M. Allison, C. D. Perry, and C. S. Kvien. 1993. Continuous in-process determination of moisture loss from curing peanuts. *Transactions of the ASAE*. 36(3): 935-942.
- American Peanut Council. 2007. About the peanut industry. Available at: <http://www.peanutsusa.com/index.cfm?fuseaction=home.page&pid=12>. Accessed 12 March 2007.
- ASAE Standards, 49th ed. 2002. S410.1: Moisture Measurement - Peanuts. St. Joseph, Mich: ASAE.
- Beasley, E. O., and J. W. Dickens. 1963. Engineering research in peanut curing. *North Carolina Agricultural Experiment Station Tech. Bull. No. 155*: North Carolina State University, Raleigh, NC.
- Blankenship, P. D., and J. I. Davidson. 1980. A method for automatic cutoff of laboratory peanut dryers. *Transactions of the ASAE*. 23(6): 1530-1537.
- Blankenship, P. D., and J. I. Davidson. 1984. Automatic monitoring and cutoff of peanut dryers. *Peanut Science*. 11(2): 58-60.
- Bussey, H. E. 1967. Measurement of the rf properties of materials - a survey. *Proceedings of the IEEE*. 55(6): 1046-1053.
- Butts, C. L. 1995. Incremental cost of overdrying farmers' stock peanuts. *Applied Engineering in Agriculture*. 11(5): 671-675.
- Butts, C. L., J. I. Davidson, M. C. Lamb, C. V. Kandala, and J. M. Troeger. 2003. A decision support system for curing farmers' stock peanuts. ASAE Paper No. 03-6047. St. Joseph, Mich.: ASAE.
- Butts, C. L., J. I. Davidson, M. C. Lamb, C. V. Kandala, and J. M. Troeger. 2004. Estimating drying time for a stock peanut curing decision support system. *Transactions of the ASAE*. 47(3): 925-932.
- Butts, C. L., and J. Hall III. 1994. Development of a graphical decision support system for a peanut curing operation. ASAE Paper No. 94-6515. St. Joseph, MI: ASAE.

- Butts, C. L., J. Tuggle, and E. J. Williams. 2008. Good agricultural practices for buying point operations. Available at: http://admin.peanutsusa.com/documents/Document_Library/2008%20Final%20Chapter%202%20%20Buying%20Point%20Operations.pdf. Accessed 13 November 2011.
- Butts, C. L., and E. J. Williams. 2004. Measuring airflow distribution in peanut drying trailers. *Applied Engineering in Agriculture*. 20(3): 335-339.
- Chen, L. F., C. K. Ong, C. P. Neo, V. V. Varadan, and V. K. Varadan. 2004. *Microwave electronics: Measurement and materials characterization*. England: John Wiley & Sons Ltd.
- Chung, S.-Y., S. Maleki, E. T. Champagne, K. L. Buhr, and D. W. Gorbet. 2002. High-oleic peanuts are not different from normal peanuts in allergenic properties. *Journal of Agricultural and Food Chemistry*. 50(4): 878-882.
- Colson, K. H., and J. H. Young. 1990. Two-component thin-layer drying model for unshelled peanuts. *Transactions of the ASAE*. 33(1): 241-246.
- Distefano III, J. J., A. R. Stubberud, and I. J. Williams. 1990. *Theory and problems of feedback and control systems*. New York, NY: McGraw-Hill, Inc.
- Foster, G. H. 1986. William v. Hukill: A pioneer in crop drying and storage. *Drying Technology*. 4(3): 461-471.
- Haenselmann, T. 2006. Sensor networks. Available at: http://www.informatik.uni-mannheim.de/~haensel/sn_book/sensor_networks.pdf. Accessed 30 October 2006.
- Haidekker, M. A. 2011. *Linear feedback controls - the essentials: A compendium*. unpublished supplement to ENGG 4220/6220.
- Hall, C. W. 1957. *Drying farm crops*. Reynoldsburg, OH: Agricultural Consulting Associates, Inc.
- Hasted, J. B. 1973. *Aqueous dielectrics*. London: Chapman and Hall.
- Heath, S. 2003. *Embedded systems design*. United Kingdom: Newnes.
- Irudayaraj, J., and C. Reh. 2008. *Nondestructive testing of food quality*. Ames, IA: Blackwell Publishing.
- Jacobsen, R., W. Meyer, and B. Schrage. 1980. Density-independent moisture meter at x-band. *Proceedings of 10th European Microwave Conference*. Warsaw, Poland. 216-220.
- King, R. J. 1997. On-line moisture and density measurement of foods with microwave sensors. *Applied Engineering in Agriculture*. 13(3): 361-371.

- Klich, M. A. 2007. *Aspergillus flavus*: The major producer of aflatoxin. *Molecular Plant Pathology*. 8(6): 713-722.
- Kraszewski, A. 1980. Microwave aquametry - a review. *Journal of Microwave Power*. 15(4): 209-220.
- Kraszewski, A. W., and S. Kulinski. 1976. An improved microwave method of moisture content measurement and control. *IEEE Transactions on Industrial Electronics and Control Instrumentation*. 23(4): 364-470.
- Lewis, M., and S. Trabelsi. 2011a. Embedded solution for a microwave moisture meter. *Proceedings of 2011 IEEE Southeastcon*. Nashville, TN. pp. 101-104.
- Lewis, M., and S. Trabelsi. 2011b. Integrating an embedded system within a microwave moisture meter. ASABE Paper No. 1110943. St. Joseph, Mich.: ASABE.
- Lewis, M., S. Trabelsi, S. O. Nelson, and E. W. Tollner. 2009. Type-independent calibration method for microwave moisture sensing in unshelled and shelled peanuts. ASABE Paper No. 096136. St. Joseph, Mich.: ASABE.
- Lewis, M., S. Trabelsi, S. O. Nelson, and E. W. Tollner. 2010. Stability and type-independence analysis of density-independent calibration functions for microwave moisture sensing in unshelled and shelled peanuts. ASABE Paper No. 1009857. St. Joseph, Mich.: ASABE.
- Li, Z., N. Wang, G. S. V. Raghavan, and W. Cheng. 2006. A microcontroller-based, feedback power control system for microwave drying processes. *Applied Engineering in Agriculture*. 22(2): 309-314.
- Loewer, O. J., T. C. Bridges, and R. A. Bucklin. 1994. *On-farm drying and storage systems*. St. Joseph, MI: American Society of Agricultural Engineers.
- Metaxas, A. C. 1996. *Foundations of electroheat: A unified approach*. Hoboken, NJ: Wiley.
- Meyer, W., and W. Schilz. 1980. A microwave method for density independent determination of the moisture content of solids. *Journal of Physics D: Applied Physics*. 13(10): 1823-1830.
- Microtherm Inc. 2000. Opticure2000 dryer control system. Available at: <http://www.microtherm.com/dryctrl.htm>. Accessed 13 January 2010.
- Nelson, S. O. 1973. Electrical properties of agricultural products - a critical review. *Transactions of the ASAE*. 16(2): 384-400.
- Nelson, S. O. 1982. Factors affecting the dielectric properties of grain. *Transactions of the ASAE*. 25(4): 1045-1049.
- Nelson, S. O. 1999. Dielectric properties measurement techniques and applications. *Transactions of the ASAE*. 42(2): 523-529.

- Nelson, S. O. 2010. Fundamentals of dielectric properties measurements and agricultural applications. *Journal of Microwave Power and Electromagnetic Energy*. 44(2): 98-113.
- Nelson, S. O., and P. G. Bartley Jr. 2002. Frequency and temperature dependence of the dielectric properties of food materials. *Transactions of the ASAE*. 45(4): 1223-1227.
- Nelson, S. O., and S. Trabelsi. 2004. Principles for microwave moisture and density measurements in grain and seed. *Journal of Microwave Power and Electromagnetic Energy*. 39(2): 107-118.
- Nelson, S. O., and S. Trabelsi. 2008. Dielectric spectroscopy measurements on fruit, meat and grain. *Transactions of the ASABE*. 51(5): 1829-1834.
- Nelson, S. O., S. Trabelsi, and A. W. Kraszewski. 1998. Advances in sensing grain moisture content by microwave measurements. *Transactions of the ASAE*. 41(2): 483-487.
- Nise, N. S. 2008. *Control systems engineering*. Hoboken, NJ: John Wiley & Sons, Inc.
- Nyfors, E., and P. Vainikainen. 1989. *Industrial measurement sensors*. Norwood, MA: Artech House, Inc.
- Paine, M. D. 1969. Constant wet-dry bulb differential controller used for peanut drier control. *Transactions of the ASAE*. 12(6): 741-744.
- Pozar, D. M. 1993. *Microwave engineering*. Reading, MA: Addison-Wesley Publishing Company.
- Putnam, D. H., E. S. Oplinger, T. M. Teynor, E. A. Oelke, K. A. Kelling, and J. D. Doll. 2000. *Peanut. Alternative field crops manual*. St. Paul, MN: University of Minnesota.
- Siyami, S., B. R. Tennes, H. R. Zapp, G. K. Brown, B. A. Klug, and J. R. Clemens. 1987. Microcontroller-based data acquisition system for impact measurement. *Transactions of the ASAE*. 30(6): 1822-1826.
- Steele, J. L. 1982. A microprocessor control system for peanut drying. *Peanut Science*. 9(2): 77-81.
- Trabelsi, S., A. W. Kraszewski, and S. O. Nelson. 1997. Simultaneous determination of density and water content by microwave sensors. *Electronic Letters*. 33(10): 874-876.
- Trabelsi, S., A. W. Kraszewski, and S. O. Nelson. 1998. New density-independent calibration function for microwave sensing of moisture content in particulate materials. *IEEE Transactions on Instrumentation and Measurement*. 47(3): 613-622.
- Trabelsi, S., A. W. Kraszewski, and S. O. Nelson. 1999a. Determining physical properties of grain by microwave permittivity measurements. *Transactions of the ASAE*. 42(2): 531-536.

- Trabelsi, S., A. W. Kraszewski, and S. O. Nelson. 1999b. Unified calibration method for nondestructive sensing of moisture content in granular materials. *Electronic Letters*. 35(16): 1346-1347.
- Trabelsi, S., A. W. Kraszewski, and S. O. Nelson. 2000. Phase-shift ambiguity in microwave dielectric properties measurements. *IEEE Transactions on Instrumentation and Measurement*. 49(1): 56-60.
- Trabelsi, S., A. W. Kraszewski, and S. O. Nelson. 2001a. New calibration technique for microwave moisture sensors. *IEEE Transactions on Instrumentation and Measurement*. 50: 877-881.
- Trabelsi, S., A. W. Kraszewski, and S. O. Nelson. 2001b. Universal calibration method for microwave moisture sensing in granular materials. *Transactions of the ASAE*. 44(3): 731-736.
- Trabelsi, S., M. A. Lewis, and S. O. Nelson. 2008a. Frequency, temperature, density, and moisture dependence of dielectric properties of unshelled and shelled peanuts. ASABE Paper No. 084412. St. Joseph, Mich.: ASABE.
- Trabelsi, S., M. A. Lewis, and S. O. Nelson. 2009a. Investigating moisture, density, and temperature dependence of dielectric properties of unshelled and shelled peanuts at microwave frequencies. *43rd Annual International Microwave Power Symposium Proceedings*. pp. 95-100.
- Trabelsi, S., M. A. Lewis, and S. O. Nelson. 2009b. Rapid and nondestructive determination of moisture content in peanut kernels from microwave measurement of dielectric properties of pods. ASABE Paper No. 097043. St. Joseph, Mich.: ASABE.
- Trabelsi, S., M. A. Lewis, and S. O. Nelson. 2010. Microwave moisture meter for rapid and nondestructive grading of peanuts. ASABE Paper No. 1009183. St. Joseph, Mich.: ASABE.
- Trabelsi, S., S. Nelson, and M. Lewis. 2009c. Microwave nondestructive sensing of moisture content in shelled peanuts independent of bulk density and with temperature compensation. *Sensing and Instrumentation for Food Quality and Safety*. 3(2): 114-121.
- Trabelsi, S., and S. O. Nelson. 1998. Density-independent functions for on-line microwave moisture meters: A general discussion. *Measurement Science and Technology*. 9(4): 570-578.
- Trabelsi, S., and S. O. Nelson. 2003a. Free-space measurement of dielectric properties of cereal grain and oilseed at microwave frequencies. *Measurement Science and Technology*. 14(5): 589-600.
- Trabelsi, S., and S. O. Nelson. 2003b. Nondestructive multiparameter microwave sensor. ASAE Paper No. 036129. St. Joseph, Mich.: ASAE.

- Trabelsi, S., and S. O. Nelson. 2004a. Calibration methods for nondestructive microwave sensing of moisture content and bulk density of granular materials. *Transactions of the ASAE*. 47(6): 1999-2008.
- Trabelsi, S., and S. O. Nelson. 2004b. Microwave dielectric properties of shelled and unshelled peanuts. *Transactions of the ASAE*. 47(4): 1215-1222.
- Trabelsi, S., and S. O. Nelson. 2006a. Microwave sensing technique for nondestructive determination of bulk density and moisture content in unshelled and shelled peanuts. *Transactions of the ASABE*. 49(5): 1563-1568.
- Trabelsi, S., and S. O. Nelson. 2006b. Microwave sensing technique for nondestructive determination of bulk density and moisture content in unshelled and shelled peanuts. *Transactions of the ASAE*. 49(5): 1563-1568.
- Trabelsi, S., and S. O. Nelson. 2006c. Temperature-dependent behavior of dielectric properties of bound water in grain at microwave frequencies. *Measurement Science and Technology*. 17(8): 2289-2294.
- Trabelsi, S., and S. O. Nelson. 2007. A low-cost microwave sensor for simultaneous and independent determination of bulk density and moisture content in grain and seed. ASAE Paper No. 076240. St. Joseph, Mich.: ASAE.
- Trabelsi, S., S. O. Nelson, and M. Lewis. 2008b. Microwave moisture sensor for grain and seed. *Biological Engineering*. 1(2): 195-202.
- Trabelsi, S., S. O. Nelson, and M. Lewis. 2008c. Practical microwave meter for sensing moisture and density of granular materials. *Instrumentation and Measurement Technology Conference Proceedings, 2008. IMTC 2008. IEEE*. 1021-1025.
- Trabelsi, S., S. O. Nelson, and M. Lewis. 2008d. Use of dielectric spectroscopy for pelleted biofuels characterization. ASABE Paper No. 084402. St. Joseph, Mich.: ASABE.
- Troeger, J. M. 1989. Modeling quality in bulk peanut curing. *Peanut Science*. 16(2): 105-108.
- University of Georgia. 2003. World geography of the peanut. Available at: <http://lanra.anthro.uga.edu/peanut/>. Accessed 20 February 2007.
- Virginia-Carolina Peanut Promotions. 2007. Everything about peanuts. Available at: <http://www.aboutpeanuts.com>. Accessed 22 March 2007.
- Von Hippel, A. R. 1954. *Dielectric materials and applications*. New York, NY: The Technology Press of MIT. and John Wiley and Sons.